Doctor Dissertation (Engineering)

Development of Solar Radiation and Atmospheric Radiation Models and Their Applications in China

中国における日射量と大気放射量モデルの開発と応用

Graduate School of Urban Innovation

Yokohama National University

常　開

March, 2020

Table of Contents

Abstract

Weather data is significant and indispensable for building simulations, in which the solar radiation and atmospheric radiation data are very important compositions. However, the solar radiation and atmospheric radiation are only observed at very few stations in China. Thus, developing models to estimate solar radiation and atmospheric radiation are necessary and valuable.

The main purpose of this study is to develop solar radiation and atmospheric radiation data used for building simulations for Chinese locations. The following works are conducted for fulfilling this purpose.

Firstly, to estimate solar radiation for the locations where solar data are not available, two different solar radiation models are developed. One is the decomposition model, which is based on the hourly/daily radiation ratio retrieved from the Zhang and Huang model and the measured daily solar radiation; the other is the hourly sunshine duration model, which is using the routine meteorological elements such as the hourly sunshine duration, the dry-bulb temperature, and the relative humidity. Comparing with the Zhang and Huang model, the average RMSE of the decomposition model is reduced by 29.54%, while the RMSE of the hourly sunshine duration model is reduced by 33.88% for Beijing.

Secondly, to estimate the atmospheric radiation for Chinese locations, atmospheric radiation models are proposed for all-sky conditions using the routine meteorological elements such as the ambient dry-bulb temperature, the water vapor pressure, and the relative humidity. The proposed models perform well comparing with the existing models. Furthermore, the distribution map of radiative cooling potential for China is created.

Finally, the Typical Meteorological Year (TMY) is improved for 24 Chinese locations based on the proposed decomposition solar model, the proposed atmospheric radiation model, and the routine meteorological elements during the period 2006 - 2016, which could be used in building simulations for these locations in China.

List of Tables

List of Figures

CHAPTER 1

Introduction

1.1 Background

The building can be regarded as a heat transfer and moisture transfer system from the perspective of thermal engineering. In order to predict the indoor temperature and humidity changes, in addition to knowing the building thermal performance, the indoor heat generation and water vapor generation, the knowledge of the weather condition around the building that is the boundary condition of heat and moisture transfer system is also necessary. With the development of computer science and technology, building thermal simulation is widely used in building science. Currently, the indoor temperature, humidity, and airflow can be calculated accurately for spatial distribution and time variation using the simulation software, which the weather data is an indispensable input parameter.

There are two widely used forms of weather data, one is the Typical Meteorological Year (TMY); the other is the Test Reference Year (TRY) (a term mainly used in Europe). In recent years, the TMY is more commonly used because it is generated from the observational data and is composed by selecting each typical calendar month separately; while the TRY is generated by selecting the specific year data with the whole 12 consecutive months. The TMY includes 8,760 hourly values of meteorological elements such as temperature, solar radiation, and relative humidity for one year period. Since the typical months come from different years in the TMY, the data smoothing connection is required for different months. The TMY can reflect the average weather characteristics of a certain region for one year period. Therefore, it is very suitable for building simulation.

With the development of computer simulation software, the concept of TMY that defined as a combination of typical meteorological months was firstly proposed in the USA. In 1978, Hall et al. [1] from the Sandia National Laboratories developed the TMY for 230 locations in the USA based on the Finkelstein-Schafer (FS) statistical method, the observational data utilized for developing this TMY are collected from 1948 to 1980. Then in 1995, the TMY was improved by the National Renewable

Energy Laboratory (NREL) using the observational data during 1961 - 1990, which is called TMY2 [2]. In 2008, the TMY3 [3] was developed for 1,020 locations in the USA by the NREL based on the observational data during 1991 - 2005. Another widely used TMY is the International Weather for Energy Calculations (IWEC), which was established by the American Society of Heating, Refrigerating and Air-Conditioning Engineers (ASHRAE) for 227 locations outside the USA and Canada in 2001 [4], and then the IWEC2 was developed for 3012 locations [5].

In 1973, Matsuo and Akasaka [6] firstly developed the TMY for about 40 locations in Japan. The Automated Meteorological Data Acquisition System (AMeDAS) is a weather observation network, which included 1,300 stations in Japan and can observe routine meteorological elements automatically. However, it has no observational data of solar radiation and atmospheric radiation. In 2000, the Expanded AMeDAS (EA) Weather Data was released for 842 locations in Japan based on the observational data during 1981 - 1995 in the AMeDAS dataset [7].

In 1988, Pissimanis et al. [8] developed the TMY for Athens, Greece, based on the observational data from 1966 to 1982. In Italy, the TMY was developed for 66 locations using the observational data from 1951 to 1970 [9]. In Spanish, the TMY was developed for 52 locations [9]. In Argentina, the TMY was generated by Facundo et al. [10] for 15 locations using observation data during the period 1994 - 2014.

In China, from 1999, Zhang et al. [11,12] initially developed the TMY for 57 locations using the observation data from 1982 to 1997, and then completed the TMY for 360 locations in 2012 based on the observational data from 1995 to 2005 [13]. In 2005, Another TMY is created by Tsinghua University and Climatic Data Center of China Meteorological Administration for 270 Chinese locations using observational data during 1971 – 2003 [14], however, in which only 93 locations have measured solar radiation data.

The TMY is created using the observational data from the National Climate Data Center (NCDC), which includes about 1,000 Chinese locations. However, it has no solar radiation and atmospheric radiation data. Therefore, in the process of developing TMY, the biggest problem is the shortage of solar radiation and atmospheric radiation

data. Moreover, solar radiation and atmospheric radiation data are more significant for building thermal simulation.

Also, solar radiation and atmospheric radiation data are indispensable for other applications. For example, solar radiation data is necessary for building air-conditioning design and photovoltaic (PV) systems; and the atmospheric radiation data is significant for building radiative cooling system design. However, the observed data on solar radiation and atmospheric radiation are very few in China.

For the solar radiation, meteorological stations for observing solar radiation are fewer than that for observing other routine meteorological parameters such as temperature, relative humidity, and wind speed. For example, in China, 2,440 meteorological stations [15] are observing the routine meteorological parameters, of which only 122 stations [16] observe solar radiation.

Furthermore, the atmospheric radiation is not observed in the routine meteorological stations and only in specific flux observation stations in current China, however, the specific flux observation stations are very few because of the expensive radiation measuring equipment and maintenance.

Therefore, to make up the deficiency of solar radiation and atmospheric radiation data especially for the development of TMY, it is necessary to develop models for estimating solar radiation and atmospheric radiation based on the routine meteorological parameters.

1.2 Purposes of the study

The primary purpose of the study is to develop solar radiation and atmospheric radiation data for building simulations for locations in China. The main highlights of the purposes are as follows:

1. To estimate the hourly solar radiation based on the proposed decomposition solar model and the hourly sunshine duration model for locations in China.
2. To estimate the atmospheric radiation based on the proposed empirical model for specific geographic and atmospheric characteristics in China.
3. To improve the Typical Meteorological Year (TMY) based on the proposed solar radiation and atmospheric radiation models and the latest routine meteorological observation data from 2006 to 2016 in China.

1.3 Outline of the dissertation

The dissertation is composed of six chapters. The outline of each chapter is as follows:

Chapter 1 briefly describes the research background, research purpose, and research significance.

In Chapter 2, to calculate solar radiation for locations without solar radiation observational records, a new decomposition model is proposed for all-sky conditions based on the hourly/daily radiation ratio retrieved from the Zhang and Huang model. To test the performance of the proposed model, the proposed model is validated and compared with the Zhang and Huang model using the measured hourly solar radiation in 2001. Compared to the existing decomposition models, the advantage of our proposed model is that it can estimate the simultaneous solar radiation not only for clear-sky conditions but also for cloudy-sky conditions. As the application to building air-conditioning design, two kinds of hourly solar radiation datasets (the frequency levels of 95% and 97.5%) are developed based on cumulative frequency function.

In Chapter 3, in order to verify whether the hourly sunshine duration parameter is effective for calculating solar radiation, two hourly solar models for all-sky conditions (Nimiya model and Zhang model) are firstly tested for Beijing, China. To improve the performance of the Nimiya model for Beijing, the Nimiya model is modified by replacing the daily mean temperature parameter with the three-hour temperature difference. With consideration of hourly sunshine duration which is rarely utilized in the previous solar models, a new solar model is developed for all-sky conditions based on regression analysis. To verify the accuracy of the proposed model, it is compared with the Zhang model for Beijing.

In Chapter 4, in order to estimate the atmospheric radiation for Chinese locations, new empirical models for estimating LW radiation (atmospheric radiation) are proposed under all-sky conditions based on the meteorological parameters such as the ambient dry-bulb temperature, the water vapor pressure and the relative humidity, which can be classified into four cases: all day, nighttime, daytime with and without considering cloud modification factor. To test the performance of the proposed models, the proposed models are compared with the existing models (Sridhar model and Crawford and Duchon model) using the validation dataset. As one of the applications of the proposed models, the long-wave radiation datasets for 351 locations of China are developed based on the current typical meteorological year (TMY). Moreover, the distribution map of radiative cooling potential in July is created using the proposed model for the nighttime.

In Chapter 5, the information about the development of the typical meteorological year (TMY) that included detailed data processing is described. Firstly, the lately measured routine meteorological data such as dry-bulb temperature, dew point temperature, and wind speed from 2006 to 2016 are downloaded for 24 locations of China. Then the data records are converted from a three-hour interval to one-hour interval based on a data interpolation method called double Fourier interpolation. Secondly, the hourly solar radiation is calculated by the new decomposition model established in Chapter 2, and then the global solar radiation is separated into the direct

normal and diffuse components using the Gompertz function. The atmospheric radiation data is calculated using the new proposed LW radiation model stated in Chapter 4. Thirdly, the typical meteorological months (TMMs) for 24 locations are selected based on the statistical methods. Lastly, five representative cities in different building climate zones of China in the new TMY are compared and discussed.

Chapter 6 makes a summary of the previous chapters and gives suggestions for further studies.

In order to show the research process more clearly, the flow diagram of the whole study is shown in Fig.1.1.

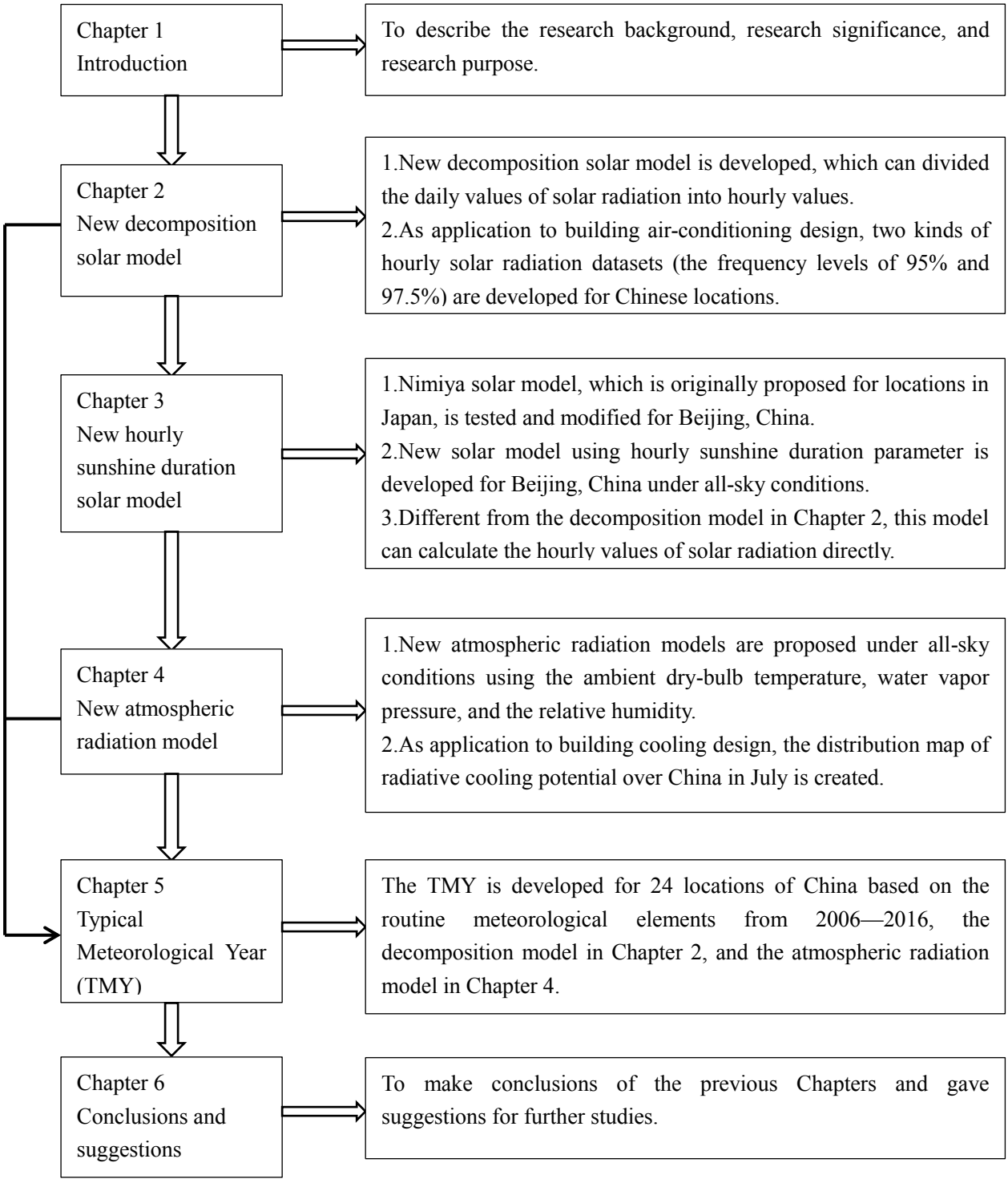

Fig.1.1 Research flow diagram

CHAPTER 2

Development of the decomposition solar model

Nomenclature

I_{he}	estimated hourly solar radiation (W/m^2)
I_0	solar constant, 1367 W/m^2
CC	cloud cover
T_n, T_{n-3}	dry-bulb temperatures at n and n-3 hour, respectively
φ	relative humidity (%)
h	solar altitude angle (°)
C_0, C_1, C_2, C_3, C_4, d, k	regression coefficients
L	local latitude (°)
δ	solar declination angle (°)
h_s	solar hour angle (°)
I_{dm}	measured daily solar radiation (W/m^2)
I_{he}/I_{de}	hourly/daily radiation ratio

2.1 Introduction

Solar radiation is one of the most important parameters for building energy simulations. Only a few meteorological stations measure solar radiation compared with other meteorological parameters such as temperature, relative humidity, wind speed because of the expensive solar measuring equipment and maintenance cost. In China, 2,440 stations [15] have records of meteorological data, while solar radiation is observed at only 122 stations [16]. Therefore, developing models to estimate solar radiation is required for the locations without solar radiation records.

The routine meteorological parameters such as temperature and relative humidity are recorded at almost all meteorological stations, so the relationships between solar radiation and other measured meteorological parameters can be established; this kind of models is called empirical models [18-20]. Empirical models can be mainly classified into four categories based on the employed meteorological parameters [18]: 1) sunshine-based models; 2) cloud-based models; 3) temperature-based models; and 4) hybrid meteorological parameter-based models. Currently, empirical models are widely used to estimate solar radiation in different regions of the world during to their simplicity [21-27]. However, not much work has been done on global solar radiation in China compared with other regions in the world. Chen et al. [27] compared two sunshine-based and three temperature-based models at 48 meteorological stations over China and concluded that the temperature-based only models were not suitable for daily global radiation estimation in China. Wu et al. [28] developed two other models for estimating daily global solar radiation based on air temperature, total precipitation and mean dew point in Nanchang station of China, but the models have not been tested at more locations.

Almost all of the solar radiation models mentioned above estimate monthly or daily solar radiation; very few studies focus on hourly solar radiation. One model for estimating hourly solar radiation is the ASHRAE model [29], which was modified to different forms such as Nijegorodov model [30], Machler and Iqbal model [31] and

Parishwad model [32] by revising the constants A, B and C in the ASHRAE model. The other kind of models is the decomposition ones, which can transform daily solar radiation values into hourly values. They can be divided into three main groups: the first kind of models considers the solar hour angle, day length and solar time such as the Whillier model [33] and the Liu and Jordan one [34]; the second kind of models is established in the form of a Gaussian function such as the Jain model [35], the Baig model [36]; the third kind is represented by the Newell model [37]. However, these models work well under clear-sky conditions and fail in mixed weather situations. Kambezidis et al. [38] communicated the latest developments performed in the Meteorological Radiation Model (MRM) for obtaining hourly solar radiation in Greece and discussed the large uncertainties in the model simulation under cloudy skies. Yao et al. [39] compared the performance of 11 existing decomposition models and proposed 4 new ones based on the observed hourly solar radiation in Shanghai, China; however, further validation is also needed for more locations.

Zhang and Huang initially developed the hourly global solar radiation model based on the dry-bulb temperature difference, relative humidity, wind velocity and cloud cover for Beijing and Guangzhou, China [11]; then Zhang improved this model by removing the wind velocity parameter and calibrated the constants within the model using hourly observed solar data for 24 locations in China [48]. Many previous studies [40,41] have verified the validity of the Zhang and Huang model; for example, Seo and Krarti [42] investigated the impact of 4 different solar radiation datasets used to estimate hourly global, diffuse, and direct solar radiation on annual building energy consumption and concluded that the Zhang and Huang model could predict the annual building energy consumption more accurately than other 3 models.

Recently, we noted that the measured daily solar radiation dataset was available for 99 locations in China; therefore it might be possible to develop a new method based on this dataset to improve the Zhang and Huang model. To achieve this goal, the empirical and decomposition methods were combined by the hourly/daily radiation ratio retrieved from the Zhang and Huang model, which would have advantages in improving estimation accuracy for all-sky conditions.

The objective of this study is to improve the original Zhang and Huang model based on measured daily global solar radiation dataset and the estimated hourly/daily radiation ratio; then the accuracy of the new model is validated using an hourly solar radiation dataset from 2001 under all-sky conditions. Based on the above evaluation, the hourly solar radiation dataset is developed for 2006 - 2016, which can be used to generate the latest Typical Meteorological Year (TMY). Furthermore, as an application of the new hourly solar radiation dataset, based on the cumulative frequency analysis, the solar radiation dataset is developed for building air-conditioning design at 17 locations.

2.2 Data collection and processing

In this study, two kinds of measured meteorological datasets were used; one concerns all meteorological elements excluding solar radiation; the other is the solar radiation dataset. The meteorological parameters were obtained from the Integrated Surface Database (ISD) of the National Climate Data Center (NCDC), which includes more than 1000 meteorological stations of China [43]. The data of dry-bulb temperature, dew-point temperature, cloud cover and air pressure from 17 locations of China were considered in this study.

The measured hourly solar radiation data in 2001 [12] was used to validate the proposed model; the measured daily solar radiation data of 17 locations in the period 2006 - 2016 [44] were used in the new model for generating the hourly solar radiation dataset. The geographical coordinates of the 17 locations are shown in Table 2.1.

Table 2.1 Geographical information of the 17 locations.

	Latitude (°N)	Longitude (°E)	Elevation (m a.m.s.l.)
Beijing	40.08	116.59	35
Changchun	43.99	125.68	215
Changsha	28.12	112.78	120
Fuzhou	26.08	119.28	85
Guangzhou	23.39	113.30	15
Harbin	45.93	126.57	118
Hefei	31.78	117.30	33
Jinan	36.68	116.98	58
Kunming	24.99	102.74	1895
Lhasa	29.67	91.13	3650
Nanchang	28.87	115.90	44
Nanjing	31.74	118.86	15
Shenyang	41.73	123.52	43
Tianjin	39.10	117.17	5
Xining	36.62	101.77	2262
Yinchuan	38.48	106.22	1112
Zhengzhou	34.52	113.84	151

Though most of the measurements intervals in the ISD dataset for meteorological parameters are three hours, the proposed model needs one-hour intervals to estimate hourly global solar radiation. Therefore, the original ISD dataset was filled with hourly values using the linear interpolation method. As far as the dry-bulb temperature and dew-point temperature are concerned, the double Fourier series was utilized according to a previous study by Zhang [12]. The following equations were used in the Fourier series interpolation process (Eqs. (2.1) - (2.4)):

$$f(t) = \sum_{n=1}^{M} a_n \sin(n\omega t) + b_0 + \sum_{n=1}^{M} b_n \cos(n\omega t) \quad (2.1)$$

$$a_n = \frac{1}{4}\sum_{k=1}^{8} f(k) \sin\frac{n\pi k}{4} \quad (2.2)$$

$$b_n = \frac{1}{4}\sum_{k=1}^{8} f(k) \cos\frac{n\pi k}{4} \quad (2.3)$$

$$b_0 = \frac{1}{8}\sum_{k=1}^{8} f(k) \tag{2.4}$$

where, M=3 and 4, respectively; ω=π/12; k is a sequential number of the measured dry-bulb temperature from 1 to 8 at three-hour intervals; t is the local standard time from 1 to 24 at one-hour intervals.

In our previous study, the Eq. (2.1) approximated the measured dry-bulb temperature most closely with M=3 or M=4 [12]; therefore, the average value of Eq. (1) between M=3 and M=4 was utilized for this study. The Fourier interpolation is very effective for variables that change periodically, and it assumes that the data interpolated in the start time of one day equal to the end time of that day, which is not always true for dry-bulb temperature; so it leads to an unsmooth connection between the two consecutive days. In order to solve this problem, the second Fourier interpolation was conducted from 2 p.m. of one day to 11 a.m. of the next day for every pair of consecutive days. An example of the comparison between single and double Fourier interpolation is shown in Fig.2.1 It is clearly seen that the dry-bulb temperature can be connected smoothly after two double Fourier series.

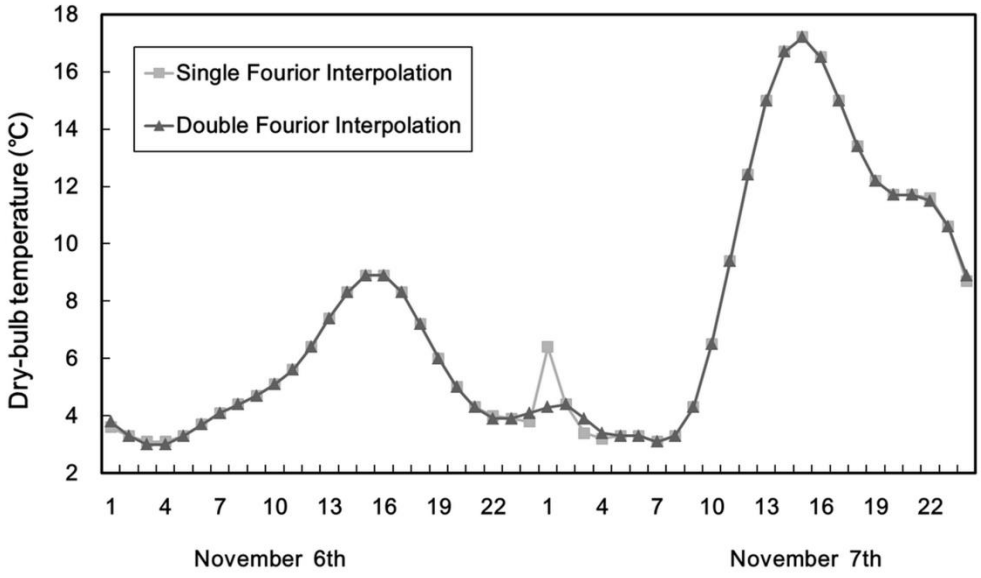

Fig.2.1 Example of dry-bulb temperature interpolation, Beijing, November 6th—November 7th, 2006. Time is LST.

2.3 Development of the decomposition model

Almost all of the empirical models were used for estimating daily or monthly global solar radiation, while few models for hourly global solar radiation. Zhang and Huang [11] developed an hourly solar radiation model for Beijing and Guangzhou in China using common meteorological elements such as temperature, relative humidity, and cloud cover. Zhang [48] subsequently improved this model by removing the wind velocity as shown in Eq. (2.5) and calibrated the constants within the model using hourly observed solar data from 24 locations in China.

$$I_{he} = \{I_0 \cdot \sin(h) \cdot [C_0 + C_1 \cdot CC + C_2 \cdot CC^2 + C_3 \cdot (T_n - T_{n-3}) + C_4 \cdot \varphi] - d\}/k \quad (2.5)$$

where, I_{he} is estimated hourly solar radiation (W/m^2); I_0 is the solar constant, 1355 W/m^2; CC is the total cloud cover in tenths; T_n, T_{n-3} are the dry-bulb temperatures at n and $n-3$ hours, respectively (^{0}C); φ is the relative humidity (%); h is the solar altitude angle (°); C_0, C_1, C_2, C_3, C_4, d, k are location specific constants as shown in Table 2.2.

$$\sin(h) = \sin(L) \cdot \sin(\delta) + \cos(L) \cdot \cos(\delta) \cdot \cos(h_s) \quad (2.6)$$

where, L is the local latitude(°); δ is the solar declination angle(°); h_s is the solar hour angle(°) [45].

Table 2.2 Regression coefficients of the Zhang model for 17 locations in China.

	C_0	C_1	C_2	C_3	C_4	d	k
Beijing	0.6584	0.4864	-0.6647	0.0203	-0.0039	36.6114	0.9300
Changchun	0.8412	0.4406	-0.6853	0.0021	-0.0047	40.2260	0.8868
Changsha	0.7085	0.7065	-0.9413	0.0230	-0.0038	42.2020	0.8747
Fuzhou	0.7960	0.7279	-0.9365	0.0200	-0.0052	35.7491	0.9112
Guangzhou	0.6050	0.5755	-0.7893	0.0278	-0.0030	36.8362	0.8998
Harbin	1.0235	0.5162	-0.6877	-0.0056	-0.0063	35.0285	0.8924
Hefei	0.8084	0.6724	-0.8846	0.0189	-0.0051	35.6732	0.9197
Jinan	0.6497	0.4679	-0.6317	0.0242	-0.0038	27.2746	0.9178
Kunming	0.4817	0.2936	-0.5768	0.0403	0.0003	43.9962	0.8745
Lhasa	0.6996	-0.0929	-0.2399	0.0162	0.0026	56.6359	0.8811
Nanchang	0.7638	0.8086	-1.0198	0.0348	-0.0048	35.5071	0.9192
Nanjing	0.7586	0.5914	-0.7919	0.0181	-0.0050	31.8024	0.9350
Shenyang	0.8199	0.6304	-0.8533	0.0035	-0.0051	39.2128	0.9047
Tianjin	0.7297	0.5113	-0.7432	0.0118	-0.0036	38.6689	0.9110
Xining	0.3856	0.6237	-0.8658	0.0376	0.0015	41.7887	0.8910
Yinchuan	0.5831	0.4261	-0.7089	0.0282	-0.0006	37.4911	0.9237
Zhengzhou	0.7085	0.5092	-0.7069	0.0165	-0.0037	37.0826	0.9250

The Zhang model was developed based on the relationship among the hourly global solar radiation, the dry-bulb temperature difference, the relative humidity and the cloud cover. Therefore, the daily global solar radiation can be calculated by summing up the hourly global solar radiation values (Eq. (2.8)); the hourly/daily radiation ratio can also be obtained. The correlation and comparison between the measured and estimated daily solar radiations for Beijing are shown in Fig.2.2 and Fig.2.3. It is seen that even though the correlation between the measured and estimated daily solar radiation is strong (Correlation coefficient r=0.95), errors still exist on some specific days in 2009.

According to the comparison shown in Fig.2.3, we suppose that the Zhang model might be improved by replacing the estimated daily solar radiation with the measured values and using the hourly/daily radiation ratio calculated by the Zhang model to decompose the measured daily solar radiation into hourly values. Therefore, we developed a new hourly global solar radiation model, which can be expressed by Eq.

(2.7):

$$I'_h = I_{dm} \cdot \frac{I_{he}}{I_{de}} \tag{2.7}$$

$$I_{de} = \sum I_{he} \tag{2.8}$$

where, I'_h is hourly solar radiation estimated by the proposed model (W/m^2); I_{dm} is the measured daily solar radiation (W/m^2); I_{de} is the daily solar radiation from Eq.(2.8) (W/m^2); I_{he} is the hourly solar radiation estimated from Eq.(2.5) (W/m^2); I_{he} /I_{de} is the hourly/daily radiation ratio.

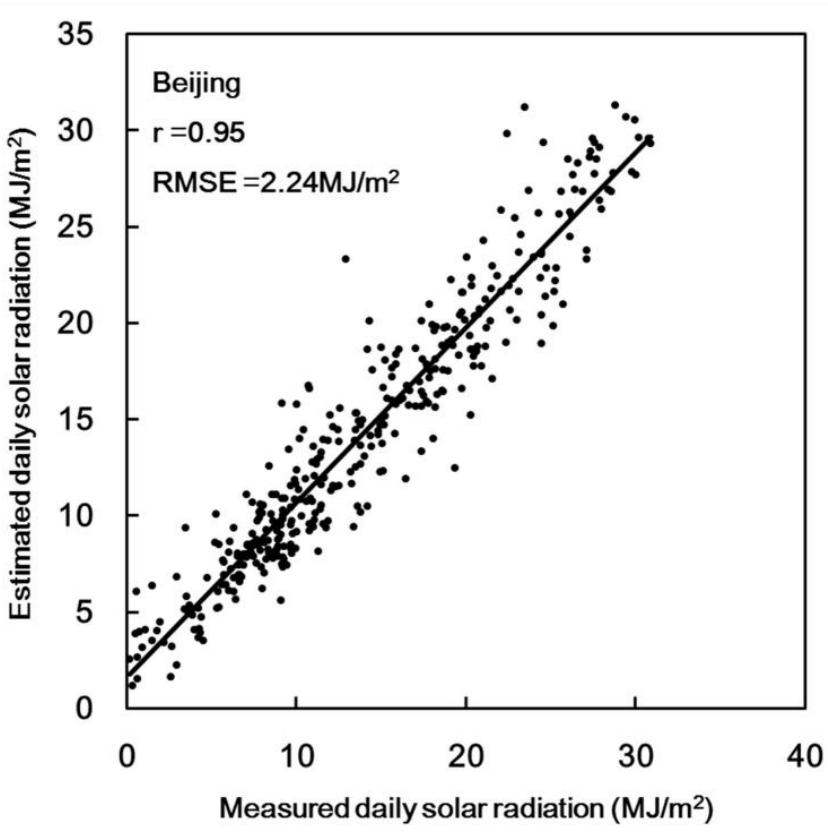

Fig.2.2 Correlation between measured and estimated daily global solar radiation for Beijing, 2009.

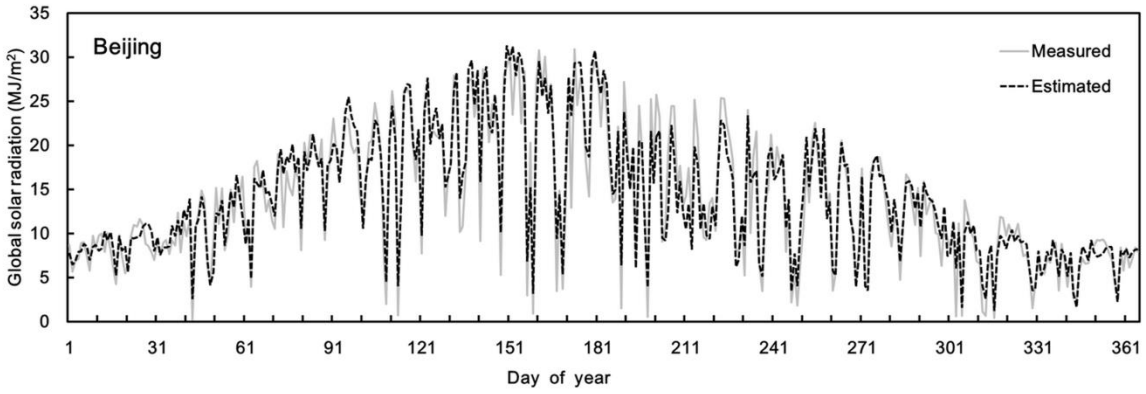

Fig.2.3 Comparison between measured and estimated daily solar radiation for Beijing, 2009.

In order to validate the performance of the proposed model, values of solar radiation between Eq. (2.5) and Eq. (2.7) were compared for the 17 locations.

The values of R^2 and RMSE were used to evaluate the two solar radiation models: Eq. (2.5) and Eq. (2.7). These indicators can be calculated as follows [46]:

$$R^2 = 1 - \frac{\sum_{i=1}^{n}\left(H_{i,m}-H_{i,c}\right)^2}{\sum_{i=1}^{n}\left(H_{i,m}-H_{m,avg}\right)^2} \tag{2.9}$$

$$\mathrm{RMSE} = \sqrt{\frac{1}{n}\sum_{i=1}^{n}\left(H_{i,m}-H_{i,c}\right)^2} \tag{2.10}$$

where, R^2 is coefficient of determination; *RMSE* is root mean square error (W/m^2); $H_{i,m}$ and $H_{i,c}$ are the i th measured and estimated values, respectively (W/m^2); $H_{m,avg}$ is the average of the measured values (W/m^2); n is the total number of measurements.

Solar radiation affects the indoor environment; therefore, it should be taken into account in the building equipment design. In winter, generally, we do not consider solar radiation, which is ignored for heating design, since the heating system must secure the indoor temperature even on cloudy days. On the contrary, solar radiation is important for air-conditioning design in summer since solar radiation affects the

cooling load of air conditioners significantly.

The summer hourly solar radiation data generated by proposed model from 2006 to 2016 (June, July, August) were used to develop two different datasets for the 17 locations: the hourly solar radiation at the frequency level of 95% and 97.5%, respectively. The cumulative frequency analysis [47] was carried out with the hourly solar radiation dataset for each location in 2006 - 2016.

2.4 Results and discussion

2.4.1 Performance of the proposed model

The hourly/daily radiation ratios were firstly calculated based on the Zhang model with meteorological parameters in 2001 for 17 locations. The correlation of hourly/daily radiation ratio between estimated and measured is shown in Fig.2.4. It is seen that the value of the correlation coefficient (r) is high, which indicates that the estimated hourly/daily radiation ratio is feasible to be applied to the proposed model. Fig.2.5 is a comparison between the measured hourly solar radiation and the estimated values calculated by the new model for Beijing, 2001. The estimated hourly solar radiation agrees well with the measured one with limited errors.

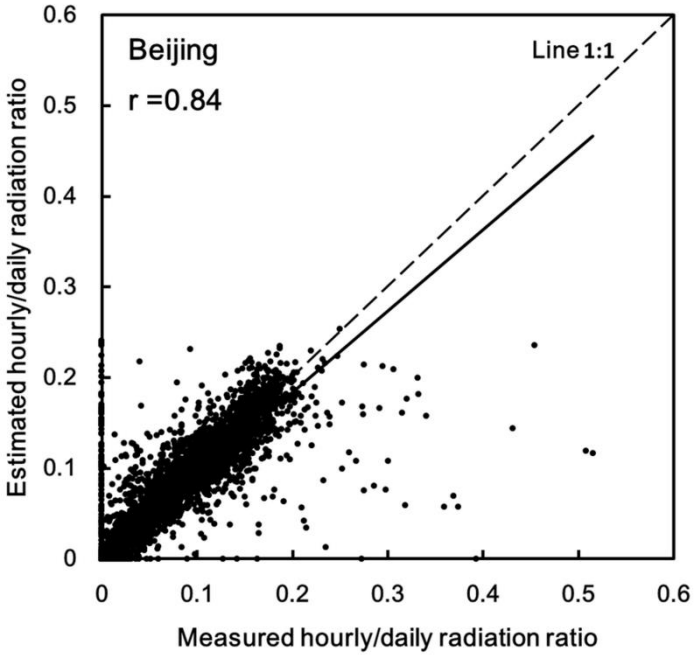

Fig.2.4 Correlation between measured and estimated hourly/daily radiation ratio, Beijing, 2001.

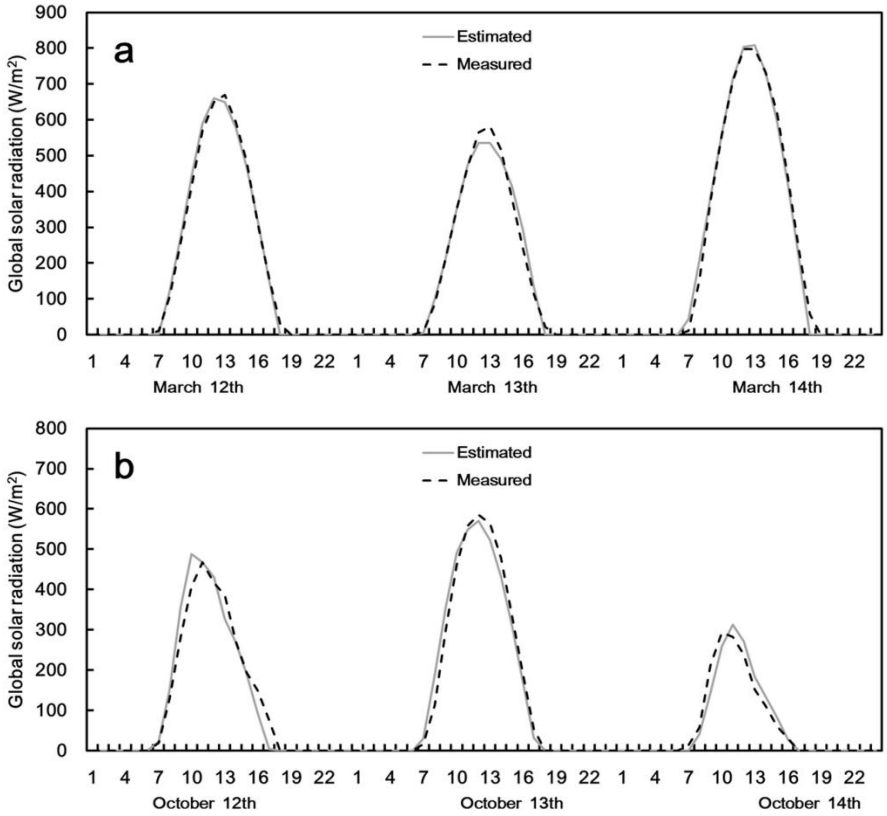

Fig.2.5 Example of the comparison of measured and estimated hourly global solar radiation for Beijing, 2001: (a) March 12th – 14th, under clear-sky conditions; (b) October 12th—14th, under all-sky conditions. Time is LST.

The proposed model was validated under all-sky conditions using the measured hourly solar radiation dataset in 2001. The comparison of R^2 and RMSE between the Zhang model and the proposed one for 17 locations are listed in Table 2.3. Both statistical indicators of the proposed model are much improved over those of the Zhang model. The average of R^2 for all the 17 locations in the Zhang model is 0.80 while that in the proposed model becomes 0.90; the average of RMSE for all the 17 locations in the Zhang model is 115.83 W/m^2, while for the new model it is 81.61 W/m^2. Between the two models, the proposed model performs well for all the 17 locations. The relationship between the measured and estimated hourly global solar radiation for 5 locations is shown in Fig.2.6. Beijing has the best results with the highest R^2, 0.93, and the lowest RMSE, 63.52 W/m^2, while Kunming has the highest RMSE, 114.04 W/m^2. The model's accuracy varies from one location to the other, but it shows a better performance over the Zhang model.

Zhang et al. [49] reviewed, classified and compared a large number of solar models used to estimate the monthly average daily, daily and hourly global radiation and made a summary that the RMSEs of the models used to estimate hourly radiation are in the range of 88.33 - 142.22 W/m^2, whose performance was worse than our results (average RMSE was 81.61 W/m^2). Yao et al. [39] tested 15 hourly solar radiation models (11 existing decomposition models and 4 new proposed models) with 6 months of measured data in Shanghai, China and obtained that the decomposition models established in the form of Gaussian function (group two) were more accurate. The RMSEs of 11 existing decomposition models ranged from 0.473 to 0.512 MJ/m^2, corresponding to 131.39 to 142.22W/m^2, and that of the 4 new ones ranged from 0.474 to 0.481 MJ/m^2, corresponding to 131.67 to 133.61 W/m^2; which are higher than that in any of our locations. From the above comparison, it reveals that our proposed model in this study works better and is suitable for more locations.

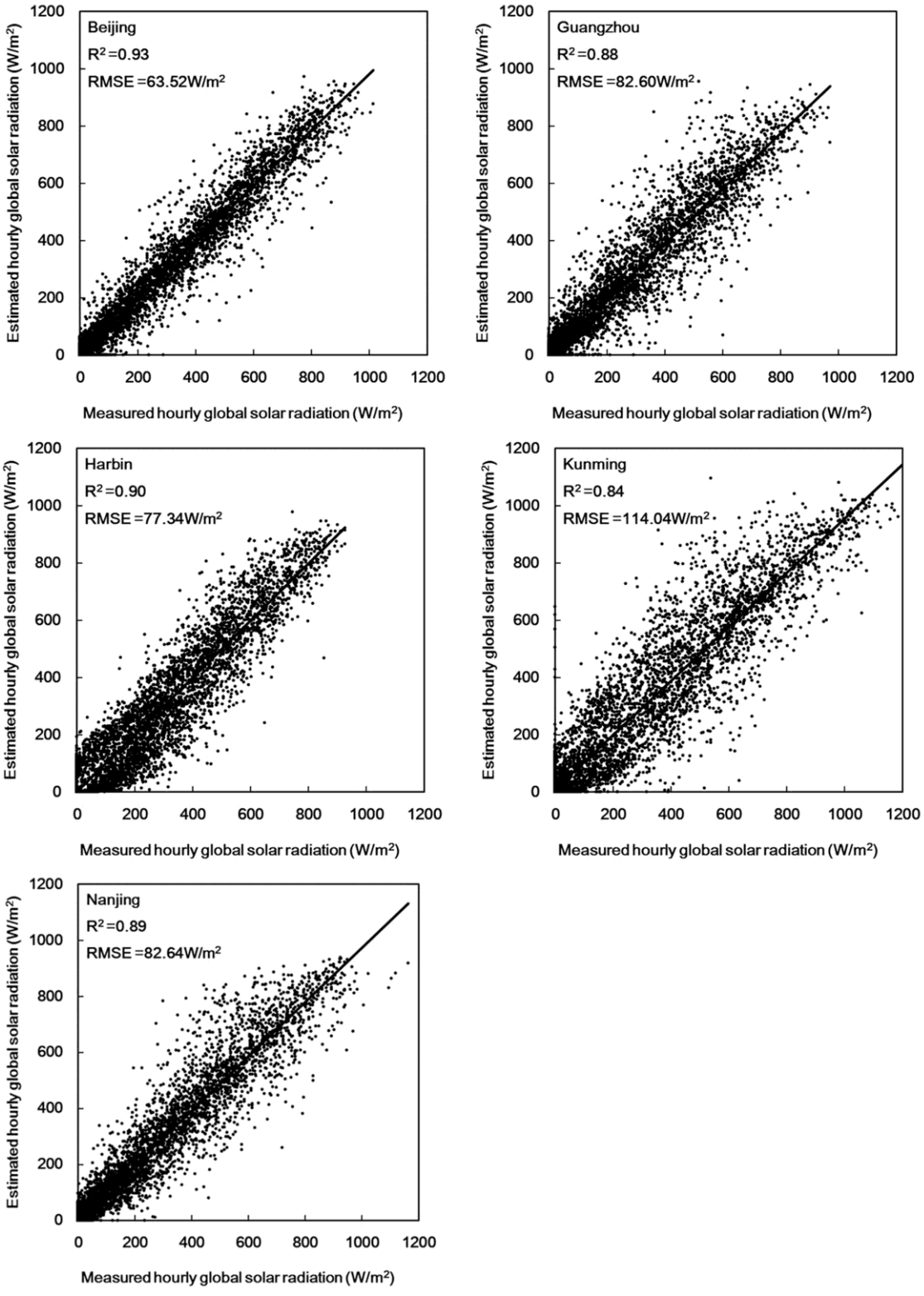

Fig.2.6 Correlation between measured and estimated hourly global solar radiation for 5 locations, 2001, under all-sky conditions.

Table 2.3 Statistical results for the proposed model and the Zhang model.

	R^2-ZH*	R^2-New**	RMSE-ZH* (W/m^2)	RMSE-New** (W/m^2)
Beijing	0.88	0.93	86.45	63.52
Changchun	0.77	0.88	123.11	88.23
Changsha	0.84	0.93	101.88	66.82
Fuzhou	0.78	0.87	118.33	89.86
Guangzhou	0.82	0.88	101.54	82.60
Harbin	0.59	0.90	156.37	77.34
Hefei	0.82	0.92	110.09	73.96
Jinan	0.78	0.93	106.48	60.88
Kunming	0.74	0.84	144.18	114.04
Lhasa	0.73	0.85	161.04	118.33
Nanchang	0.87	0.94	98.80	69.22
Nanjing	0.81	0.89	108.52	82.64
Shenyang	0.74	0.84	126.49	96.97
Tianjin	0.87	0.94	92.74	62.40
Xining	0.79	0.87	128.18	102.96
Yinchuan	0.86	0.92	101.89	75.63
Zhengzhou	0.84	0.94	103.06	62.02

*ZH: Zhang model.

**New: proposed model.

2.4.2 Solar radiation for air-conditioning design

An hourly weather dataset such as the Typical Meteorological Year (TMY) is necessary for building thermal simulations; the quality of this dataset affects the accuracy of thermal simulations. In the weather dataset, the hourly solar radiation is one of the most important parameters, which influences the indoor thermal environment and energy consumption. The Typical Meteorological Year (TMY) dataset for China was developed by Zhang with solar radiation estimated using the Zhang model [12]. In this study, the hourly solar radiation dataset is calculated based on the proposed model for 2006 - 2016, which can be used for developing the typical meteorological year.

In this study, we focus on the building cooling design as an application of this solar radiation dataset. When the air-conditioning equipment design is carried out, the

indoor thermal environment under most weather conditions should be guaranteed excluding extreme weather; therefore, we need to select the solar radiation value at different frequency levels such as 95% and 97.5% for a specific location from long-term solar radiation records. Long-term records of at least 10 years are commonly used [50].

Since solar radiation is always ignored for heating system design during winter, while it is also significant for air-conditioning design in summer. In this study, the hourly solar radiation data in summer (June, July, August) were used for statistical processing based on the cumulative frequency analysis. Fig.2.7 shows the cumulative frequency function of hourly solar radiation at noon in Beijing from 2006 to 2016. The value of solar radiation corresponding to the cumulative frequency of 100% is the maximum solar radiation in 11 years (2006 - 2016) at noon, which will lead to the excessive capability of an air-conditioner. Therefore, the cumulative frequency of 95% and 97.5% corresponding to solar radiation values were selected as the design reference value according to the building design standard.

Fig.2.8 shows the comparison for values of hourly solar radiation at frequency levels of 95% and 97.5% in Beijing. The suggested hourly global solar radiation values for the air-conditioning design of the 17 locations are shown in Tables 2.4 and 2.5, which are useful for building air-conditioning design.

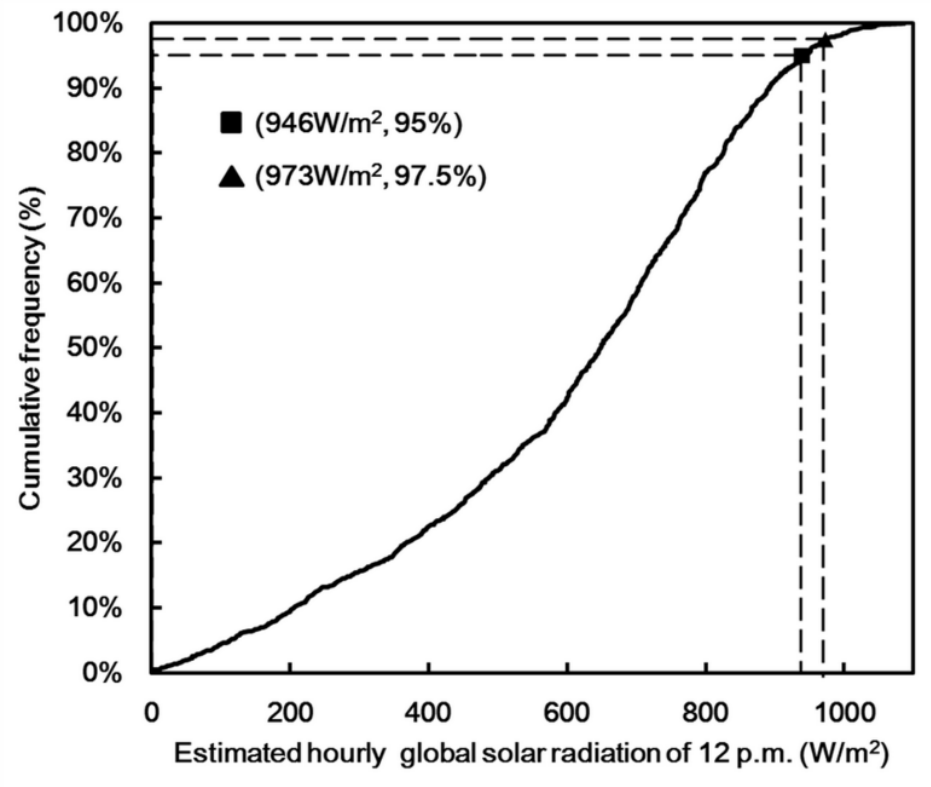

Fig.2.7 Cumulative frequency function of global solar radiation at noon in Beijing from 2006 to 2016.

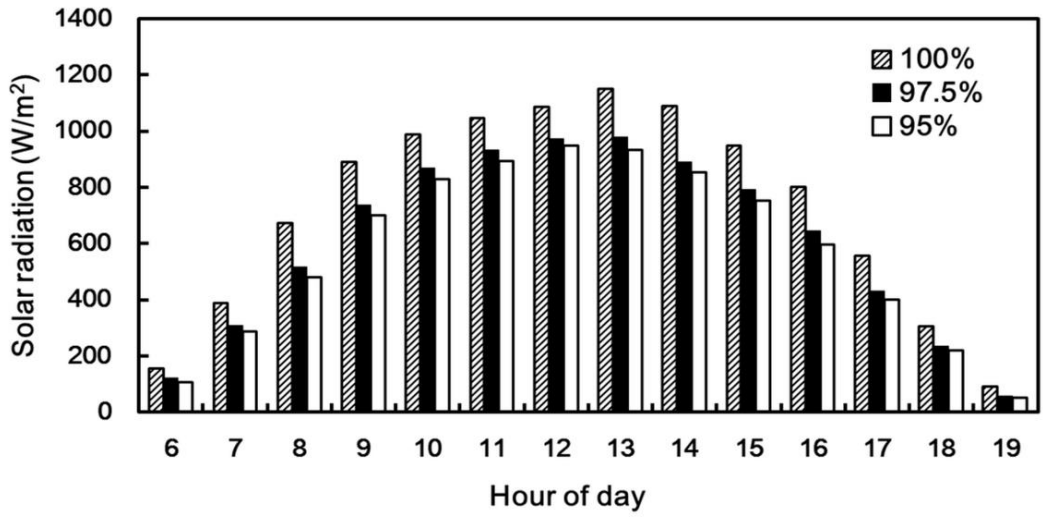

Fig.2.8 Hourly solar radiation values at frequency levels of 97.5% and 95% for air-conditioning design in Beijing from 2006 to 2016. Time is LST.

Table 2.4 Hourly solar radiation values (W/m^2) at the frequency level of 97.5% for air-conditioning design in 17 locations.

Time (h) / Location	5	6	7	8	9	10	11	12	13	14	15	16	17	18	19	20
Beijing	0	122	311	516	737	867	933	973	980	889	793	644	430	237	60	0
Changchun	94	264	459	644	892	961	985	1042	1020	921	806	658	443	210	0	0
Changsha	0	20	209	399	638	805	931	1022	1047	973	860	677	460	230	26	0
Fuzhou	0	91	307	521	755	922	990	1042	1037	949	780	577	348	129	0	0
Guangzhou	0	0	181	419	653	817	916	947	946	869	768	648	416	186	0	0
Harbin	129	284	445	590	733	836	904	924	900	809	700	553	378	199	22	0
Hefei	0	86	268	473	709	886	974	1022	1010	937	850	702	447	207	0	0
Jinan	0	125	311	490	725	850	904	964	983	880	774	601	404	206	36	0
Kunming	0	0	60	276	541	787	1018	1103	1116	1058	936	785	574	313	102	0
Lhasa	0	0	0	186	439	688	890	1031	1096	1119	1044	935	790	579	358	133
Nanchang	0	60	245	456	691	819	927	984	1039	951	836	645	425	190	0	0
Nanjing	0	95	287	500	750	874	955	1010	991	900	798	663	426	182	0	0
Shenyang	46	203	381	557	781	898	940	993	999	921	811	643	429	206	8	0
Tianjin	0	146	313	499	688	895	1038	1087	1101	1037	912	704	484	260	57	0
Xining	0	0	147	361	633	850	999	1101	1135	1051	925	764	567	357	169	18
Yinchuan	0	24	222	450	684	845	972	1051	1086	1044	932	774	575	367	169	0
Zhengzhou	0	70	245	432	647	796	898	963	961	899	795	634	439	245	59	0

Table 2.5 Hourly solar radiation values (W/m^2) at the frequency level of 95% for air-conditioning design in 17 locations.

Time (h) / Location	5	6	7	8	9	10	11	12	13	14	15	16	17	18	19	20
Beijing	0	107	288	479	700	828	893	946	932	853	753	598	400	220	52	0
Changchun	85	246	425	597	804	884	922	951	957	868	746	603	394	188	0	0
Changsha	0	17	196	373	602	775	887	964	983	912	812	652	440	220	22	0
Fuzhou	0	79	285	486	704	871	942	993	990	898	745	544	323	116	0	0
Guangzhou	0	0	162	378	604	774	850	899	887	818	714	593	388	172	0	0
Harbin	117	260	414	554	709	813	871	895	870	785	676	534	362	190	20	0
Hefei	0	76	250	435	659	830	925	987	969	886	779	637	410	188	0	0
Jinan	0	114	287	453	668	806	867	931	922	837	726	570	365	192	32	0
Kunming	0	0	43	236	488	736	924	1034	1053	1003	876	730	528	283	89	0
Lhasa	0	0	0	172	416	655	856	995	1073	1084	1022	907	766	562	339	123
Nanchang	0	53	232	425	654	790	903	957	990	908	798	615	401	181	0	0
Nanjing	0	84	269	455	693	839	915	961	938	856	748	615	386	172	0	0
Shenyang	0	186	361	512	735	844	902	960	964	880	758	597	392	190	0	0
Tianjin	0	129	293	457	647	841	949	999	994	924	821	641	431	233	49	0
Xining	0	0	134	341	600	808	955	1055	1098	1008	894	742	547	341	157	10
Yinchuan	0	21	210	424	652	819	937	1009	1037	978	892	735	549	348	160	0
Zhengzhou	0	62	228	398	613	764	846	928	930	851	761	607	413	229	56	0

2.5 Summary

In this study, a new hourly solar radiation model was proposed using the hourly/daily radiation ratio. The main conclusions from this study are as follows:

(1) Compared with the Zhang model, the proposed model is more accurate with the average of R^2, 0.90 and RMSE, 81.61 W/m^2. The proposed model also can estimate the hourly solar radiation better for all-sky conditions and wider locations compared with other existing decomposition models in China.

(2) The latest hourly global solar radiation dataset from 2006 to 2016 for the 17 locations was developed using the proposed model, which can be used to generate the Typical Meteorological Year (TMY).

(3) As an application of the new hourly solar radiation dataset, two kinds of datasets (frequency levels of 95% and 97.5%) for air-conditioning were developed, which can provide a valuable reference for air-conditioning design.

More works are needed for expanding solar radiation dataset to more locations in China based on the proposed model and applying the new solar radiation dataset to generate the Typical Meteorological Year (TMY) in the future.

CHAPTER 3

Improvement of solar models using the hourly sunshine duration for all-sky conditions

Nomenclature

a,b	regression coefficients
a_1, a_2	regression coefficients
b_1, b_2	regression coefficients
c_1, c_2, c_3	regression coefficients
C_0, C_1, C_2, C_3, C_4	regression coefficients
CC	cloud cover in tenths
d_1, d_2, d_3	regression coefficients
e_0, e_1, e_2, e_3, e_4	regression coefficients
h	solar altitude angle (°)
h_s	solar hour angle (°)
I_{h1}, I_{h2}, I_{h3}	hourly solar radiation classified by values of sunshine hour (W/m^2)
I_{he}	hourly solar radiation (W/m^2)
I_0	hourly extraterrestrial solar radiation (W/m^2)
I_{sc}	solar constant, 1367 W/m^2
L	latitude of the location (°)
n	Julian day of the year
Rs	daily global solar radiation (MJ/m^2day)
Ra	daily extraterrestrial solar radiation (MJ/m^2day)
SD_{daily}	daily total sunshine hours (h)
SD_{max}	daily maximum possible sunshine hours (h)
SD_{ratio}	daily sunshine ratio
SD_{hourly}	hourly sunshine duration (h)
T_{daily}	daily mean temperature (℃)
T_n, T_{n-3}	temperature at n and n-3 hours, respectively
δ	solar declination angle (°)
φ	relative humidity (%)
ω_1, ω_2	solar hour angle at the beginning and end of one-hour interval (°)
ω_s	sunset hour angle (°)

3.1 Introduction

Solar radiation data is significant for various applications in the building field, such as building thermal simulation, air-conditioning design, passive solar house design, and photovoltaic (PV) system. Meteorological stations for observing solar radiation are much less than those for observing the general meteorological elements (temperature, relative humidity, wind speed and sunshine duration). For example, in China, 2440 meteorological stations are observing routine meteorological parameters, of which only 122 stations observe solar radiation [16]. Therefore, it is necessary to develop models for estimating solar radiation based on the general meteorological parameters since the deficiency of solar radiation data.

Currently, empirical models, which were developed based on the relationships between solar radiation and general meteorological parameters through regression analysis, were widely used in the world [51]. One of the commonly used parameters in such empirical solar models was the daily sunshine duration for its readily available [52]. Therefore, Angstrom [53] proposed the initial sunshine duration model through regression analysis of two ratios: one is the ratio of measured daily solar radiation to the theoretical clear-sky solar radiation; the other is the ratio of measured daily sunshine duration to the theoretical maximum possible sunshine duration. Then Prescott [19] modified this model using the theoretical extraterrestrial solar radiation to replace the clear-sky solar radiation, because the theoretical extraterrestrial solar radiation was easier to calculate; this modified form was called the Angstrom-Prescott model. Other sunshine duration-based model appeared subsequently based on different forms of the Angstrom-Prescott one; however, almost all of them were proposed for calculating the daily values or monthly average daily values, and the hourly values were paid little attention.

Hourly values of solar radiation were more necessary than daily values for some applications, for example, for building thermal simulation software, the hourly values of solar radiation were essential and critical input parameters. Currently, the existing

hourly solar models could be divided into three categories: the first category was the ASHRAE model [54] and its different modification forms such as the Nijegorodov model [30]. The second kind of model was the decomposition model, which could decompose daily values into hourly values such as Liu and Jordan model [34]. The third kind of model was complicated and needed detailed information of atmospheric components (aerosols, water vapor, and ozone) as model parameters such as the Ineichen model [55], the MRM model [38], and the ESRA model [56]. However, some of the models mentioned above estimated the monthly average hourly values only, which means that only the representative day of each month, not the consecutive days of each month could be calculated. Moreover, almost all of them were only suitable for clear-sky conditions, not for all-sky conditions.

Since the appearance of clouds had a significant influence on solar radiation, developing hourly solar models for all-sky conditions included clouds was more complex and difficult than for clear-sky conditions. An hourly solar model was initially developed by Zhang and Huang for Beijing and Guangzhou City, China, which used the observing cloud cover data to reflect the impact of clouds on solar radiation under all-sky conditions [11]; then this model was subsequently modified and recalibrated the regression coefficients by Zhang based on the regression analysis and the measured hourly solar data at 24 locations [48]. For other countries and regions, another hourly solar model for all-sky conditions was proposed by Nimiya et al. [57] based on the hourly sunshine duration, the extraterrestrial solar radiation, and other meteorological parameters, which had good performance with high accuracy for locations in Japan.

The solar models with consideration of daily sunshine duration such as the Angstrom-Prescott equation were compared and analyzed in many previous studies for China. For example, Chen et al. [27] calibrated two daily sunshine duration-based models using measured daily data for 48 locations in China. Yao et al. [58] analyzed 108 existing daily sunshine duration-based models using 42 years of meteorological data in Shanghai station, China. However, the hourly sunshine duration, not the daily sunshine duration, was being paid little attention on model development. Therefore, in

this study, the hourly sunshine duration was employed in developing the hourly solar model.

The purpose of this study is to discuss the effectiveness of hourly sunshine duration in the existing solar models, and to propose new hourly solar model using the hourly sunshine duration parameter under all-sky conditions. To achieve this goal, the following steps were being carried out: 1) the performance of original Nimiya model was analyzed using the measured hourly solar data in Beijing, China; 2) the original Nimiya model was improved by replacing the daily mean temperature with the three-hour temperature difference; 3) the new solar model was proposed with the hourly sunshine duration parameter based on Zhang model.

3.2 Data collection and statistical evaluation

The hourly routine meteorological elements (temperature, cloud cover, relative humidity) were downloaded from the Integrated Surface Database (ISD) of the National Climate Data Center (NCDC) [43] for Beijing, 2017. More than 1000 Chinese meteorological stations were included in the ISD datasets; however, most of the measurement intervals of meteorological elements are three hours, while the one-hour interval of meteorological parameters was necessary for Zhang model. Therefore, the linear and Fourier series interpolation methods were applied to obtain one-hour values from three hours values, and the detailed formulas and processes can refer to our previous research [12][59].

The hourly solar radiation, hourly sunshine duration, and daily mean temperature were obtained from the China Meteorological Data Service Center (CMDC) [60] for Beijing, 2017. The daily sunshine duration parameter used in the Nimiya model can be calculated by adding up the values of hourly sunshine duration for each day.

The four common statistical indicators: r, RMSE, MBE, and t-statistic were applied to evaluate the performance of hourly solar radiation models, and could be expressed as follows [18]:

$$\mathrm{r} = \frac{\Sigma\left(\left(H_{i,m}-H_{m,avg}\right)\left(H_{i,c}-H_{c,avg}\right)\right)}{\sqrt{\Sigma\left(H_{i,m}-H_{m,avg}\right)^2 \Sigma\left(H_{i,c}-H_{c,avg}\right)^2}} \quad (3.1)$$

$$\mathrm{RMSE} = \sqrt{\frac{1}{n}\sum_{i=1}^{n}\left(H_{i,c}-H_{i,m}\right)^2} \quad (3.2)$$

$$\mathrm{MBE} = \frac{1}{n}\sum_{i=1}^{n}\left(H_{i,c}-H_{i,m}\right) \quad (3.3)$$

$$\mathrm{t-statistic} = \sqrt{\frac{(n-1)(MBE)^2}{(RMSE)^2-(MBE)^2}} \quad (3.4)$$

where, *r* is the correlation coefficient; *RMSE* is the root mean square error; *MBE* is the mean bias error; and *t-statistic* is the t-Test statistic; *n* is the total number of data; $H_{i,m}$ and $H_{i,c}$ are the *i*th measured and estimated values of the solar radiation, respectively (W/m^2); $H_{m,avg}$ and $H_{c,avg}$ are the average of the measured and estimated values, respectively (W/m^2).

3.3 Nimiya hourly solar radiation model

3.3.1 Original Nimiya solar model for Japan

The Angstrom-Prescott model was widely used for calculating the daily solar radiation in the world, in which one of the most significant meteorological parameter was the daily sunshine duration. The main calculation formulas of this model were shown in Eq. (3.5) and the detailed information was shown as follows.

$$\frac{R_s}{R_a} = \mathrm{a} + \mathrm{b}(SD_{ratio}) \quad (3.5)$$

$$SD_{ratio} = \frac{SD_{daily}}{SD_{max}} \quad (3.6)$$

where, R_s is the daily global solar radiation (MJ/m^{2}day); R_a is the daily extraterrestrial solar radiation (MJ/m^{2}day); SD_{ratio} is the daily sunshine ratio; SD_{daily} is the daily total sunshine hours (h); SD_{max} is the daily maximum possible sunshine hours (h); *a, b* are the empirical regression coefficients.

The daily extraterrestrial solar radiation, R_a is calculated as follows,

$$R_a = \frac{24}{\pi} \cdot I_{sc} \cdot \left(1 + 0.033\, cos\frac{360n}{365}\right) \cdot \left(cos\, L \cdot cos\, \delta \cdot sin\, \omega_s + \frac{\pi}{180}\omega_s \cdot sin\, L \cdot sin\, \delta\right) \tag{3.7}$$

Where, I_{sc} is the solar constant, 1367 W/m^2; L is the latitude of the location (°); δ is the solar declination (°); ω_s is the sunset hour angle (°);

The solar declination δ and the sunset hour angle ω_s can be calculated as,

$$\delta = 23.45 \sin\left[\frac{360}{365}(284 + n)\right] \tag{3.8}$$

$$\omega_s = \cos^{-1}(-\tan L \cdot \tan \delta) \tag{3.9}$$

The maximum possible sunshine hours SD_{max} can be calculated as,

$$SD_{max} = \frac{2}{15}\omega_s \tag{3.10}$$

For the Angstrom-Prescott model, the daily sunshine hours could indirectly reflect the influence of weather conditions, mainly the cloudiness, on solar radiation; therefore, the performance of this model was very well based on the model accuracies had been evaluated in different regions of the world [52] [58]. However, the Angstrom-Prescott model using daily sunshine duration parameter could only calculate the daily or monthly average daily values; moreover, the measured daily sunshine hours are obtained by adding up the hourly value for each day. Therefore, whether it is possible to apply the hourly sunshine duration to develop hourly solar models is worth discussing.

In the Angstrom-Prescott equation, the daily sunshine duration and daily extraterrestrial solar radiation may be replaced by the hourly sunshine duration and

hourly extraterrestrial solar radiation respectively for calculating hourly solar values. Therefore, the Nimiya model was proposed for locations in Japan using the hourly sunshine duration.

Since a large number of hourly values of sunshine duration were 0 or 1, the regression analysis between the hourly measured solar radiation and the extraterrestrial solar radiation was primarily conducted for 0 and 1 values of sunshine hour respectively. The specific constants of the Nimiya model were then calculated based on the daily sunshine ratio, hourly solar altitude angle, and daily mean temperature. The detailed formulas of the Nimiya model can be expressed as follows:

For $SD_{hourly} = 0$:

$$I_{h1} = a_1 \cdot I_0 + b_1 \tag{3.11}$$

$$a_1 = c_1 + c_2 \cdot SD_{ratio} + c_3 \cdot \sin(h) \tag{3.12}$$

For $SD_{hourly} = 1$:

$$I_{h2} = a_2 \cdot I_0 + b_2 \tag{3.13}$$

$$a_2 = d_1 + d_2 \cdot SD_{ratio} + d_3 \cdot T_{daily} \tag{3.14}$$

For $SD_{hourly} = 0.1 – 0.9$:

$$I_{h3} = I_{h1(SD_{hourly}=0)} \cdot \left(1 - SD_{hourly}\right) + I_{h2(SD_{hourly}=1)} \cdot SD_{hourly} \tag{3.15}$$

where, I_{h1}, I_{h2}, I_{h3} are hourly solar radiations classified by values of hourly sunshine duration (W/m^2); I_0 is hourly extraterrestrial solar radiation (W/m^2); SD_{ratio} is daily sunshine ratio (Eq.(3.6)); SD_{hourly} is the hourly sunshine duration (h); h the is solar altitude angle (°); T_{daily} is the daily mean temperature (℃); a_1, a_2, b_1, b_2, c_1, c_2, c_3, d_1, d_2, d_3 are regression coefficients as shown in Table 3.1(A).

The hourly extraterrestrial solar radiation can be expressed as follows,

$$I_0=\frac{12\cdot3600}{\pi}\cdot I_{sc}\cdot\left(1+0.033\,cos\frac{360n}{365}\right)\cdot\left[cos\,L\cdot cos\,\delta\cdot(sin\,\omega_2-sin\,\omega_1)+\frac{\pi(\omega_2-\omega_1)}{180}\cdot sin\,L\cdot sin\,\delta\right] \quad (3.16)$$

where, I_0 is hourly extraterrestrial solar radiation (W/m^2) [61]; I_{sc} is the solar constant, 1367 W/m^2; n is the Julian day of one year; L is the local latitude (°); δ is the solar declination angle(°); ω_1, ω_2 are the hour angle at the beginning and end of the time interval (one-hour) (°).

3.3.2 Performance of Nimiya model for Beijing

In this study, the original Nimiya solar model was firstly tested using the measured hourly solar radiation and hourly sunshine duration for Beijing, 2017. The correlation between the measured and extraterrestrial hourly solar radiation can be classified into three parts based on the values of the sunshine hour (0, 1 and 0.1—0.9).

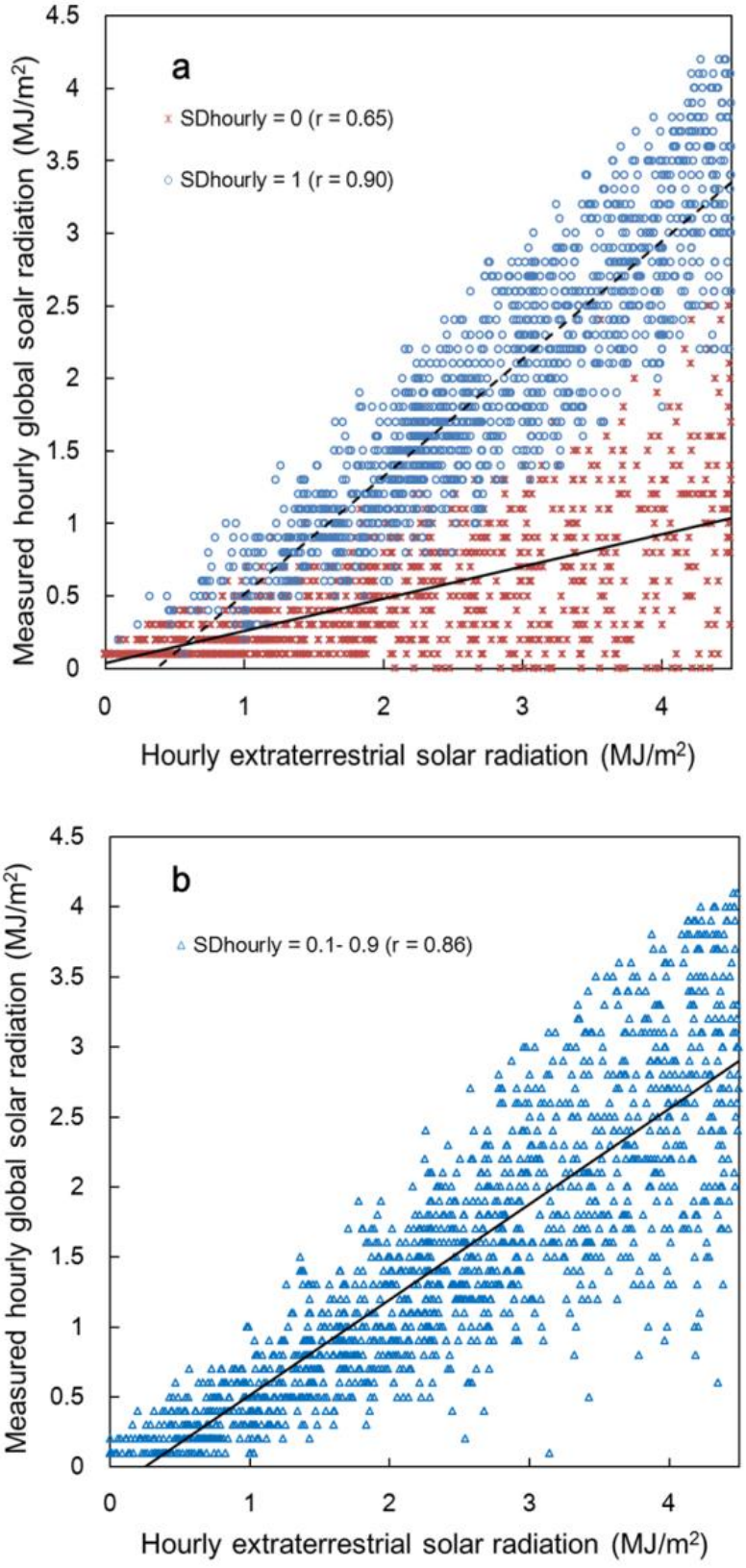

Fig.3.1 Correlation between measured and extraterrestrial solar radiation based on hourly values of sunshine duration for Beijing, 2017: (a) 0 and 1 values of the sunshine hour, respectively; (b) 0.1—0.9 values of the sunshine hour.

From Fig.3.1, it can be seen that the correlation between measured and extraterrestrial hourly solar radiation was the best (r=0.90) for the part where the sunshine hour was 1. The sunshine hour value of 1 may indicate a clear-sky condition within one hour while that of 0 may indicate a completely cloudy-sky condition. Therefore, the sunshine hour value can indirectly reflect the impact of weather conditions on solar radiation for one location.

The hourly values of solar radiation was then estimated according to the original Nimiya model (regression coefficients in Table 3.1(A).) with measured daily mean temperature, hourly sunshine duration, and daily sunshine ratio for Beijing, 2017. The regression coefficients in the original Nimiya model was general for locations in Japan since it was obtained based on 8 locations selected with high regression accuracy in Japan. However, it may not be suitable for locations in China because of different geography and atmospheric conditions.

The regression coefficients in the original Nimiya model were subsequently calibrated based on measured meteorological data in Beijing, 2017, and the new regression coefficients were shown in Table 3.1(B). The correlations between measured and estimated values for the original and calibrated Nimiya model were shown in Fig.3.2, respectively. From Table 3.2, it can be seen that the calibrated Nimiya model has better performance than the original one for Beijing, with the RMSE of 94.53 W/m^2, which was reduced by 8.43%.

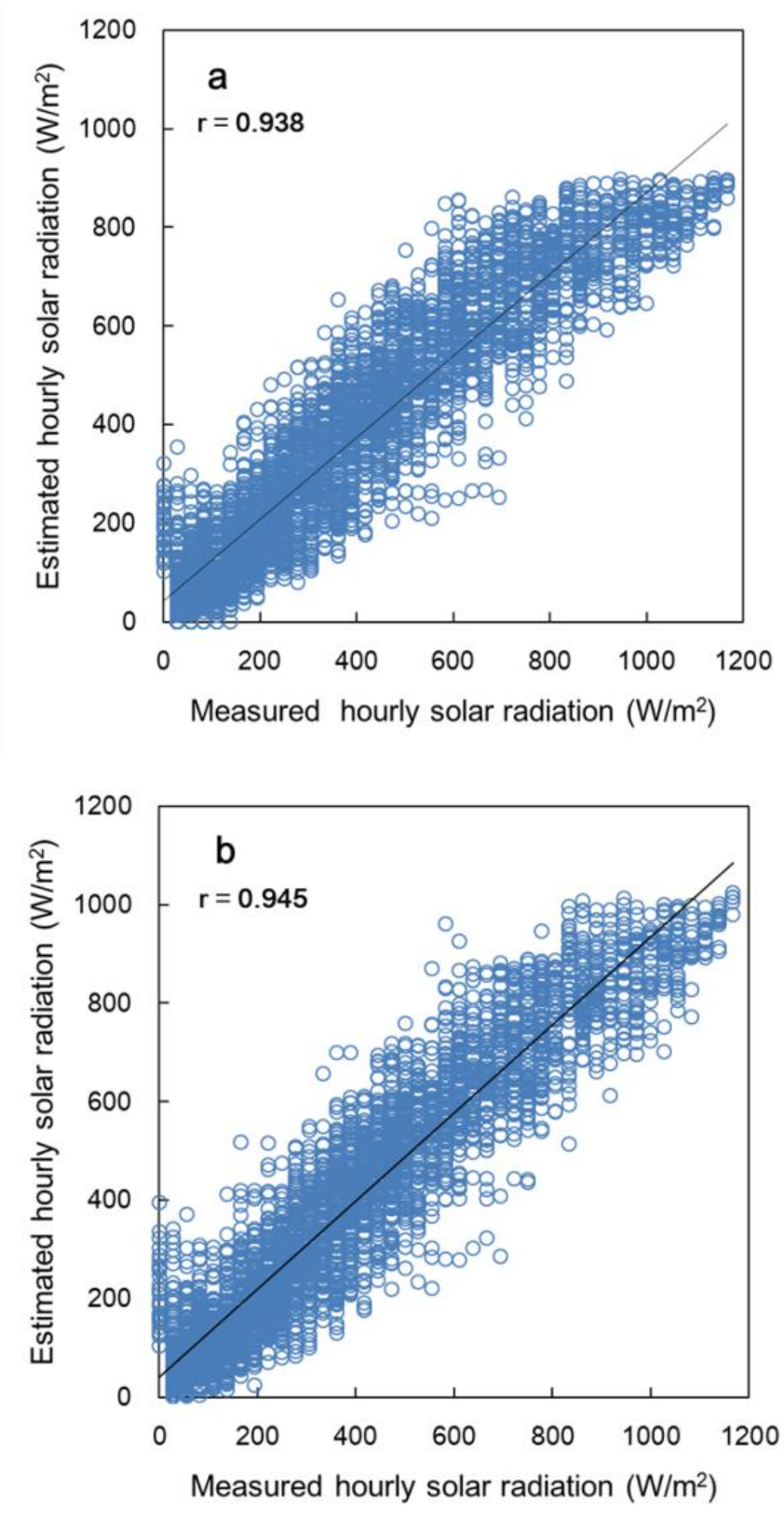

Fig.3.2 Correlation between measured and estimated hourly solar radiation for Beijing, 2017, under all-sky conditions: (a) original Nimiya model; (b) calibrated Nimiya model. The sampling number is 4086.

3.3.3 Modification of Nimiya model for Beijing

In the process of regression analysis using measured solar radiation and meteorological parameters for Beijing, we found out that the hourly solar radiation had a better correlation with the three-hour temperature difference than that with the daily mean temperature. It can be clearly shown in Fig.3.3 that the correlation coefficient of hourly solar radiation and three-hour temperature difference was 0.48, which was better than that of hourly solar radiation and daily mean temperature (r=0.22). Therefore, we modified Eq. (3.14) of the original Nimiya model by replacing the daily mean temperature (T_{daily}) with the three-hour temperature difference (T_n-T_{n-3}). The modified formula was Eq. (3.17) and the new regression coefficients of this modified Nimiya model for Beijing were shown in Table 3.1(C).

$$a_2 = d_1 + d_2 \cdot SD_{ratio} + d_3 \cdot (T_n - T_{n-3}) \tag{3.17}$$

where, SD_{ratio} is the daily sunshine ratio; T_n, T_{n-3} are the temperatures at n and n-3 hours, respectively (℃).

Table 3.1 Regression coefficients of different forms of the Nimiya model.

	a_1			b_1	a_2			b_2
	c_1	c_2	c_3		d_1	d_2	d_3	
A	0.1312	0.1762	0.0853	0.00586	0.7696	0.0740	-0.00231	-0.2889
B	0.0108	0.2730	0.2172	0.1256	0.6691	0.3585	-0.0030	-0.4719
C	0.0324	0.2782	0.1966	0.1038	0.5211	0.3456	0.0147	-0.3376

A: original Nimiya model for locations in Japan; B: calibrated Nimiya model for Beijing, 2017; C: modified Nimiya model for Beijing, 2017.

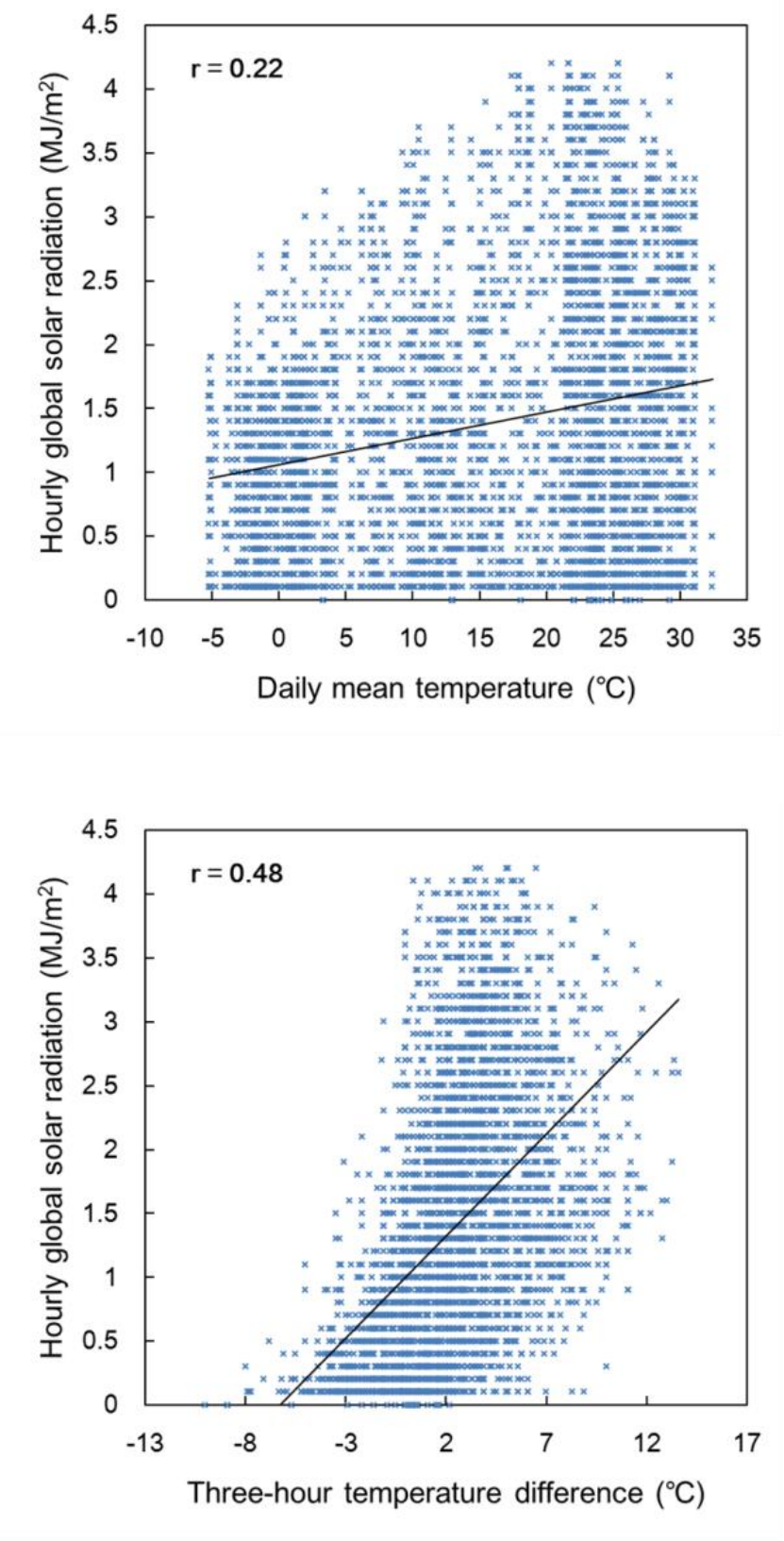

Fig.3.3 Correlation between measured hourly solar radiation and daily mean temperature or three-hour temperature difference for Beijing, 2017.

The correlation between the measured and estimated solar values using the modified Nimiya model was shown in Fig.3.4 for Beijing. Then the performance of the modified Nimiya model for Beijing was compared with the original and the calibrated Nimiya model based on statistical evaluation. From Table 3.2, It can be seen that the modified Nimiya model had the best performance with the correlation coefficient of 0.948 and the RMSE of 92.08 W/m^2; however, more locations of China were also needed for comparison in further research.

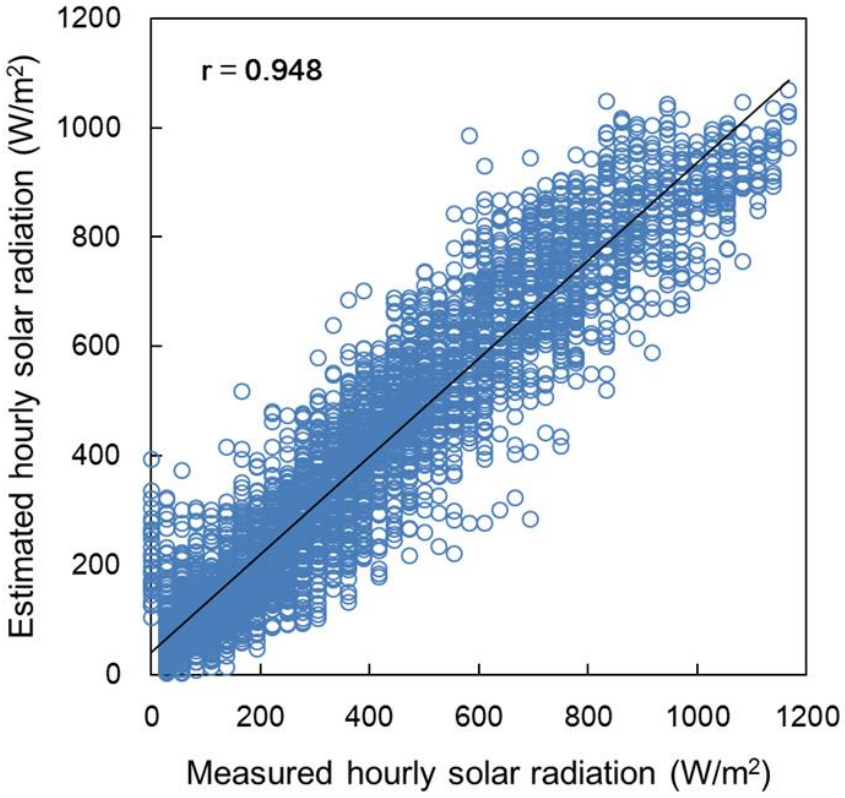

Fig.3.4 Correlation between measured and estimated hourly solar radiation for Beijing, 2017, under all-sky conditions. The sampling number is 4086.

Table 3.2 Statistical results for the original, calibrated and modified Nimiya model, Beijing, 2017

	Original Nimiya model	Calibrated Nimiya model	Modified Nimiya model
r	0.938	0.945	0.948
RMSE	103.23	94.53	92.08
MBE	-22.87	-0.03	0.03
t-statistic	14.52	0.02	0.02

Sampling number: 4086

3.4 The hourly solar model considering the hourly sunshine duration

3.4.1 Zhang model

The empirical models which utilized the relationship between solar radiation and general meteorological elements (temperature, relative humidity, daily sunshine hours) were widely used in the world. However, a large number of these existing empirical models were suitable for calculating the daily values, and very few of them was suitable for the hourly values currently.

An hourly empirical model for all-sky conditions was developed by Zhang and Huang for Beijing and Guangzhou City, China [11], and this model was then modified by deleting the wind velocity parameter and recalibrated the regression coefficients by Zhang based on the regression analysis and the measured hourly solar data at 24 locations [48]. Chang and Zhang recently improved the performance of the Zhang model by decomposing the daily solar values into hourly values according to the hourly/daily radiation ratio [59]. The accuracy of the Zhang model had been evaluated by many previous studies [40-42] in different regions, and the detailed formulas were expressed as follows:

$$I_{he} = \{I_{sc} \cdot \sin(h) \cdot [C_0 + C_1 \cdot CC + C_2 \cdot CC^2 + C_3 \cdot (T_n - T_{n-3}) + C_4 \cdot \varphi] - d\}/k \quad (3.18)$$

where, I_{he} is the estimated hourly solar radiation (W/m^2); I_{sc} is the solar constant, 1367 W/m^2; h is the solar altitude angle (°); CC is the total cloud cover in tenth; T_n, T_{n-3} are the temperatures at n and $n-3$ hour, respectively (^{0}C); φ is the relative humidity (%); C_0, C_1, C_2, C_3, C_4, d, k are the regression coefficients as shown in Table 3.3.

$$\sin(h) = \sin L \cdot \sin \delta + \cos L \cdot \cos \delta \cdot \cos h_s \tag{3.19}$$

where, L is latitude of the location(°); h_s is solar hour angle (°); δ is solar declination angle (°).

Table 3.3 Regresstion coefficients in Zhang model for Beijing, China.

C_0	C_1	C_2	C_3	C_4	d	k
0.6584	0.4864	-0.6647	0.0203	-0.0039	36.6114	0.9300

3.4.2 The improved model

The routine meteorological parameters used for Zhang model were obtained from ISD dataset, which had data records for more than 1000 Chinese meteorological stations; however, the cloud cover in ISD dataset was not recorded as numerical values but as description words such as clear, scattered, broken, overcast, obscured and partial obscured. Zhang et al. establishing the corresponding relations between them and converted the description words into corresponding numerical values of the cloud cover in the previous study [12]. The accuracy of these conversion values of cloud cover may be lower than the directly measured values and the hourly sunshine duration may indirectly reflect the weather conditions, mainly cloudiness on solar radiation, therefore, a new model was proposed by replacing the cloud cover parameter with hourly sunshine duration in the Zhang model for all-sky conditions.

It was worthy to note that there was polynomial correlation between hourly solar radiation and cloud cover parameter in the Zhang model; however, there was no particular difference between the linear correlation and polynomial correlation for the

hourly sunshine duration parameter based on regression analysis (shown in Fig.3.5). Therefore, the linear correlation was employed in the new proposed model for simplicity. The detailed formulas of the new model were shown as follows:

$$I_{he} = I_{sc} \cdot \sin(h) \cdot \left(e_0 + e_1 \cdot SD_{hourly} + e_2 \cdot (T_n - T_{n-3}) + e_3 \cdot \varphi\right) + e_4 \quad (3.20)$$

where, I_{sc} is solar constant, 1367 W/m^2; SD_{hourly} is the hourly sunshine duration (h); e_0, e_1, e_2, e_3, e_4 are regression coefficients as shown in Table 3.4.

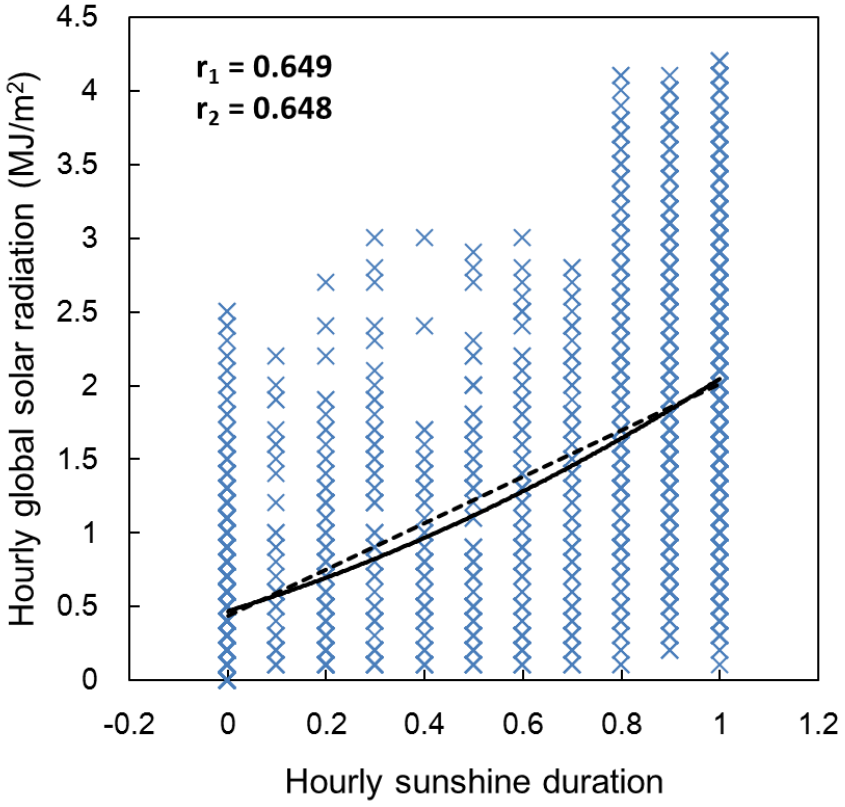

Fig.3.5 Correlation between hourly solar radiation and hourly sunshine duration for Beijing, 2017. r_1: polynomial correlation coefficient; r_2: linear correlation coefficient.

Table 3.4 Regression coefficients in new proposed model for Beijing, China.

e_0	e_1	e_2	e_3	e_4
0.5360	0.3483	0.0027	-0.0041	-23.8598

The performance of the new proposed model was much better than that of the original Zhang model for Beijing. It was shown in Table 3.5 that the RMSE of the new proposed model was 84.59 W/m^2, which was reduced by 33.88% compared to the original Zhang model. The hourly values of solar radiation were underestimated by the Zhang model for the negative value of MBE. The comparisons of measured and estimated values between the Zhang model and the new proposed model were shown in Fig.3.6 and the performance of the proposed model for some consecutive days was shown in Fig.3.7. Through the above comparison, it can be proved that the hourly sunshine duration parameter was effective for employing in solar models under all-sky conditions.

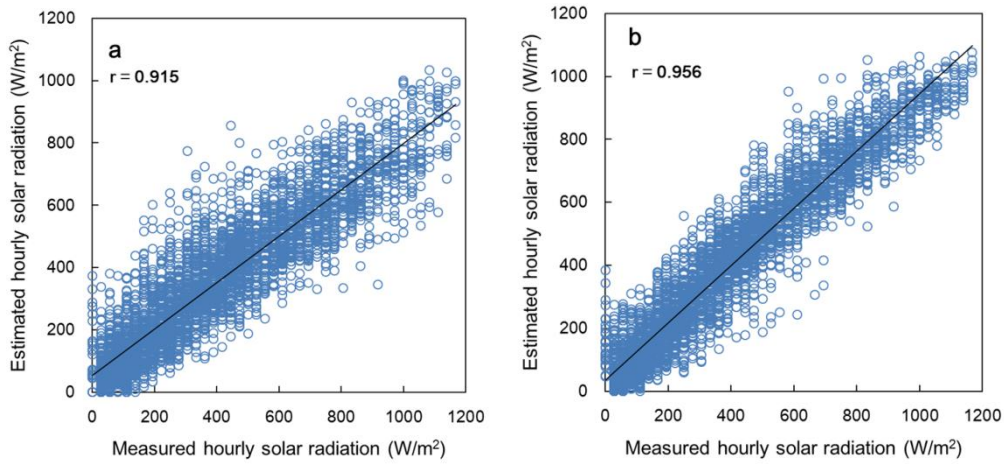

Fig.3.6 Correlation between measured and estimated hourly solar radiation for Beijing, 2017. (a) Zhang model; (b) new proposed model.

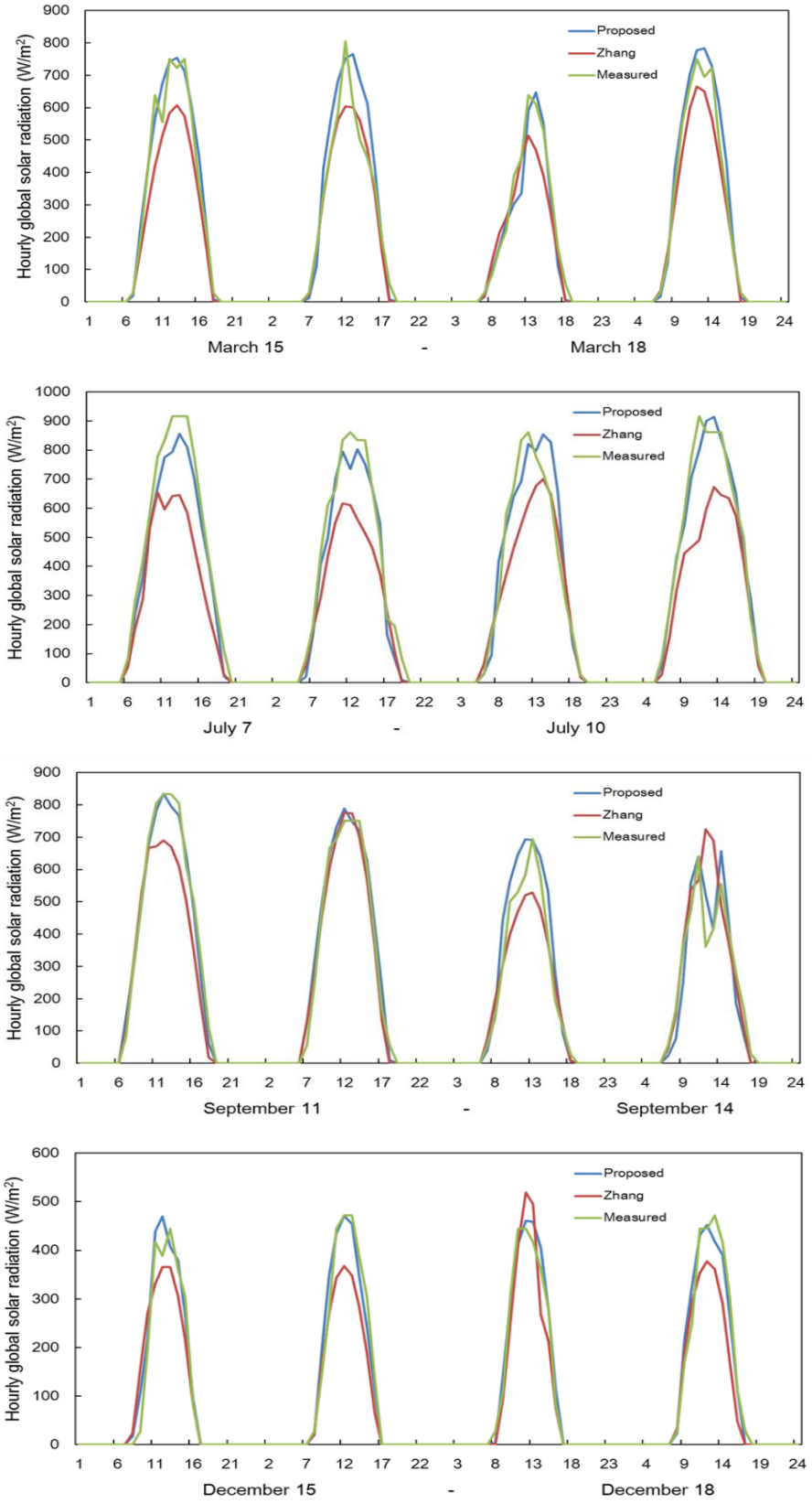

Fig.3.7 Example of the comparison of measured and estimated hourly solar radiation for Beijing, 2017 under all-sky conditions. Time is LST.

Table 3.5 Statistical results for the original Zhang model and new proposed model, Beijing, 2017

	Original Zhang model	New proposed model
r	0.915	0.956
RMSE	127.94	84.59
MBE	-45.50	0.37
t-statistic	24.32	0.28

3.5 Discussion

3.5.1 Performance of hourly solar models for Beijing

The proposed model in this study had better performance with a higher correlation coefficient (0.956) and lower RMSE (84.59 W/m^2) for Beijing compared with the modified Nimiya model. Since calculation formulas of the Nimiya model were complicated, one of the greater advantages of this proposed model is that it is very simple and easy to apply. The most significant parameter in this proposed model was the hourly sunshine duration, which was readily accessible for locations having daily sunshine duration records; the daily sunshine duration was used widely in many empirical solar models such as Angstrom-Prescott model and the hourly sunshine duration should be considered more in future research.

Numerous empirical models were employed in calculating the daily solar values in China currently; while the hourly values were paid little attention since estimating the hourly values was more difficult. The existing solar models focused on daily, monthly average daily and hourly values were reviewed and compared by Zhang et al. [49], and the accuracies of different types of solar models was also concluded. One of the conclusions was that the RMSEs of the hourly solar models were in the range of 88.33 - 142.22 W/m^2. Compared with this summary, the proposed model in this study had very well performance with more precise.

3.5.2 Daily and Monthly values of solar radiation

The proposed model in this study also can be applied to calculate the daily values by adding up the hourly values for each day. The comparison between the measured and estimated daily solar values was shown in Fig.3.8. It can be seen that the daily variable tendencies of measured and estimated solar radiations were consistent. Furthermore, based on the summary that made by Zhang et al. [49] in the reviews of daily solar models, the RMSEs of the existing daily sunshine duration-based models were in the range of 1.11 - 4.50 MJ/(m^2day), while the RMSE of this proposed model was 2.06 MJ/(m^2day). Therefore, it was indicated that the proposed model also performed very well for calculating the daily solar values. The monthly values of solar radiation also can be calculated by adding up the daily values for each month and the comparison results were shown in Fig.3.9.

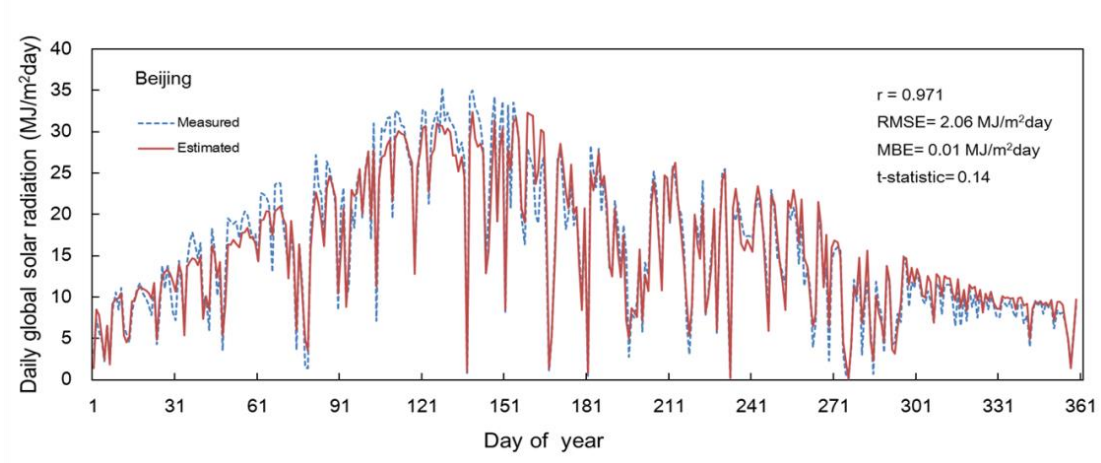

Fig.3.8 Comparison between measured and estimated daily values of solar radiation for Beijing, 2017.

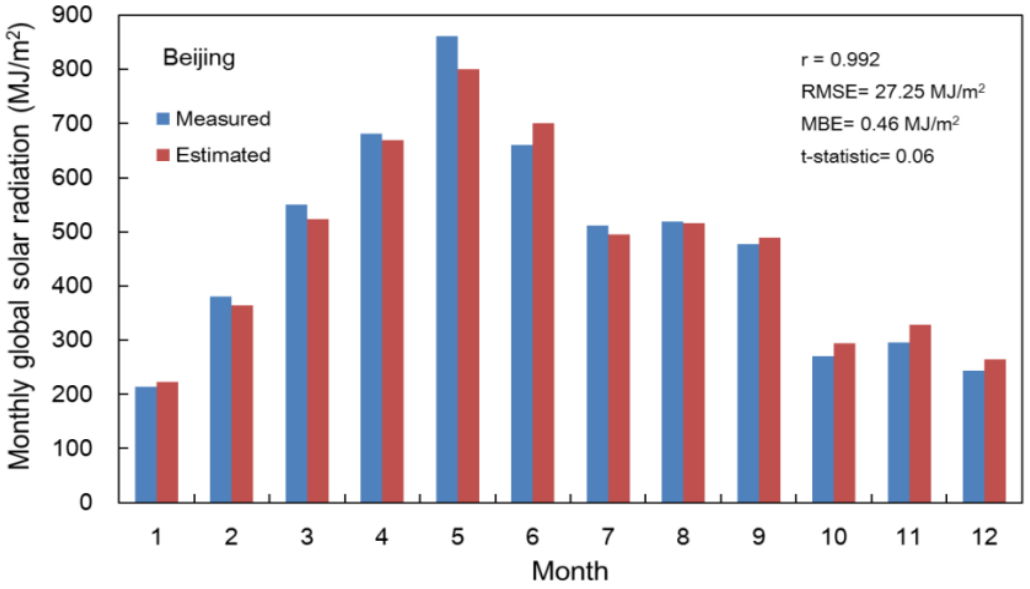

Fig.3.9 Comparison between measured and estimated monthly values of solar radiation for Beijing, 2017.

3.5.3 Hourly solar radiation models for clear-sky or all-sky conditions

Almost all of the hourly solar models were established for clear-sky conditions, which assumed that there was no effect of weather conditions on solar radiation and usually considered the atmospheric attenuation parameter. The clear-sky solar models could estimate the upper limit of surface solar radiation for one location and these practical maximum values of solar radiation were valuable for some applications, for example, the maximum output potential of solar power generation was important for designing photovoltaic (PV) system under clear-sky conditions. Antonanzas-Torres et al. reviewed and evaluated 70 clear-sky models for offering advice on choosing the appropriate models [62]. However, only knowing the maximum values of solar radiation in one location may not be enough for some applications, the mean values of solar radiation with long-term variations under all-sky conditions was also very necessary, for example, the building thermal simulation needed the Typical Meteorological Year (TMY) dataset which included long-term hourly solar values under all-sky conditions.

As far as we know, there were almost no hourly solar models for all-sky conditions in China currently; therefore, the proposed model with consideration of hourly sunshine duration in this study would be meaningful for some applications. However, the measured data for more locations are also needed to evaluate the model performance in further study.

3.6 Summary

In this study, the hourly sunshine duration was introduced and employed in empirical solar models for all-sky conditions. Two existing hourly solar models: Nimiya model and Zhang model were analyzed and improved for Beijing. Moreover, the new hourly solar model was developed using hourly sunshine duration under all-sky conditions. The main conclusions of this study are as follows:

(1) The hourly sunshine duration parameter was very effective for estimating solar radiation under all-sky conditions, which should be considered more in future empirical solar models.

(2) The Nimiya model was modified by replacing the daily mean temperature with the three-hour temperature difference, the performance of which was better than the original Nimiya model for Beijing.

(3) The proposed model in this study had better performance with a higher correlation coefficient (0.956) and lower RMSE (84.59 W/m^2) compared with the modified Nimiya model for Beijing.

(4) The proposed model also performed very well for estimating the daily solar values by adding up the hourly values for each day.

As a case study, the regression coefficients of the proposed model were only calculated for Beijing. More work is needed to apply this model to more locations in further research.

CHAPTER 4

Modeling of the atmospheric radiation and radiative cooling potential in China

Nomenclature

$R_{\downarrow}$	downward longwave radiation (W/m^2)
$R_{\uparrow}$	ground surface longwave radiation (W/m^2)
$R_{cooling}$	radiative cooling potential (W/m^2)
T_a	ambient dry-bulb temperature (K)
T_s	ground surface temperature (K)
e_a	water vapor pressure (hPa)
φ	relative humidity (%)
σ	Stefan-Boltzmann constant, $5.67 \cdot 10^{-8}$ (W·m^{-2}·K^{-4})
a, b, c	empirical coefficients
clf'	cloud fraction
clf	cloud modification factor
S	ratio of the measured solar radiation to the clear-sky radiation
K_t	clearness index
H_c	clear-sky solar radiation (W/m^2)
c_1, c_2, f_1, f_2	altitude correction coefficients
I_0	extraterrestrial irradiance (W/m^2)
h	solar altitude angle (°)
AM	air mass
T_L	Linke turbidity factor
Alt	altitude (m)
DOY	Julian day of the year
H_m	hourly measured solar radiation (W/m^2)
H_0	hourly extraterrestrial solar radiation (W/m^2)
G_{sc}	solar constant, 1367 W/m^2
L	local latitude (°)
δ	declination angle (°)
ω_1, ω_2	hour angle at the beginning and end of the time interval (°)

4.1 Introduction

The downward longwave (LW hereafter) radiation is a significant factor in energy balance on the earth surface, as well as in the design of building radiative cooling system [63]. The LW radiation is usually observed at very few stations, while the routine meteorological parameters such as temperature and relative humidity are easy to access; therefore, developing models to estimate LW radiation is necessary based on the available routine meteorological elements.

The LW radiation originates from gases composed the atmosphere such as water vapor, carbon dioxide and ozone, among which the water vapor plays a major role. Moreover, 90% of the LW radiation at ground level comes from the first 800-1600 m above the earth surface [64]. Therefore, the water vapor pressure and the ambient temperature of earth surface are closely related to LW radiation. In addition, the cloud and the relative humidity can also affect LW radiation [65-67].

Currently, there are three main methods to estimate the LW radiation. The first type is the empirical model [68], which established the relationship between the measured LW radiation and routine meteorological parameters such as the water vapor pressure and ambient temperature. The second type is the physical model, which is based on the atmospheric radiative transfer phenomena, such as the LOWTRAN [69] and MODTRAN [70]. However, the detailed profiles of atmospheric constituents utilized in the model are not often available. The last type is the remote sensing method, which can estimate the LW radiation in large-scale based on the retrieval of some meteorological parameters such as the earth surface temperature [71]. However, the estimation accuracy for specific location needs to be improved.

The empirical models are widely used for estimating the LW radiation in the world. Brunt [72] proposed a model based on the water vapor pressure under clear-sky conditions for California. Some models were established [73-76] subsequently just based on the ambient temperature and water vapor pressure for different locations. Then other meteorological parameters such as dew point temperature, relative

humidity were used for establishing LW radiation models [77-79]. The empirical models mentioned above were only suitable for clear-sky conditions, while the existence of clouds could increase LW radiation [64]. Moreover, for the design of building passive cooling system, the data utilized should reflect the long-term change in LW radiation under all-sky conditions, especially for the nighttime. Therefore, it is also significant to develop empirical models for all-sky conditions. So far, very few models can be used for all-sky conditions, though Crawford and Duchon [80] proposed a model under all-sky conditions by considering the cloud cover.

Few studies were conducted to estimate LW radiation for China since little measured LW radiation data was available. Wang et al. [81] addressed the estimation of LW radiation using remote sensing method with the Moderate resolution imaging spectroradiometer (MODIS) data for the Tibetan Plateau region, China, but no empirical model was proposed in this study. Zhang et al. [82] estimated the LW radiation in different locations to obtain the radiative cooling potential over China, however, the calculation results were not validated due to the lack of measured LW radiation data. Therefore, it is necessary to develop the empirical models that can be utilized for meteorological and geographic conditions of China.

The primary objective of this study is to develop new empirical models of LW radiation based on the routine meteorological parameters for locations in China. To accomplish this objective, the following steps were carried out: 1) the empirical models were established between the LW radiation and the ambient temperature, water vapor pressure and relative humidity under all-sky conditions, which can be classified into four cases: all day, nighttime, daytimes with and without considering cloud modification factor; 2) the proposed LW radiation models were validated using measured LW radiation in four locations of China: Changbaishan, Haibei, Qinghai and Yucheng; 3) the hourly LW radiation dataset was developed based on the typical meteorological year (TMY) dataset [13] for 351 locations in China; 4) the distribution maps of the LW radiation and the radiative cooling potential were generated over China, which can provide a valuable reference for building cooling design.

4.2 Methodology

4.2.1 Measured data

Since the routine meteorological stations do not provide the LW radiation data in China, the LW radiation data in this study was obtained from the AsiaFlux Database [83]. Then the LW radiation (W/m^2), solar radiation (W/m^2), water vapor pressure (hPa), ambient temperature (K), relative humidity (%) with one-hour intervals were selected from the AsiaFlux Database in four locations of China (Changbaishan, Haibei, Qinghai and Yucheng, as shown in Fig.4.1). The detailed geographic information of the four locations, as well as the time period of the measurement was summarized in Table 4.1. The measured data was divided into two parts according to its use: one was used for developing new LW radiation models; the other was used for validating the proposed models.

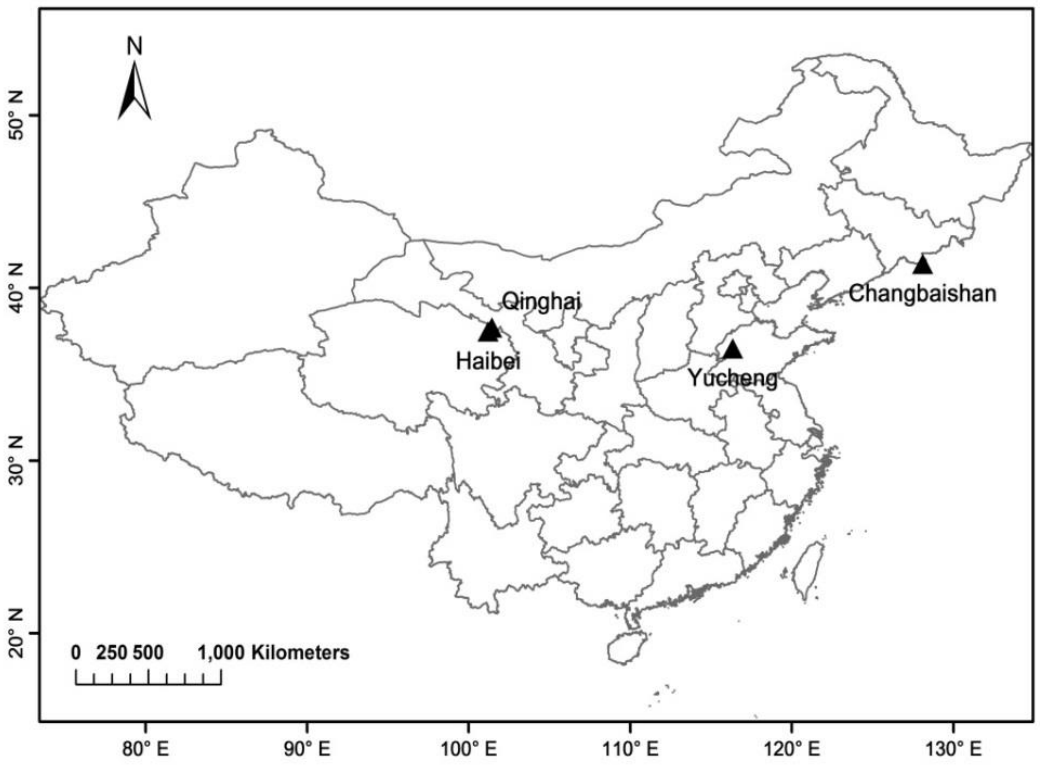

Fig.4.1 Distribution of the four observation locations in China.

Table 4.1 Information related to the four observation locations.

No.	Location	Latitude (°N)	Longitude (°E)	Elevation (m MSL)	Period-a	Period-b
1	Changbaishan	41.40	128.10	736	2003,2004	2005
2	Haibei	37.48	101.20	3200	2004	2003
3	Qinghai	37.61	101.33	3250	2002,2003	2004
4	Yucheng	36.50	116.34	28	2003,2004	2005

*Period-a: used for model development.

Period-b: used for model validation.

4.2.2 Development of new models

Because measured LW radiation data are not available in the routine meteorological stations, empirical models of the LW radiation were established based on different meteorological parameters from previous studies, where, ambient dry-bulb temperature and water vapor pressure were commonly used.

In this study, the correlation analysis was firstly conducted between the LW radiation and various meteorological parameters. The correlations between the LW radiation and the different meteorological parameters were shown in Fig. 2 and Fig. 3 (taking Yucheng as an example). It can be seen that the LW radiation has a strong correlation with the ratio of the water vapor pressure to the ambient temperature, which complies with the natural logarithm function. Based on the ideal gas state equation, the ratio of the water vapor pressure to the ambient temperature can represent the water vapor density and with the increase of that, the LW radiation will also increase. Moreover, the LW radiation also has a correlation with relative humidity. Therefore, the ambient dry-bulb temperature (T_a), water vapor pressure (e_a) and relative humidity (%) were employed in developing the new models as shown in Eq. (1).

The LW radiation during the daytime is necessary for the energy balance application, while that during the nighttime is more favorable for the building passive cooling system [65]. Therefore, the empirical coefficients in Eq. (4.1) were calculated

through regression analysis for the all day, nighttime and daytime, respectively.

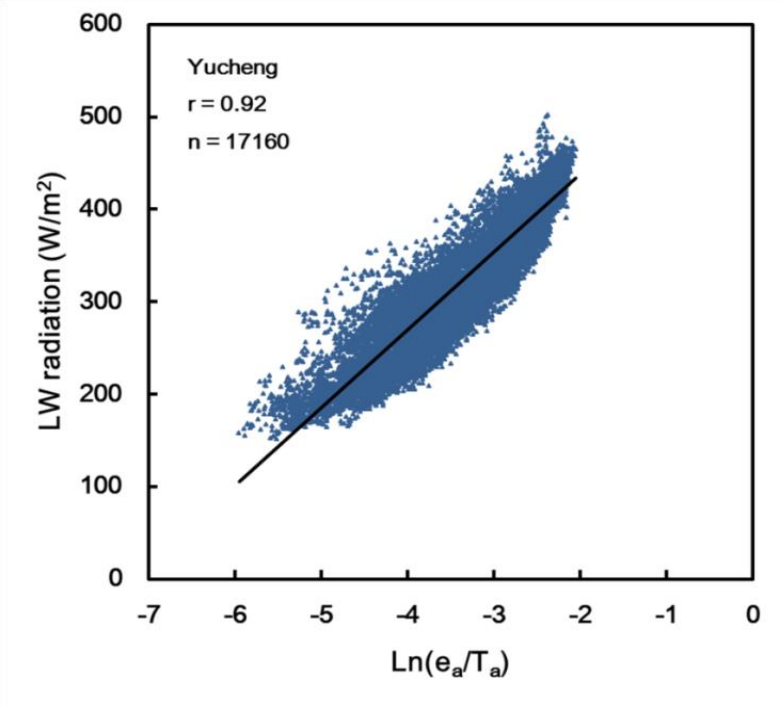

Fig.4.2 Correlation between LW radiation and $\ln(e_a/T_a)$, Yucheng, 2003-2004. n is the sampling number.

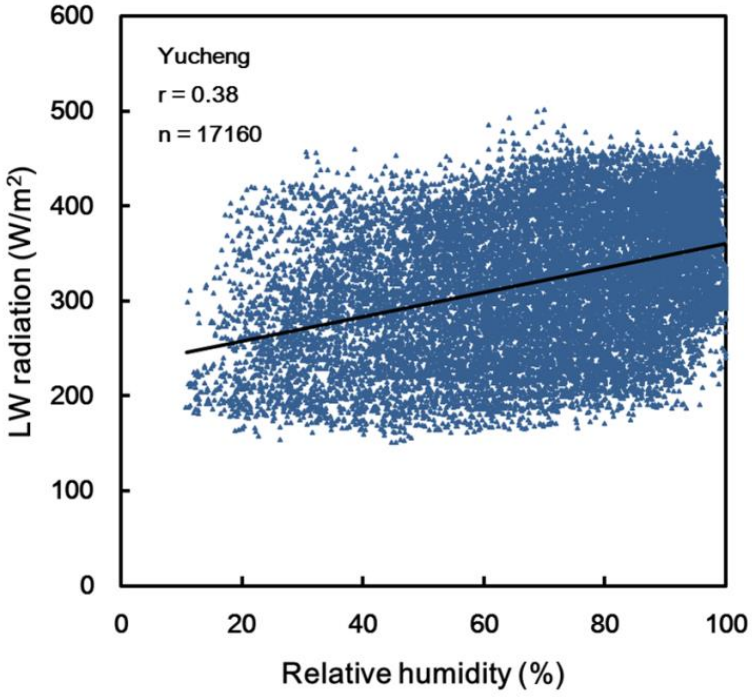

Fig.4.3 Correlation between LW radiation and the relative humidity, Yucheng, 2003-2004. n is the sampling number.

$$R_{\downarrow} = \sigma \cdot (T_a)^4 \cdot \left[a \cdot \ln\left(\frac{e_a}{T_a}\right) + b \cdot \varphi + c\right] \quad (4.1)$$

where, $R_{\downarrow}$ is the downward longwave radiation (W/m^2) under all-sky conditions; T_a is the ambient dry-bulb temperature (K); e_a is the water vapor pressure (hPa); φ is the relative humidity (%);σ is the Stefan-Boltzmann constant, $5.67 \cdot 10^{-8}$ (W·m^{-2}·K^{-4}); *a, b, c* are the empirical coefficients.

Clouds can increase the LW radiation up to 34% with 100% cloud cover of low (< 2 km) clouds [66], therefore it should be considered in the LW radiation model. Crawford and Duchon [80] proposed an LW radiation model for all-sky conditions with a cloud fraction instead of the cloud cover data, where the cloud fraction (in Eq. (4.2)) was defined as the ratio of the measured solar radiation to the clear-sky radiation.

In this study, the cloud cover data in the four locations of China was unavailable, while the global solar radiation was measured in the daytime. The clearness index which defined as the ratio of the measured solar radiation to the extraterrestrial solar radiation (Eq. (4.4)) can be regarded as an indicator of cloud cover [84]. Therefore, for the daytime, another LW radiation model (Eq. (4.6)) was proposed with a cloud modification factor based on the clearness index.

$$clf' = 1 - S \quad (4.2)$$

$$clf = 1 - K_t \quad (4.3)$$

where, clf' is the cloud fraction in Crawford and Duchon model; *clf* is the cloud modification factor in this study; *S* is the ratio of the measured solar radiation to the clear-sky radiation; K_t is the clearness index.

The Ineichen clear-sky global solar radiation in Eq. (4.2) can be expressed as [65,

88-90],

$$H_c = c_1 \cdot I_0 \cdot \sin(h) \cdot e^{0.01 \cdot AM^{1.8} - c_2 \cdot AM \cdot (f_1 + f_2 \cdot (T_L - 1))} \quad (4.4)$$

where, H_c is the clear-sky solar radiation (W/m^2); c_1, c_2, f_1 and f_2 are altitude correction coefficients; I_0 is the extraterrestrial irradiance (W/m^2); h is the solar altitude angle(°); AM is the air mass; T_L is the Linke turbidity factor.

The altitude correction coefficients are:

$$C_1 = 5.09 * 10^{-5} \cdot Alt + 0.868 \quad (4.5)$$

$$C_2 = 3.92 * 10^{-5} \cdot Alt + 0.0387 \quad (4.6)$$

$$f_1 = e^{-Alt/8000} \quad (4.7)$$

$$f_2 = e^{-Alt/1250} \quad (4.8)$$

where, Alt is the altitude (m).

The extraterrestrial irradiance I_0 is expressed as,

$$I_0 = 1367 * \left(1 + 0.033 \cos\left(\frac{2\pi}{365} \cdot DOY\right)\right) \quad (4.9)$$

where, DOY is the Julian day of the year.

The air mass AM is expressed as a function of solar altitude angel,

$$\mathrm{AM} = \frac{1}{\sin(h) + 0.50572 * (h + 6.07995)^{-1.6364}} \quad (4.10)$$

The Linke turbidity factor T_L is extracted from monthly Link turbidity images [91].

The clearness index can be calculated as follows:

$$K_t = \frac{H_m}{H_0} \tag{4.11}$$

$$H_0 = \frac{12 \cdot 3600}{\pi} \cdot G_{sc} \cdot \left(1 + 0.033\, cos \frac{360n}{365}\right) \cdot \left[cos\, L \cdot cos\, \delta \cdot (sin\, \omega_2 - sin\, \omega_1) + \frac{\pi(\omega_2 - \omega_1)}{180} \cdot sin\, L \cdot sin\, \delta\right] \tag{4.12}$$

where, H_m is the hourly measured solar radiation (W/m^2); H_0 is the hourly extraterrestrial solar radiation (W/m^2) [61]; G_{sc} is the solar constant, 1367 W/m^2; n is the Julian day of the year; L is the local latitude (°); δ is the declination angle (°); ω_1, ω_2 are the hour angle at the beginning and end of the time interval (°).

The proposed model with cloud modification factor for the daytime was expressed as follows:

$$R_{\downarrow} = \sigma \cdot (T_a)^4 \cdot \left[clf + (1 - clf) \cdot \left(a \cdot \ln\left(\frac{e_a}{T_a}\right) + b \cdot \varphi + c\right)\right] \tag{4.13}$$

where, *clf* is the cloud modification factor in Eq. (4.3).

4.2.3 Existing LW radiation models

Two existing LW radiation models developed for all-sky conditions were selected to compare with our proposed models.

(1) Sridhar model

Brutsaert [79] proposed a model based on the water vapor pressure and ambient

temperature for clear-sky condition, Sridhar et al. [85] then calibrated the Brutsaert model for four locations representing different geographical and climatological conditions. Therefore, the Sridhar model can be used for all-sky conditions (clear and cloudy) (Eq. (4.14)), which was compared with our proposed model for the all day in this study.

$$R_{\downarrow} = \sigma \cdot (T_a)^4 \cdot \left[1.31 \cdot \left(\frac{e_a}{T_a}\right)^{\frac{1}{7}}\right] \tag{4.14}$$

(2) Crawford and Duchon model

As mentioned above, Crawford and Duchon model was used for all-sky conditions with consideration of the cloud fraction, which can be expressed by Eq. (4.15):

$$R_{\downarrow} = \sigma \cdot (T_a)^4 \cdot \left\{clf' + (1 - clf') \cdot \left(1.22 + 0.06 \cdot sin\left[(month + 2) \cdot \left(\frac{\pi}{6}\right)\right]\right) \cdot \left(\frac{e_a}{T_a}\right)^{\frac{1}{7}}\right\} \tag{4.15}$$

where, *month* is the number of months in a year; *clf'* is the cloud fraction in Eq. (4.2).

4.2.4 Assessment metrics

The values of R^2 and RMSE were used to evaluate the accuracy of the proposed and existing LW radiation models. These indicators can be calculated as follows:

$$R^2 = 1 - \frac{\sum_{i=1}^{n}\left(LW_{i,m} - LW_{i,c}\right)^2}{\sum_{i=1}^{n}\left(LW_{i,m} - LW_{m,avg}\right)^2} \tag{4.16}$$

$$\text{RMSE} = \sqrt{\frac{1}{n}\sum_{i=1}^{n}\left(LW_{i,m} - LW_{i,c}\right)^2} \tag{4.17}$$

where, R^2 is the coefficient of determination; *RMSE* is the root mean square error;

$LW_{i,m}$ and $LW_{i,c}$ are the i th measured and estimated values, respectively (W/m^2); $LW_{m,avg}$ is the average of the measured values (W/m^2); n is the total number of measurements.

4.2.5 Radiative cooling potential

Radiative cooling is a thermal process, the heat from which is transferred from a high-temperature object to a low-temperature one through emitting longwave radiation. For the buildings, the radiative cooling is a kind of passive cooling technique which uses radiative heat transfer effect to cool the building facing a colder atmosphere [64]. The building envelope can be cooled by radiative heat transfer especially during nighttime since it can obtain more heat from solar radiation during daytime. Radiative cooling can reduce the energy consumption for building cooling in summer; therefore, it is necessary to calculate the radiative cooling potential of different locations in summer.

In this study, the radiative cooling potential of the ground surface was defined as the difference between the longwave radiation emitted by the ground surface and the atmospheric downward longwave radiation (Eq. (4.18)) [82]. Assuming that the ground surface temperature (T_s) in Eq. (4.19) is equal to the ambient temperature (T_a) for simplicity ($T_s = T_a$), then the radiative cooling potential can be calculated as follows:

$$R_{cooling} = R_{\uparrow} - R_{\downarrow} \tag{4.18}$$

$$R_{\uparrow} = \sigma \cdot (T_s)^4 \tag{4.19}$$

where, $R_{cooling}$ is the radiative cooling potential (W/m^2); $R_{\uparrow}$ is the ground surface longwave radiation (W/m^2); $R_{\downarrow}$ is the LW downward radiation (W/m^2); T_s is the ground surface temperature (K).

4.3 Results and discussion

4.3.1 Empirical coefficients

The empirical coefficients in Eq. (4.1) were firstly calculated using the measured LW radiation, the ambient dry-bulb temperature, the water vapor pressure and the relative humidity based on the regression analysis. Regression analysis was conducted on each of the four locations respectively, as well as on the whole dataset (All locations) combining the four locations. The empirical coefficients of Eq. (4.1) for the all day, nighttime and daytime were shown in Table 4.2, 4.3 and 4.4, respectively.

Table 4.2 Empirical coefficients in Eq. (4.1) for the all day.

No.	Location	a	b	c	r	RMSE (W/m^2)	n
1	Changbaishan	0.080	0.0013	1.037	0.92	30.28	14040
2	Haibei	0.101	0.0026	1.036	0.88	32.10	8688
3	Qinghai	0.080	0.0015	1.032	0.89	27.88	15216
4	Yucheng	0.080	0.0011	1.022	0.92	28.12	17160
5	All locations	0.080	0.0011	1.029	0.92	31.54	55104

*n: sampling number.

Table 4.3 Empirical coefficients in Eq. (4.1) for the nighttime.

No.	Location	a	b	c	r	RMSE (W/m^2)	n
1	Changbaishan	0.080	0.0013	1.030	0.91	30.68	7046
2	Haibei	0.100	0.0027	1.025	0.89	30.13	4600
3	Qinghai	0.074	0.0017	1.017	0.92	24.10	7538
4	Yucheng	0.087	0.0012	1.037	0.92	28.34	8574
5	All locations	0.080	0.0014	1.026	0.92	29.87	27758

*n: sampling number.

Table 4.4 Empirical coefficients in Eq. (4.1) for the daytime.

No.	Location	a	b	c	r	RMSE (W/m^2)	n
1	Changbaishan	0.045	0.0025	0.837	0.93	27.68	6994
2	Haibei	0.052	0.0038	0.762	0.86	32.50	4088
3	Qinghai	0.037	0.0029	0.778	0.87	28.12	7678
4	Yucheng	0.093	0.0012	1.054	0.93	28.25	8586
5	All locations	0.086	0.0014	1.044	0.92	31.26	27346

*n: sampling number.

For the daytime, if cloud cover or solar radiation data was unavailable for one location, the Eq. (4.1) can be employed simply with only routine meteorological parameters. To further explore the effects of clouds on LW radiation, the Eq. (4.13) was proposed with a cloud fraction parameter subsequently. The empirical coefficients of Eq. (4.13) were shown in Table 4.5.

Table 4.5 Empirical coefficients in Eq. (4.6) for the daytime with cloud modification factor.

No.	Location	a	b	c	r	RMSE (W/m^2)	n
1	Changbaishan	0.074	0.0008	0.858	0.95	23.59	6994
2	Haibei	0.111	0.0003	1.021	0.85	33.99	4088
3	Qinghai	0.103	0.0004	1.035	0.91	24.35	7678
4	Yucheng	0.139	0.0004	1.045	0.93	26.56	8586
5	All locations	0.118	0	1.033	0.93	28.67	27346

*n: sampling number.

The empirical coefficients of the four locations had a little difference with each other, in order to obtain more general LW radiation models for applying in different locations of China; they were also calculated using the whole dataset (All locations) combining the four locations. It can be seen that the correlation coefficients (r) of the whole dataset (All locations) were all very good in Table 4.2, 4.3, 4.4 and 4.5. The correlation between measured and estimated hourly LW radiation for the whole dataset was also shown in Fig.4.4.

Comparing the empirical coefficients in Table 4.4 and Table 4.5, it was worthy to notice that the values of b were very small in Table 4.5, even became zero for the whole dataset (All locations). It may be due to that the relative humidity can indirectly represent the effect of clouds on LW radiation. The relative humidity had a correlation with the cloud modification factor as shown in Fig.4.5 in this study; however, the accurate relationship between the relative humidity and the cloud cover need further investigation.

Based on the above discussion, the proposed models for four cases in this study were shown in Table 4.6, which were validated using the measured LW radiation (shown in Table 4.1) subsequently.

Table 4.6 LW radiation models for all day, daytime and nighttime.

Period	Formulation	
All day	$R_{\downarrow} = \sigma \cdot (T_a)^4 \cdot \left[0.08 \cdot \ln\left(\frac{e_a}{T_a}\right) + 0.0011 \cdot \varphi + 1.029\right]$	(4.20)
Daytime	$R_{\downarrow} = \sigma \cdot (T_a)^4 \cdot \left[0.086 \cdot \ln\left(\frac{e_a}{T_a}\right) + 0.0014 \cdot \varphi + 1.044\right]$	(4.21)
Daytime with cloud modification factor	$R_{\downarrow} = \sigma \cdot (T_a)^4 \cdot \left[clf + (1 - clf) \cdot \left(0.118 \cdot \ln\left(\frac{e_a}{T_a}\right) + 1.033\right)\right]$	(4.22)
Nighttime	$R_{\downarrow} = \sigma \cdot (T_a)^4 \cdot \left[0.08 \cdot \ln\left(\frac{e_a}{T_a}\right) + 0.0014 \cdot \varphi + 1.026\right]$	(4.23)

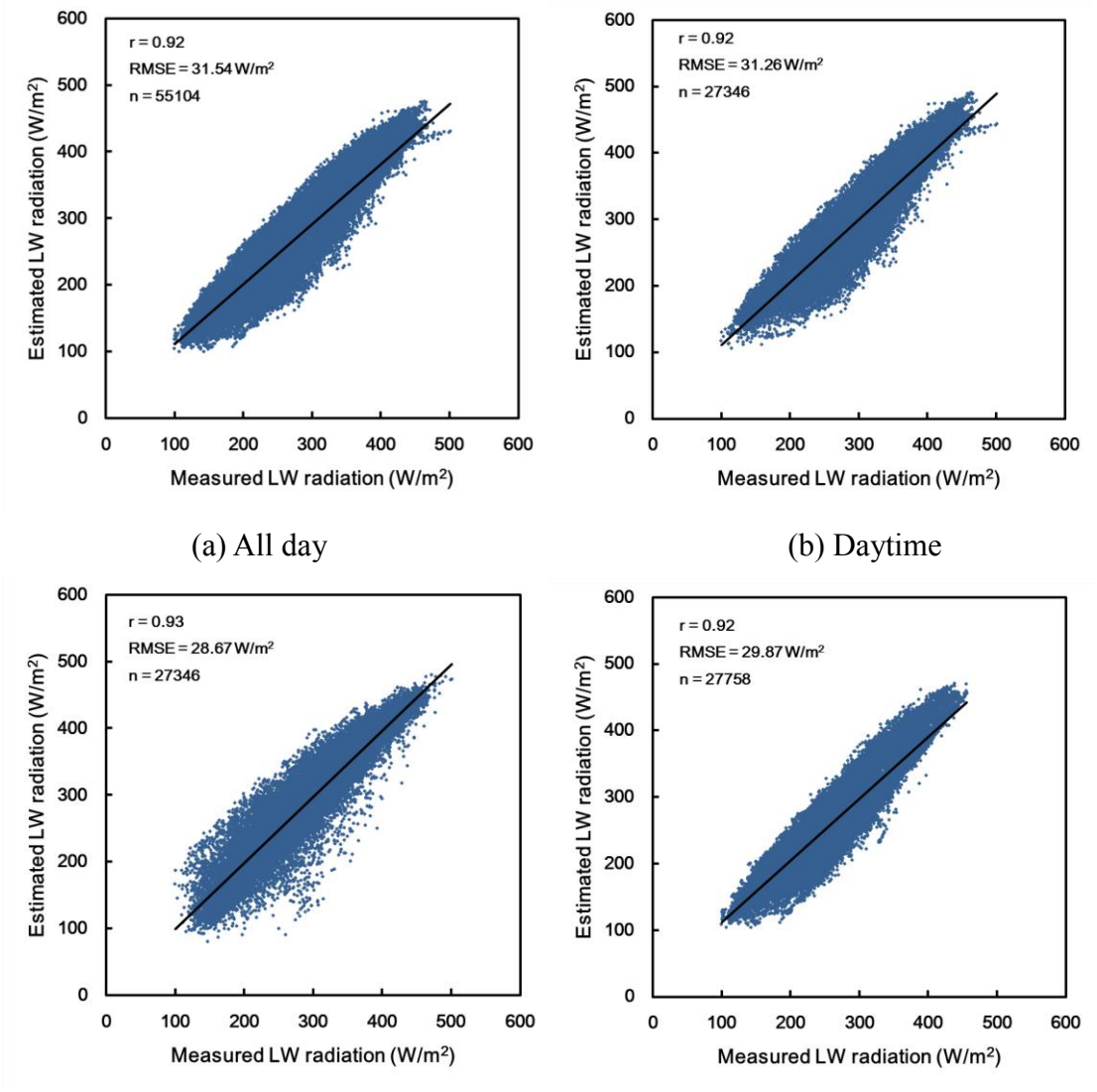

Fig.4.4 Correlation between measured and estimated hourly LW radiation using the whole dataset for four cases. n is the sampling number.

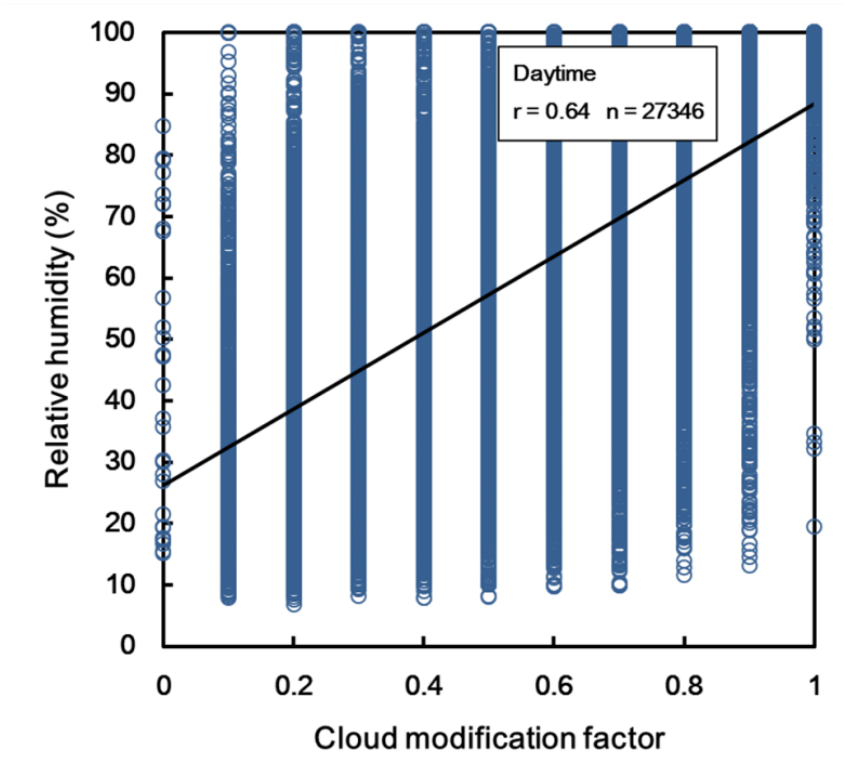

Fig.4.5 Correlation between cloud modification factor and the relative humidity during daytime periods for the whole dataset. n is the sampling number.

4.3.2 Model validation

The model validation was firstly conducted on each of the four locations respectively; then on the whole dataset (All locations) combining the four locations. The determination coefficient (R^2) and the root mean square error (RMSE) were shown for the four cases in Table 4.7, 4.8 and 4.9, respectively.

For the all day, the performance of the proposed model (Eq. (4.20)) had a little difference, among which, the Yucheng showed the best performance with the largest R^2 and smallest RMSE, while the All locations also had very good performance with R^2 of 0.86 and RMSE of 30.26 W/m^2, which means that the general proposed model is suitable for application in China.

For the nighttime, the performance of Eq. (4.23) was very good, which the RMSE of Haibei and Qinghai were both smaller than that in Table 4.7. The radiative cooling usually operates during nighttime since the solar radiation existed in the daytime,

therefore, the Eq. (4.23) was recommended to apply in calculating the radiative cooling potential for locations in China.

For the daytime, it can be seen that the performance of the proposed model was improved in Changbaishan and Haibei by adding the cloud modification factor, and the Eq. (4.22) performed better than Eq. (4.21) with R^2 of 0.87 and RMSE of 28.59 W/m^2 for the whole dataset. Therefore, Eq. (4.22) is more favorable than Eq. (4.21) if the cloud data or cloud modification factor was available. Otherwise, Eq. (4.21) was also acceptable to be applied with routine meteorological parameters only.

Table 4.7 Validation results of the proposed model (Eq. (4.20)) for the all day.

No.	Location	R^2	RMSE (W/m^2)	n
1	Changbaishan	0.86	31.33	7320
2	Haibei	0.77	35.04	4968
3	Qinghai	0.76	30.52	8352
4	Yucheng	0.90	25.39	7968
5	All locations	0.86	30.26	28608

*n: sampling number.

Table 4.8 Validation results of the proposed model (Eq. (4.23)) for the nighttime.

No.	Location	R^2	RMSE(W/m^2)	n
1	Changbaishan	0.86	31.04	3648
2	Haibei	0.83	30.20	2743
3	Qinghai	0.82	25.86	4157
4	Yucheng	0.87	27.82	4005
5	All locations	0.87	28.59	14553

*n: sampling number.

Table 4.9 Validation results of the proposed models (Eq. (4.21) and (4.22)) for the daytime.

No.	Location	R^2-a	RMSE-a (W/m^2)	R^2-b	RMSE-b (W/m^2)	n
1	Changbaishan	0.87	30.09	0.90	26.14	3672
2	Haibei	0.75	35.50	0.80	31.59	2225
3	Qinghai	0.75	29.24	0.75	29.13	4195
4	Yucheng	0.87	28.38	0.87	28.41	3963
5	All locations	0.85	30.30	0.87	28.59	14055

*a: Eq. (4.21). b: Eq. (4.22). n: sampling number.

4.3.3 Comparison with existing models

In order to better discuss the performance of the proposed LW radiation model, the proposed models were compared with some previous models. Since the existing models used for all-sky conditions were fewer compared with those for clear-sky conditions, two existing models for all-sky conditions were selected for comparison using the validation dataset (shown in Table 4.1) in this study.

For the all day, the proposed model (Eq. (4.20)) and Sridhar model (Eq. (4.14)) were both using the whole dataset (All locations) combining the four locations, and the comparison results were shown in Fig.4.6. Results showed that the proposed model performed much better than the Sridhar one with the RMSE was reduce by 17.73%. Although the Sridhar model was proposed with different geographical and climatological conditions, the new proposed model (Eq. (4.20)) was more suitable for China.

For the daytime, the proposed model (Eq. (4.22)) and the Crawford and Duchon model (Eq. (4.15)) were compared based on the whole dataset (All locations) combining the four locations. The new proposed model has better performance than the Crawford and Duchon one with smaller RMSE (shown in Fig.4.7). Therefore, it was recommended to employ for the daytime in China.

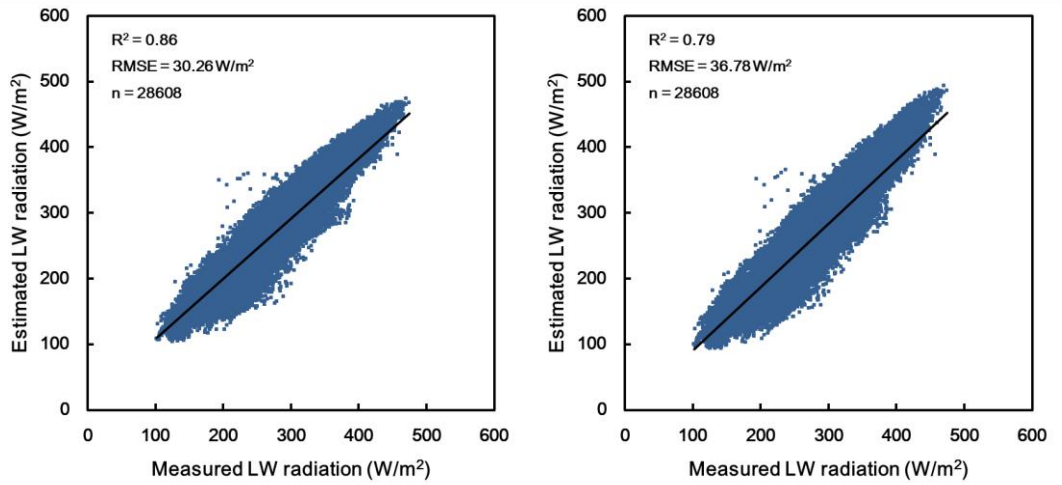

(a) Proposed model (Eq. (13)) (b) Sridhar model

Fig.4.6 Estimated LW radiation with respect to measured LW radiation for the all day. n is the sampling number.

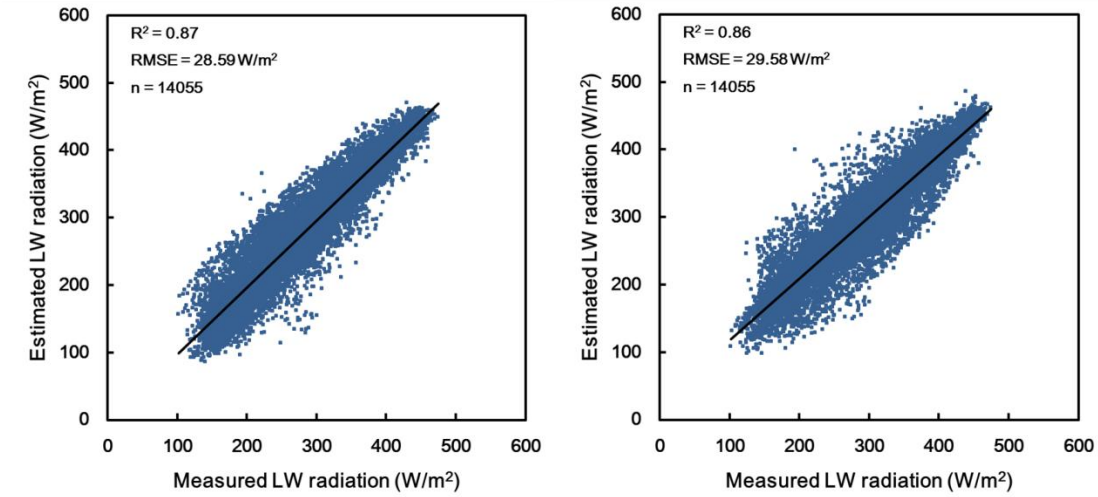

(a) Proposed model (Eq. (15)) (b) Crawford and Duchon model

Fig.4.7 Estimated LW radiation with respect to measured LW radiation for the daytime. n is the sampling number.

4.3.4 Distribution of LW radiation and radiative cooling potential

The hourly LW radiation was required for building energy simulation, and the calculation of LW radiation exchange between the building surface and the atmosphere was also necessary for building radiative cooling design. Zhang et al. [13] developed the typical meteorological year (TMY) for 360 locations in China for building simulation. The TMY dataset can represent the long-term typical weather conditions over a year for one location, however, which was lacking hourly LW radiation data. Therefore, the hourly LW radiation was calculated using Eq. (4.20) for 351 locations in China based on the TMY dataset, which can be a valuable supplement to TMY.

Building envelops can be cooled by effective radiation especially during nighttime since solar radiation was significantly stronger than LW radiation during daytime. Recently, it is demonstrated that the new glass-polymer hybrid metamaterials have a high reflectance in the solar spectrum and high emittance in the longwave spectrum for the daytime [86]; however, further research is also needed for building radiative cooling during daytime. In most regions of China, the hottest month is July; therefore, the hourly average of radiative cooling potential was calculated in July for the nighttime based on the Eq. (4.18), (4.19) and (4.23).

In order to describe the spatial distribution of LW radiation and radiative cooling potential [87], the values for 351 locations were interpolated using the Kriging method in ArcGIS 10.0 software; then the distribution maps of LW radiation and radiative cooling potential were obtained over China.

For the distribution map of LW radiation (shown in Fig.4.8), the LW radiation gradually decreases from Southeast to Northwest China excluding the Xinjiang area; and it is the smallest in the Tibetan Plateau region. It may be because the temperature in Southeast is higher than that in Northwest in summer, and the Tibetan Plateau region has the lowest temperature with the highest altitude. For the distribution map of radiative cooling potential (shown in Fig.4.9), the radiative cooling potential is

large in Northwest, while is small in Southeast. It is well-understand that the LW radiation is strongly related to the absolute water vapor content in the atmosphere, so it is larger for more humid conditions. Based on Eq. (4.18), the radiative cooling potential will be smaller for more humid conditions such as Southeast China.

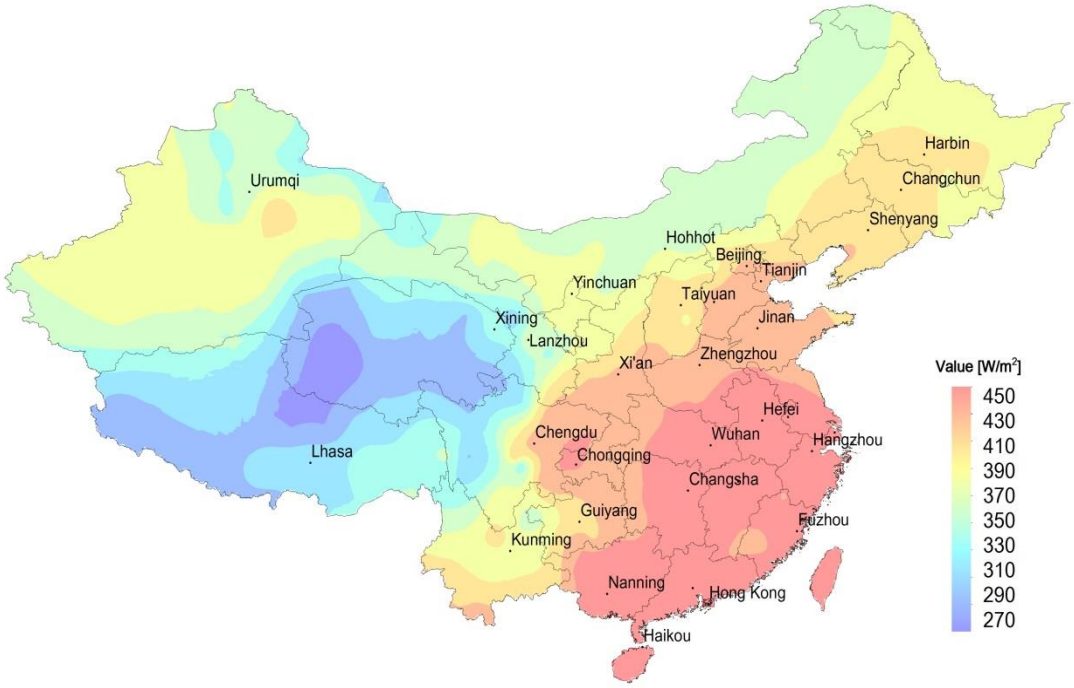

Fig.4.8 Distribution map of LW radiation (W/m^2) over parts of China for the all day in July.

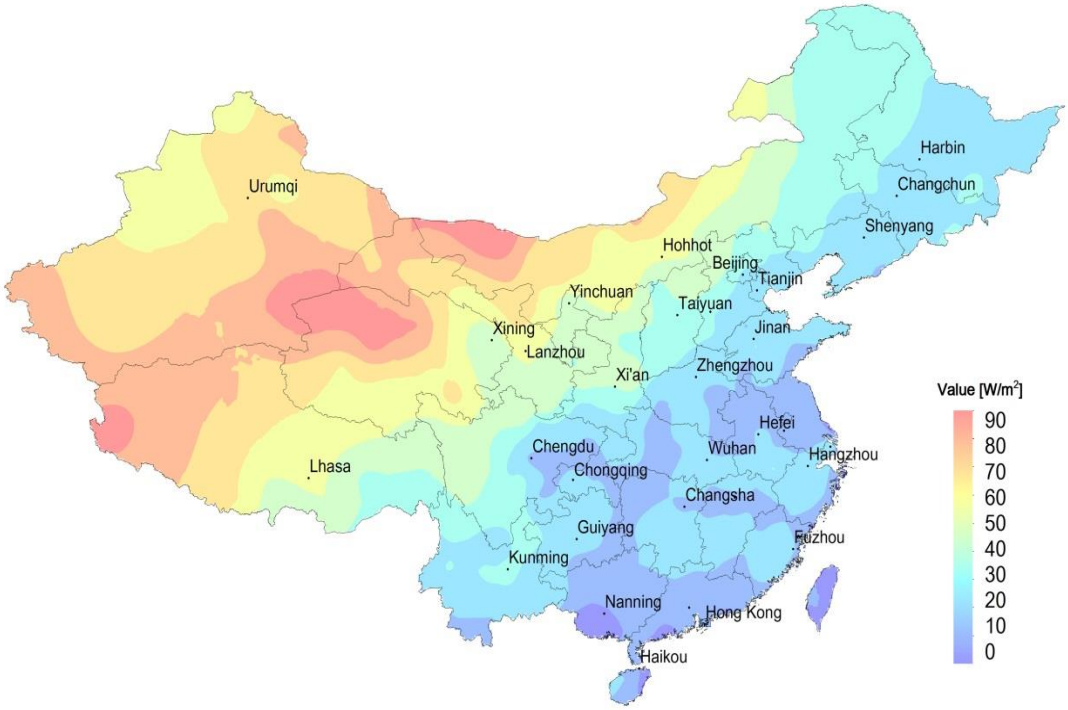

Fig.4.9 Distribution map of radiative cooling potential (W/m^2) over parts of China for the nighttime in July.

4.3.5 Applicable range of proposed models

As shown in Table 4.1, the longitude ranges of the four observation locations were 101.2° E - 128.1° E, while the latitude ranges of that were 36.5° N - 41.4° N, and there is no observation station for South China in this study. Therefore, the adaptability of the proposed models to the geographic and meteorological conditions in South China needs further verification. Moreover, further investigation is also needed to apply the proposed models and LW radiation dataset in the building simulation and the design of the building radiative cooling system.

4.4 Summary

In this study, new hourly LW radiation models were proposed under all-sky

conditions with the measured LW radiation dataset in four locations (Changbaishan, Haibei, Qinghai and Yucheng) of China. The new hourly LW radiation models (shown in Table 4.6) can be classified into four cases: all day, nighttime, daytimes with and without cloud modification factor. The main conclusions of this study are as follows:

(1) For the all day, the proposed LW radiation (Eq. (4.20)) performs well with R^2 of 0.86 and RMSE of 30.26 W/m^2, which is more accurate than the Sridhar model under all-sky conditions for locations in China.

(2) For the daytime, if the hourly cloud data or the solar radiation data are available, the model with cloud modification factor (Eq. (4.22)) is favorable, which is more accurate than the Crawford and Duchon model with R^2 of 0.87 and RMSE of 28.59 W/m^2; otherwise, the Eq. (4.21) is recommended for simplicity with limited errors.

(3) For the nighttime, the proposed model (Eq. (4.23)) was employed in calculating the radiative cooling potential of 351 locations in China, which can provide a valuable reference for the design of building radiative cooling system.

(4) The hourly LW radiation dataset of 351 locations in China was developed using Eq. (4.20), which can be a valuable supplement to the typical meteorological year (TMY).

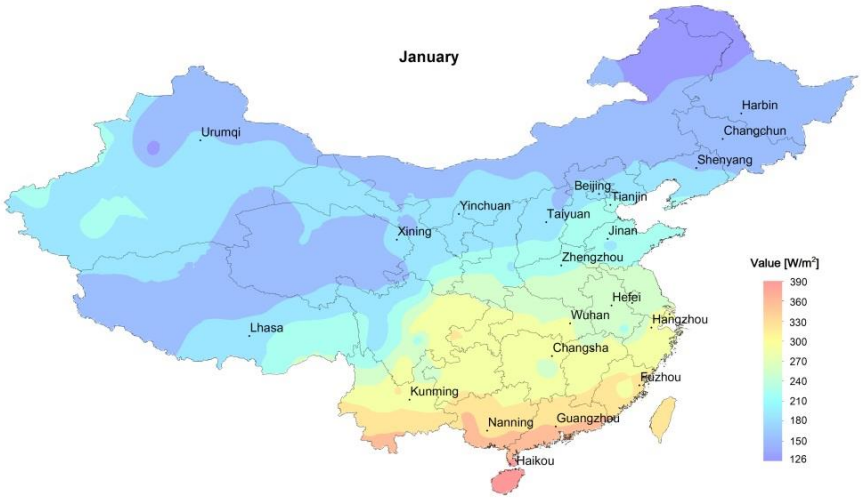

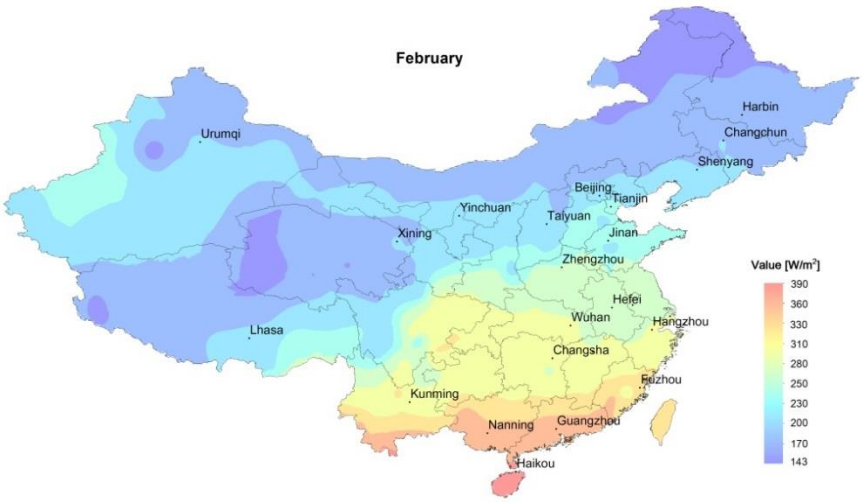

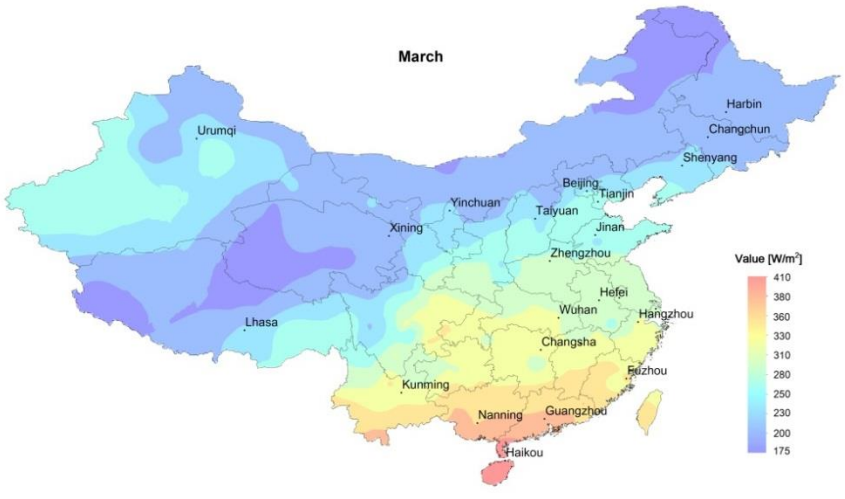

Distribution map of LW radiation (W/m^2) over parts of China for the all day

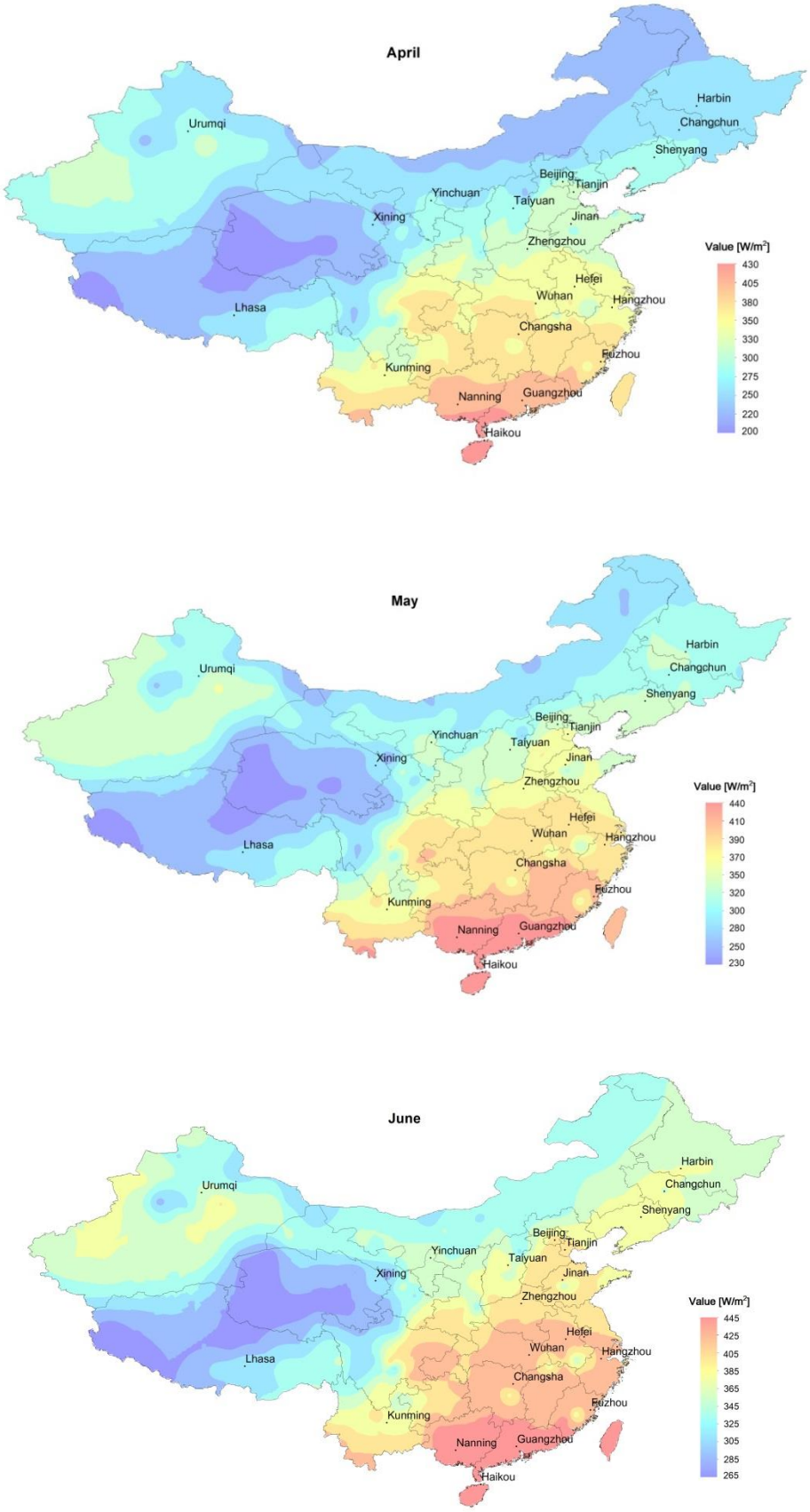

Distribution map of LW radiation (W/m^2) over parts of China for the all day

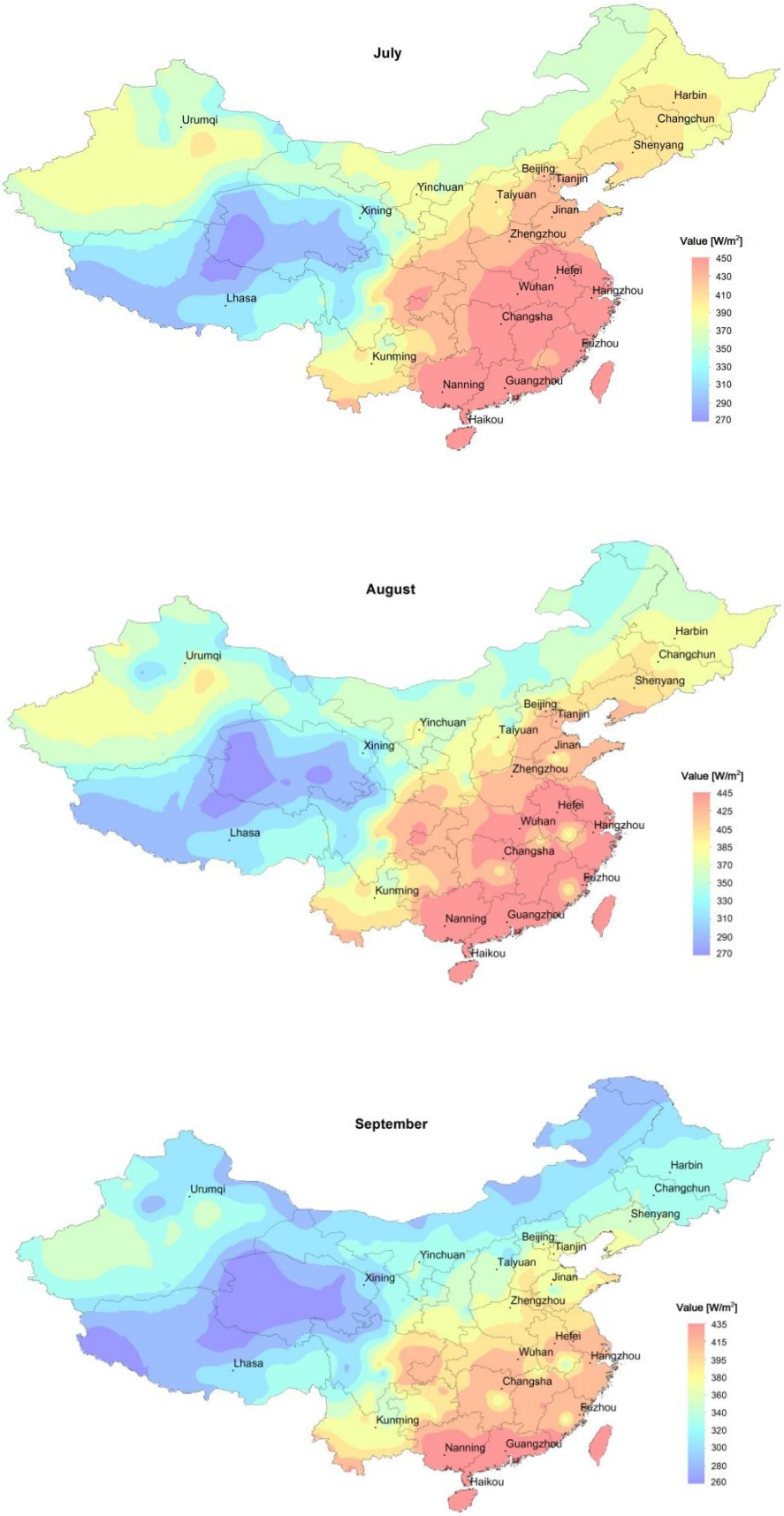

Distribution map of LW radiation (W/m^2) over parts of China for the all day

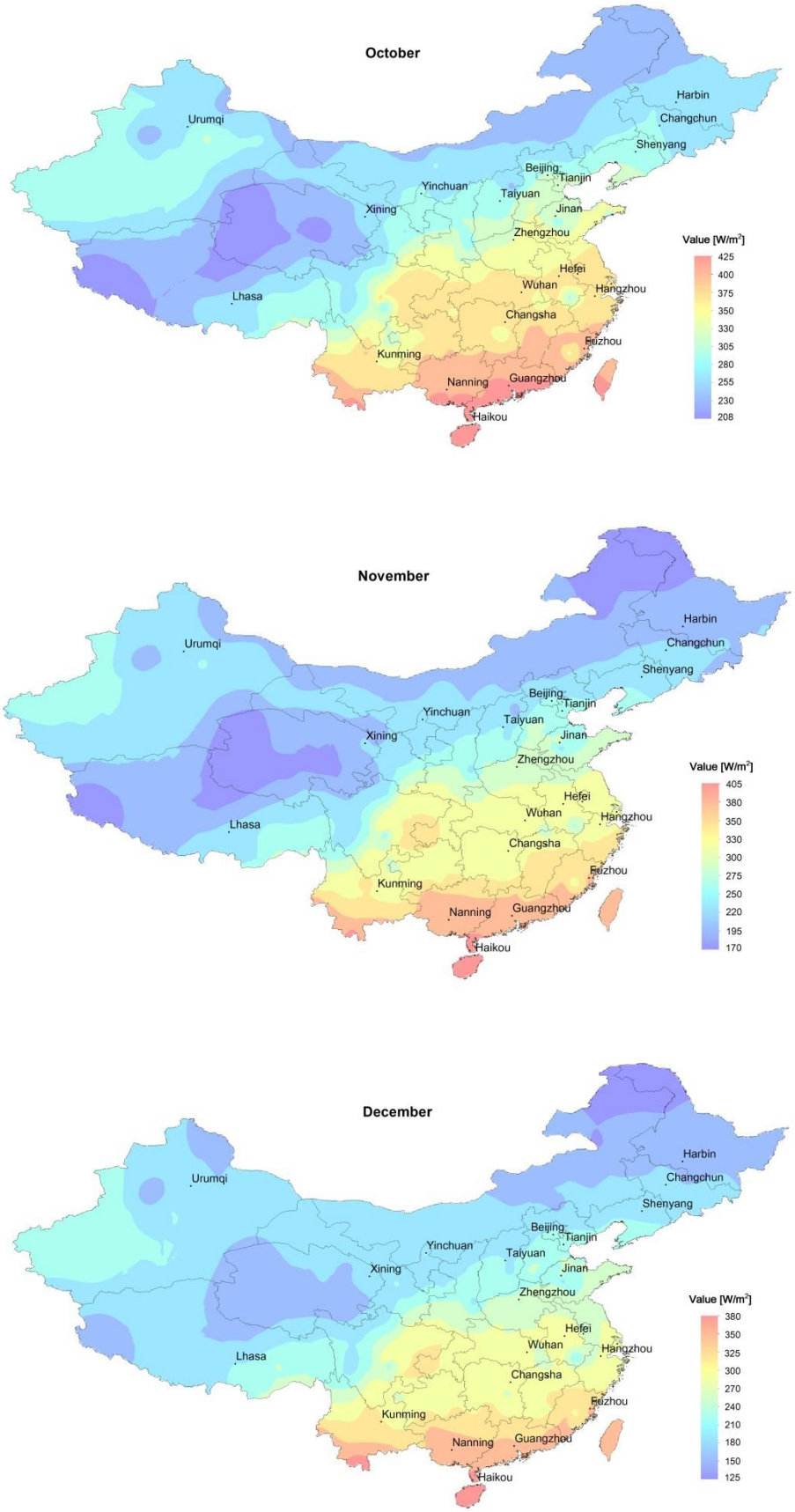

Distribution map of LW radiation (W/m^2) over parts of China for the all day

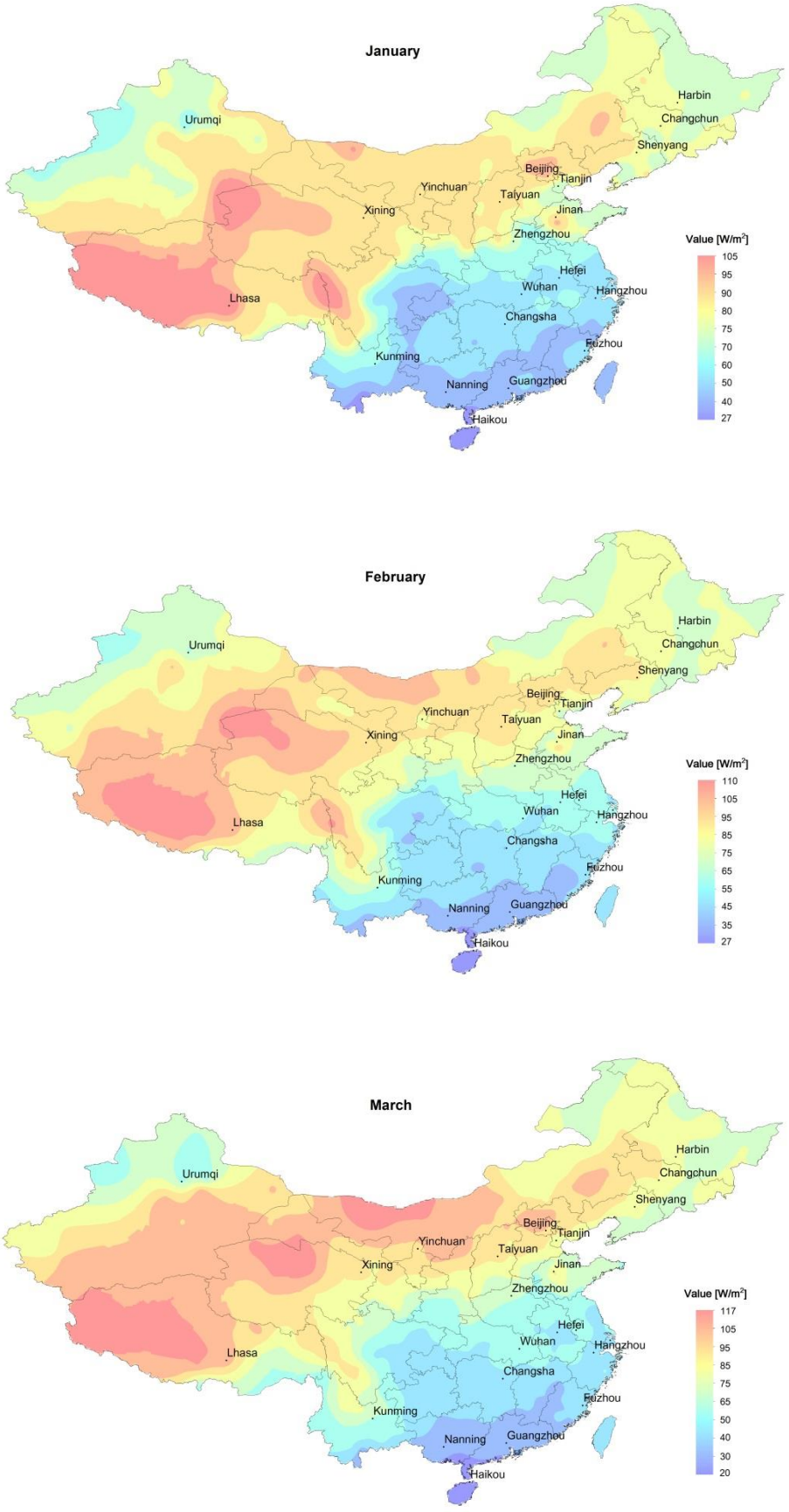

Distribution map of radiative cooling potential (W/m^2) over parts of China for the nighttime

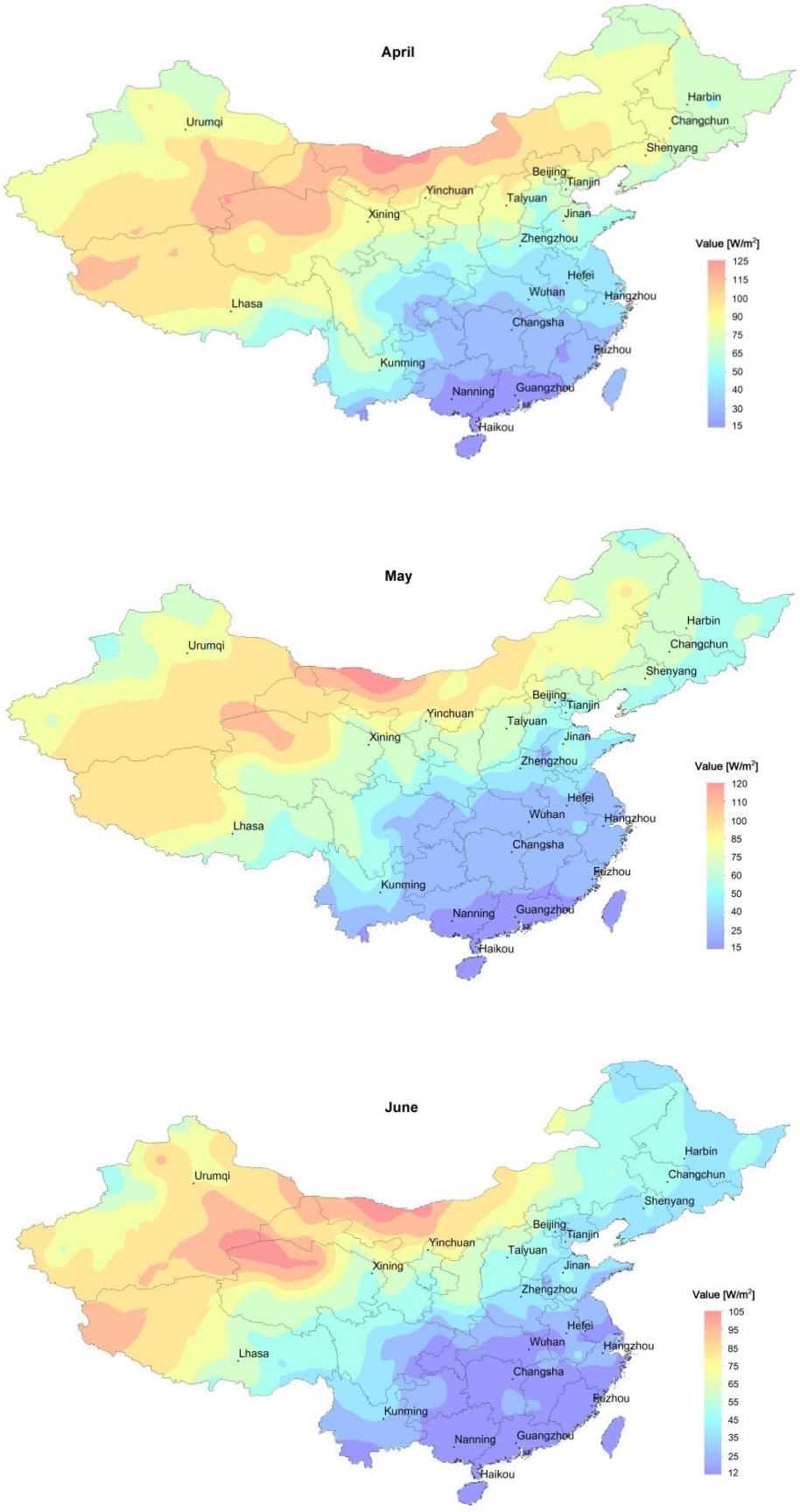

Distribution map of radiative cooling potential (W/m^2) over parts of China for the nighttime

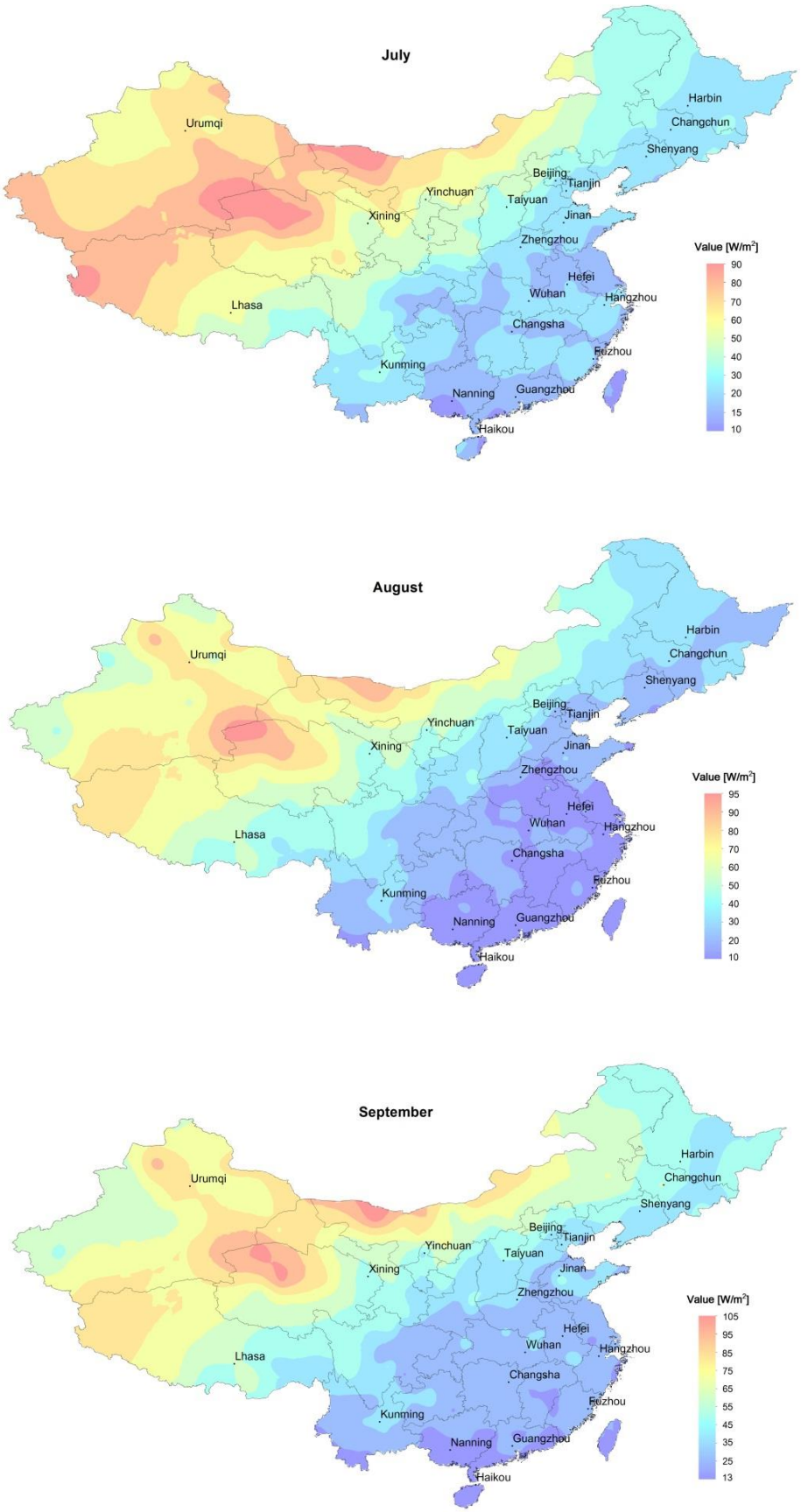

Distribution map of radiative cooling potential (W/m^2) over parts of China for the nighttime

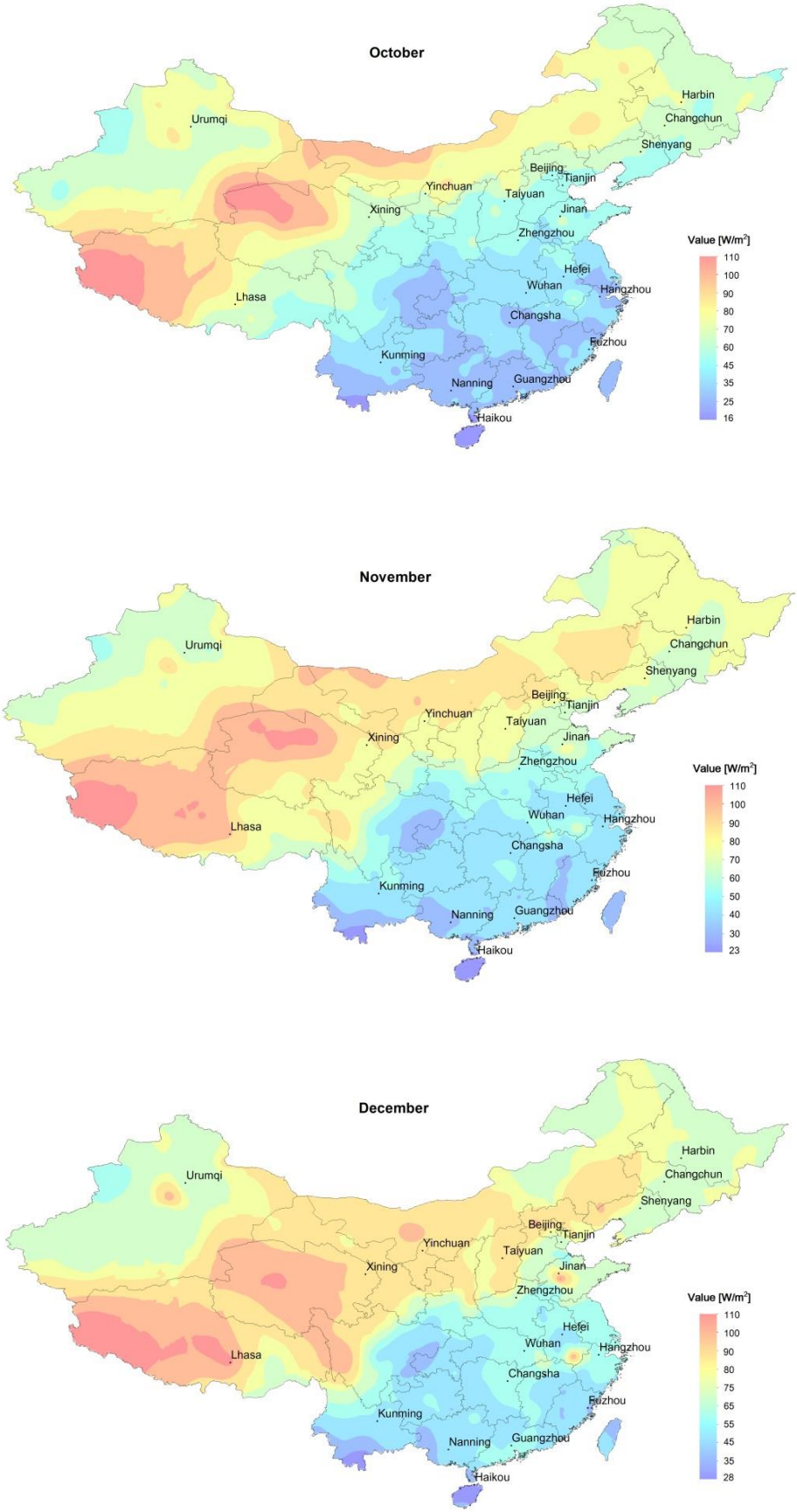

Distribution map of radiative cooling potential (W/m^2) over parts of China for the nighttime

CHAPTER 5

Improvement of the Typical Meteorological Year (TMY) for Chinese locations

Nomenclature

X	humidity ratio (0.1g/kg)
f	water vapor pressure (hPa)
P	atmospheric pressure (hPa)
P_0	sea level pressure (hPa)
H	altitude above sea level (m)
θ	dew point temperature (℃)
f_s	saturated water vapor pressure
T	dry-bulb temperature (℃)
φ	relative humidity (%)
K_t	clearness index
I_{sc}	solar constant, 1367 W/m^2
h	solar altitude angle (°)
K_n	direct beam transmittance
I_{he}	global horizontal solar radiation (W/m^2)
I_n	direct normal solar radiation (W/m^2)
I_d	diffuse solar radiation (W/m^2)
A_1, A_2, A_3, A_4	model coefficients
WS	sum of weights
W_i	weight of each meteorological element
FS_i	Finkelstein-Schafer statistic
θ_i	temperature after data smoothing (℃)
θ_i'	temperature of the last day of the previous month (℃)
θ_i''	temperature of the first day of the next month (℃)

5.1 Introduction

Research on building thermal environment and energy consumption requires building simulation software [92], which contains many kinds such as the Energy Plus, the Transient System Simulation Tool (TRNSYS), and the Building Energy Simulation Tool (BEST). The building simulation results can provide significant guidance for building designer to optimize the Heating Ventilation and Air-Conditioning (HVAC) system, to improve the building thermal conditions, and to conserve the building energy consumption. The general simulation process can be divided into three steps: 1).drawing a typical building model; 2).conducting the simulation with corresponding weather data as input parameters; 3).analyzing and optimizing the simulation results. It is worthy to note that the input of the weather data parameter is indispensable and can affect the accuracy of simulation results. Moreover, the impact of climate change such as global warming in different climate zones on building energy consumption can also be simulated by Future Weather Data. Wang et al. [93] calculated the energy consumption of cooling and heating for different building types in the U.S by Energy Plus with typical meteorological year (TMY) datasets: the historical and future.

Since the quality and accuracy of weather data are critical to the results of building simulations, many previous studies have focused on the development of weather data. One of the widely used forms of weather data is the typical meteorological year (TMY). The TMY included 8760 hourly records of meteorological parameters such as temperature, relative humidity, wind speed and solar radiation for one year period, which is selected from long-term recorded data in a certain region and can represent the typical weather conditions in this area. Numerous researches have been conducted to develop the TMY for different locations in the world. Pissimanis et al. [8] developed the TMY for Athens, Greece based on the measurement of meteorological elements for 17 years. Said et al. [94] produced the TMY for 5 cities of Saudi Arabia using 22 years of meteorological data. Thevenard et

al. [4, 95] discussed in detail the problems encountered in the establishment of the TMY for locations outside the U.S and Canada and evaluated the performance of the TMY.

In China, Zhang et al. [11] developed the TMY (named ChinaTMY1) for 28 Chinese locations based on the measured routine meteorological data in 16 years (1982 - 1997) and the estimated solar radiation data that calculated by the Zhang solar model [48]. Zhang et al. [12] subsequently improved this TMY by expanding the locations to 57 and discussed in detail the TMY establishment process. Ultimately, the TMY (named ChinaTMY2) for 360 locations of China was completed by Zhang [13] in 2012. However, The ChinaTMY2 was developed using the observed routine meteorological elements (temperature, relative humidity, wind speed, cloud cover) from 1995 to 2005, which was a bit early and not the latest years. Moreover, the hourly solar radiation data in the ChinaTMY2 was calculated by the Zhang solar model, which can be improved by our new proposed decomposition model in Chapter 2. It is worthy to note that the cloud cover data in the ChinaTMY2 can be utilized to estimate the atmospheric radiation indirectly; however, there are no records of atmospheric radiation in the ChinaTMY2, which can be improved by our proposed atmospheric radiation model in Chapter 4.

The primary purpose of this study is to improve the current TMY for locations in China based on our proposed solar radiation and atmospheric radiation models in Chapter 2 and Chapter 4 respectively. To achieve this goal, the following steps are conducted (shown in Fig.5.1): (1) the lately measured meteorological data from 2006 to 2016 was downloaded from the NCDC dataset [43]; (2) the proposed decomposition model (see Chapter 2) was employed in calculating the hourly solar radiation for 24 locations from 2006 to 2016; (3) the proposed downward LW radiation model (see Chapter 4) was applied to calculating the hourly atmospheric radiation for the all-day; (4) the latest TMY (2006 - 2016) was developed for 24 locations based on the previous chapters.

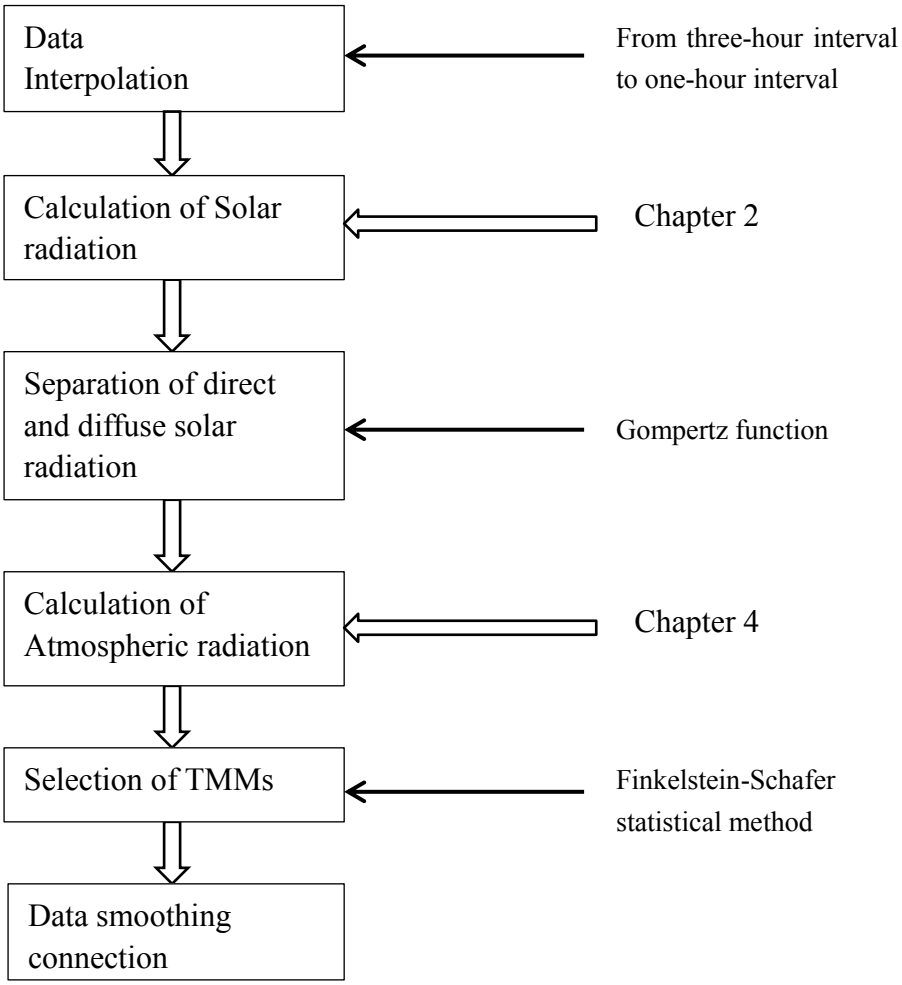

Fig.5.1 Flow diagram of development of TMY

5.2 Development of the Typical Meteorological Year (TMY)

5.2.1 Data collection and processing

The routine meteorological elements such as dry-bulb temperature, dew point temperature, wind speed and cloud cover were downloaded from the Integrated Surface Database (ISD) in the National Climate Data Center (NCDC) [43] for 24 Chinese locations during the period 2006 - 2016; while the measured daily solar radiation was coming from the China Meteorological Data Service Center (CMDC)

[60] for 24 Chinese locations during the same period 2006 - 2016. The geographical distribution of the 24 locations in this study was shown in Fig.5.2.

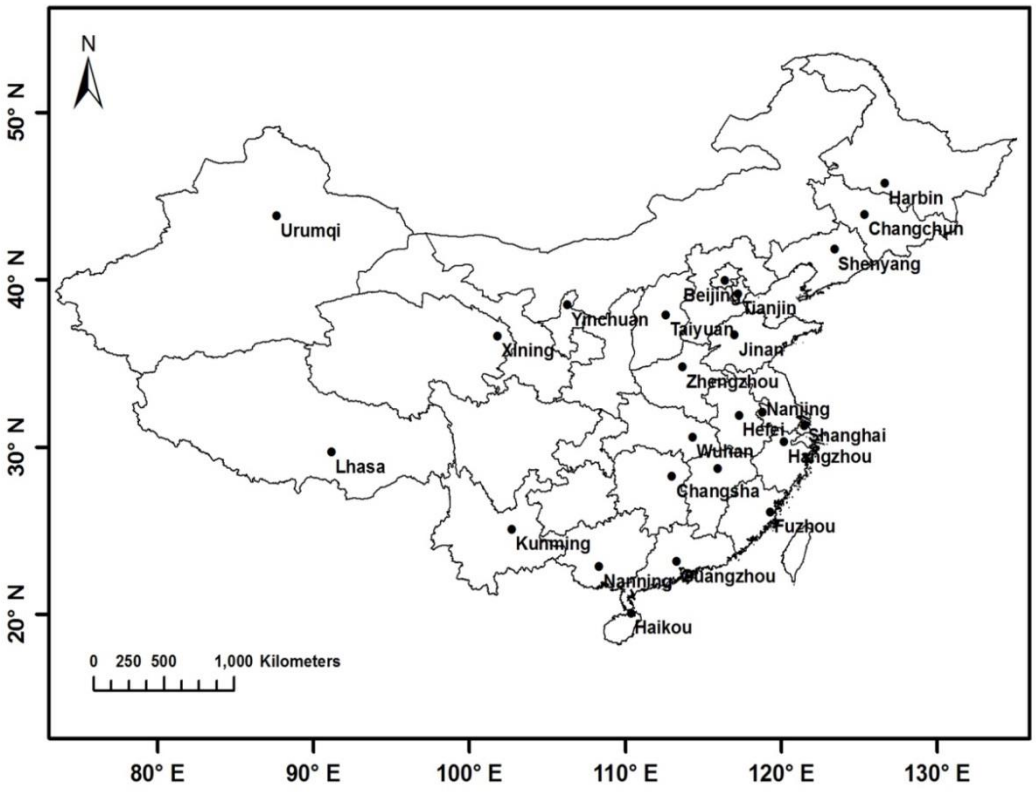

Fig.5.2 Spatial distribution of the 24 locations in this study.

The ISD dataset included more than 1000 Chinese meteorological stations, and the data records in the majority of these stations are the three-hour interval, however, the development of the TMY requires a one-hour interval. Therefore, the first step in data processing is data interpolation. According to our previous studies on the interpolation methods for meteorological elements, two different interpolation methods were applied in this study [12]: for the dry-bulb and dew point temperature parameters, the double Fourier series was utilized; as for other meteorological elements such as wind speed, station pressure, the linear interpolation was utilized. The detailed formulas of the double Fourier series were described in Chapter 2.

It is worthy to note that the cloud cover data in ISD dataset was not recorded as numerical values, which was recorded as the description words included “clear”,

“scattered”, “broken”, “overcast”, “obscured” and “partial obscured”. The conversion method from the description words to corresponding numerical values was shown in Table 5.2. Another point to note is the data missing for certain times of one day. The solution in this study is to replace the missing data record with the data from the previous or next moment.

The main meteorological elements in this TMY included the dry-bulb temperature (℃), dew point temperature (℃), relative humidity (%), humidity ratio (0.1g/kg), global horizontal solar radiation (W/m^2), direct normal solar radiation (W/m^2), diffuse solar radiation (W/m^2), wind direction, wind speed (m/s), cloud cover (one-tenth), atmospheric pressure (hPa) and the atmospheric radiation (W/m^2). Some of these elements should be calculated based on the downloaded meteorological elements in NCDC shown in Table 5.1. The detailed formulas were expressed as follows:

The humidity ratio, X, can be calculated as follows:

$$X = \frac{0.622f}{P-f} \tag{5.1}$$

where, X is the humidity ratio (0.1g/kg); f is the water vapor pressure (hPa); P is the atmospheric pressure (hPa) of the meteorological stations.

The atmospheric pressure, P, can be calculated as follows:

$$P = \frac{P_0}{(10)^{\frac{H}{18410}}} \tag{5.2}$$

where, P_0 is the sea level pressure (hPa); H is the altitude above sea level (m).

The water vapor pressure, f, can be calculated as follows:

$$f = \frac{1013.25}{760} \cdot 10^{8.10765-\frac{1750.29}{235+\theta}} \quad (5.3)$$

where, θ is the dew point temperature (℃).

The saturated water vapor pressure, f_s, can be calculated as follows:

$$f_s = \frac{1013.25}{760} \cdot 10^{8.10765-\frac{1750.29}{235+T}} \quad (5.4)$$

where, T is the dry-bulb temperature (℃).

The relative humidity, φ, can be calculated as follows:

$$\varphi = \frac{f}{f_s} \cdot 100\% \quad (5.5)$$

where, f is the water vapor pressure (hPa); f_s is the saturated water vapor pressure (hPa).

Table 5.1 Data sources for different parameters in this study.

Source	Parameter
NCDC	Wind speed Wind direction Dry-bulb temperature Dew point temperature Sea level pressure Station pressure Cloud cover
CMDC	Daily solar radiation

Table 5.2 Correspondences between the description words and the numerical values for cloud cover.

Record	Meaning	Value
CLR	Clear	0
SCT	Scattered	3.125
BKN	Broken	7.5
OVC	Overcast	10
OBS	Obscured	6
POB	Partial obscuration	3

5.2.2 Separation of direct and diffuse solar radiation

The hourly solar radiation is one of the most important elements in the TMY, which is difficult to obtain the observational values since numerous locations have no records of solar radiation. Moreover, the record of solar radiation for a long period such as 10 years will have some problems such as data missing and errors. Therefore, the estimation of solar radiation using other routine meteorological parameters such as temperature, sunshine duration is necessary and significant, this kind of solar model is called the empirical model. There are three different forms of solar radiation in this TMY: global, direct normal and diffuse solar radiation. The global solar radiation can be calculated by the proposed decomposition model and the detailed description of this model can be seen in Chapter 2.

The global solar radiation is composed of the direct and diffuse solar radiation, so it can also be divided into direct and diffuse components based on various separation models. If we want to calculate the solar radiation not only for horizontal surface, but also for inclined surface, the knowledge of direct and diffuse solar radiation are significant and indispensable. The solar radiation data on the inclined surface can be used as the fundamental reference for the design of the photovoltaic (PV) system, the building cooling load estimation as well as the building thermal simulation. Therefore, many previous studies focused on developing separation models to divide the global solar radiation into the direct normal and diffuse components [34, 96] in the world,

Zhang et al. [97] proposed a separation model based on the Gompertz function for locations in China, which had very high estimation accuracy. The detailed formulas of this model are expressed as follows [98]:

$$K_t = \frac{I_{he}}{I_{sc} \cdot \sin h} \tag{5.6}$$

$$K_n = A_1 \cdot A_2^{-A_3 \cdot A_2^{-A_4 \cdot K_t}} \tag{5.7}$$

$$I_n = K_n \cdot I_{sc} \tag{5.8}$$

$$I_d = I_{he} - I_n \cdot \sin h \tag{5.9}$$

where, K_t is the clearness index; I_{sc} is the solar constant, 1367 W/m^2; h is the solar altitude angle (°); K_n is the direct beam transmittance; I_{he} is the global horizontal solar radiation (W/m^2); I_n is the direct normal solar radiation (W/m^2); I_d is the diffuse solar radiation (W/m^2); A_1, A_2, A_3, A_4 is the model coefficients.

$$A_1 = -0.1556(\sin h)^2 + 0.1028 \sin h + 1.3748 \tag{5.10}$$

$$A_2 = 0.7973(\sin h)^2 + 0.1509 \sin h + 3.035 \tag{5.11}$$

$$A_3 = 5.4307 \sin h + 7.2182 \tag{5.12}$$

$$A_4 = 2.99 \tag{5.13}$$

5.2.3 Selection of Typical Meteorological Months (TMMs)

The TMY is composed of 12 Typical Meteorological Months (TMMs), which are defined as the month closest to the "average month" for a long period and each typical

calendar month is selected separately. Since there are 11 years data (2006 - 2016) to develop the TMY, each month in the TMMs such as January, February, March, etc. is selected respectively from the total corresponding 11 months (11 months for 11 years) based on the statistical methods. In this study, the TMMs are determined based on the sum of weights of different meteorological elements included daily maximum, minimum and average dry-bulb temperature, daily maximum, minimum and average of dew point temperature, daily maximum and average of wind speed and global solar radiation, among which the global solar radiation has the largest weight and accounts for one half. The weight value of global solar radiation can indicate the importance of solar radiation in the TMY.

The selection process for each typical meteorological month should firstly refer to the standard deviation of each meteorological element for each month, and then follow the cumulative distribution function and Finkelstein-Schafer statistic methods. The detailed processes are according to the following steps: (1) the target month in which the average dry-bulb temperature, dew point temperature, wind speed and global solar radiation for different standard deviation ranges (0.6 times, 0.8 times and 1, in sequence) was selected; (2) the sum of weights values of the target months passed through step (1) were compared (one, two or more months), and the month with the smallest value was selected as the typical meteorological month.

The sum of weights value can be calculated as follows [48]:

$$\mathrm{WS} = \sum(W_i \cdot FS_i) \tag{5.14}$$

where, WS is the sum of weights; W_i is the weight of each meteorological element; FS_i is the Finkelstein-Schafer statistic of each meteorological element.

The FS_i value can be calculated as follows:

$$FS_i = \frac{1}{n} \cdot \sum_{i=1}^{n} \delta_i \quad (5.15)$$

where, δ_i is the difference between the cumulative distribution function and the data value; n is the total days of each month.

5.2.4 Data smoothing connection

Since the month in the TMMs comes from different years, the values of meteorological elements for two adjacent months may be discontinuous. For example, if in the TMMs, January comes from 2008, while the February comes from 2014, the temperature values of 24:00, January 31 and of 1:00, February 1 may be discontinuous and need to make a smooth connection. The data smoothing connection was conducted only for the dry-bulb temperature, dew point temperature and relative humidity in this study since solar radiation had no nighttime values. The formula used for data smoothing connection can be expressed as follows:

$$\theta_i = \frac{12-i}{12} \cdot \theta_i' + \frac{i}{12} \cdot \theta_i'' \quad (5.16)$$

where, θ_i is the temperature after data smoothing (℃); θ_i' is the temperature of the last day of the previous month (℃); θ_i'' is the temperature of the first day of the next month (℃).

5.2.5 Improvement of the TMY

The first version of TMY named “ChinaTMY1” developed by Zhang used the meteorological data from 1982 to 1997, which included 57 cities of China. Then Zhang improved the first version and developed the current TMY named “ChinaTMY2”, which included 360 cities of China. Since the current TMY established by Zhang used the meteorological data from 1995 to 2005, which may be

a little out of date and need to be updated. Moreover, there was no atmospheric radiation data in this TMY; therefore, we improved the current TMY in this study based on the good research results in Chapter 2 and 4, which mainly included three aspects: first, the routine meteorological elements such as temperature, wind speed used for developing the TMY are from 2006 to 2016, which are the observed data of the last 11 years and can better reflect the characteristics of climate change in China; then, for the very significant solar radiation data, the new decomposition solar model was employed in calculating the hourly global solar radiation under all-sky conditions, which used the hourly/daily radiation ration and the measured daily values and had better estimation accuracy than the original Zhang model; last, the atmospheric radiation data was calculated using our new proposed LW radiation model, which will be a very significant supplement to the original TMY. The new TMY for 24 cities of China were completed according to the above stated development methods.

5.3 Results and discussion

5.3.1 Building climate zone in China

Since the area and range of China are large, the climate characteristics of different places are rather complicated. To conserve building energy consumption and improve the building thermal environment, the Thermal Design Code for Civil Buildings was established. In the Thermal Design Code for Civil Buildings, five climate zones in China (very cold, cold, hot-summer and cold-winter, hot-summer and warm-winter, mild regions) was identified based on the average temperatures of the coldest and warmest months [99]. Table 5.3 showed the five building climate zones and the 24 cities included.

Tabel 5.3 Study Cities in building climate zone of China

Climate zone	Cities in this study
Very cold	Harbin, Changchun, Shenyang, Xining, Urumqi,
Cold	Beijing, Jinan, Lhasa, Tianjin, Taiyuan, Yinchuan, Zhengzhou
Hot-summer and cold-winter	Shanghai, Changsha, Hefei, Nanchang, Wuhan, Nanjing, Hangzhou
Hot-summer and warm-winter	Guangzhou, Fuzhou, Nanning, Haikou
Mild	Kunming

Since a large number of cities in this study, to avoid duplication of contents, five representative cities (Harbin, Beijing, Shanghai, Guangzhou, and Kunming) in different building climate zones were selected for explanation and discussion. The distribution of the building climate zone and the five cities was shown in Fig.5.3.

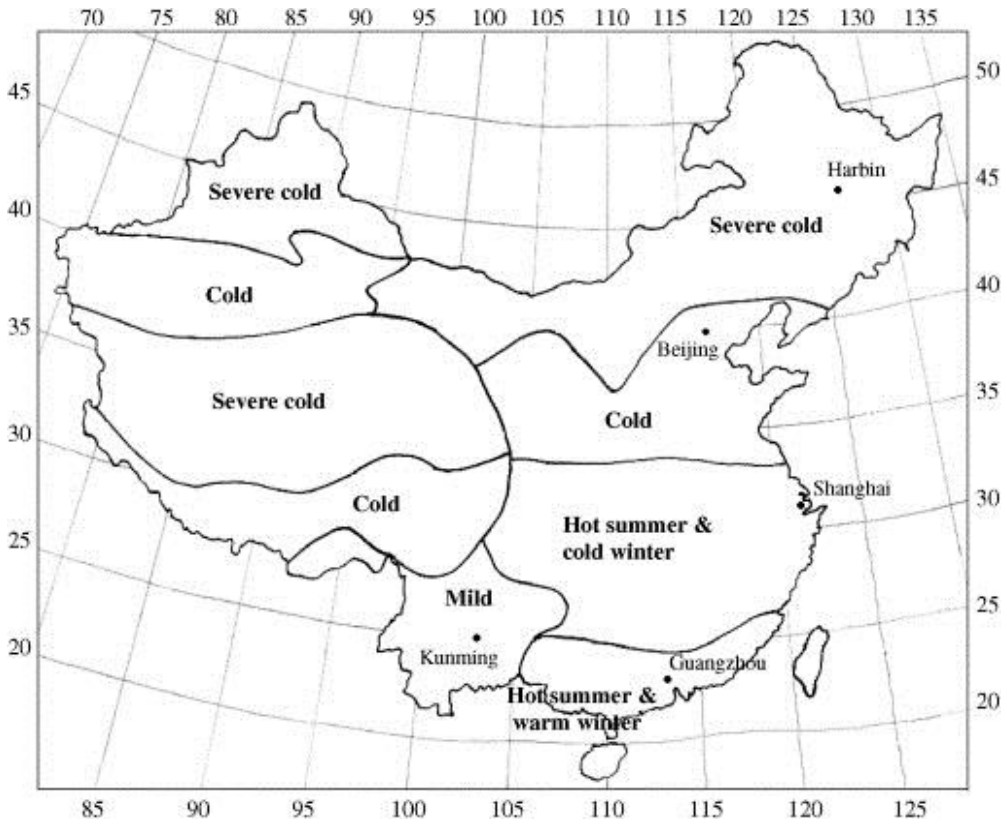

Fig.5.3 Distribution of five representative cities (Harbin, Beijing, Shanghai, Guangzhou, and Kunming) in building climate zone of China [100].

5.3.2 Selection results of typical meteorological months (TMMs)

According to the selection strategies described in Section 5.2.3, the TMMs were selected from the total 11 years data (2006 - 2016) and Table 5.4 showed the selected years for each city in the TMMs. The Comparison between the selected month and the 11-year "average month" for the five representative cities (Harbin, Beijing, Shanghai, Guangzhou, and Kunming) was shown in Table 5.5, 5.6, 5.7, 5.8 and 5.9, respectively. From these tables, we can see that the daily average values of the selected month for different meteorological elements such as global solar radiation, dry-bulb temperature, dew point temperature and wind speed in the TMMs have no much difference with the values of the "average month" of the 11 years (2006 - 2016). Therefore, the comparison results indicated that using the TMMs to compose the TMY is reasonable, which can reflect the change characteristics of the meteorological elements for a long time.

Table 5.4 The selected years of the TMMs for 24 locations in China.

	January	February	March	April	May	June	July	August	September	October	November	December
Harbin	2008	2015	2012	2011	2007	2011	2012	2009	2015	2012	2015	2011
Urumqi	2014	2009	2007	2006	2013	2010	2010	2011	2008	2011	2008	2008
Xining	2007	2010	2016	2016	2013	2009	2007	2013	2008	2008	2016	2009
Yinchuan	2016	2011	2012	2012	2009	2016	2008	2010	2015	2010	2014	2006
Taiyuan	2013	2006	2006	2006	2008	2006	2008	2008	2006	2008	2006	2013
Changchun	2006	2011	2007	2012	2007	2011	2006	2008	2015	2009	2008	2013
Shenyang	2008	2014	2009	2007	2016	2006	2012	2015	2013	2007	2007	2013
Beijing	2009	2006	2009	2007	2010	2012	2007	2012	2010	2007	2012	2008
Tianjin	2008	2011	2015	2007	2013	2016	2013	2015	2008	2008	2006	2013
Jinan	2007	2014	2008	2009	2010	2016	2011	2008	2008	2008	2007	2006
Lhasa	2012	2009	2012	2008	2011	2013	2007	2007	2007	2010	2013	2007
Kunming	2012	2011	2012	2006	2011	2009	2014	2006	2006	2011	2013	2010
Zhengzhou	2010	2015	2009	2007	2010	2006	2009	2008	2008	2011	2008	2013
Wuhan	2010	2013	2015	2007	2014	2014	2011	2010	2008	2012	2010	2015
Changsha	2007	2010	2009	2009	2009	2008	2012	2006	2015	2008	2013	2006
Nanjing	2013	2011	2013	2015	2012	2014	2009	2008	2013	2008	2013	2009
Hefei	2010	2006	2013	2007	2006	2014	2006	2012	2011	2007	2012	2009
Shanghai	2016	2013	2013	2007	2010	2011	2012	2008	2014	2008	2007	2008
Hangzhou	2010	2015	2015	2011	2015	2007	2008	2007	2015	2007	2008	2008
Nanchang	2007	2014	2006	2015	2006	2006	2008	2007	2013	2008	2008	2006
Fuzhou	2013	2011	2006	2008	2010	2007	2006	2012	2010	2007	2012	2006
Guangzhou	2013	2015	2016	2014	2013	2012	2013	2008	2008	2015	2014	2006
Nanning	2007	2011	2009	2009	2013	2009	2012	2012	2008	2009	2013	2009
Haikou	2007	2015	2012	2015	2016	2013	2009	2013	2010	2011	2012	2007

Table 5.5 Comparison between the 11-year average and selected month of TMMs in Harbin.

Month	Years when TMMS are selected	Global solar radiation (W/m^2)		Dry-bulb temperature (℃)		Dew point temperature (℃)		Wind speed (m/s)	
		Daily average of 11 years	Daily average of selected months	Daily average of 11 years	Daily average of selected months	Daily average of 11 years	Daily average of selected months	Daily average of 11 years	Daily average of selected months
Jan	2008	194.7	201.1	-17.3	-17.3	-21.7	-22.9	1.9	1.6
Feb	2015	278.7	298.6	-12.2	-11	-18.3	-16.2	2.2	2.5
Mar	2012	339.1	350.3	-2.7	-3.2	-10.7	-11	2.7	2.5
Apr	2011	366.5	367.8	7.7	7.5	-4.3	-4.4	3.1	2.7
May	2007	367.6	327.5	15.8	14.9	5.1	4.8	2.8	2.4
Jun	2011	378.8	365.6	21.8	21.6	13.8	14.2	2.3	2.1
Jul	2012	358.1	331.8	23.6	23.9	18.4	19.3	2	1.7
Aug	2009	352.9	352.1	22.5	22.2	17.2	17.5	2	1.9
Sep	2015	340.6	354.2	16.1	16.2	9.2	9.9	2	2
Oct	2012	265.5	251.3	6.9	6.3	-0.9	0.1	2.2	1.9
Nov	2015	199.3	202.9	-4.6	-5	-10.6	-10.6	2.4	2.6
Dec	2011	160.4	134.5	-14.3	-14	-18.3	-19.3	2	1.8

Table 5.6 Comparison between the 11-year average and selected month of TMMs in Beijing.

Month	Years when TMMS are selected	Global solar radiation(W/m^2)		Dry-bulb temperature (℃)		Dew point temperature (℃)		Wind speed (m/s)	
		Daily average of 11 years	Daily average of selected months	Daily average of 11 years	Daily average of selected months	Daily average of 11 years	Daily average of selected months	Daily average of 11 years	Daily average of selected months
Jan	2009	248	259.3	-3	-2.8	-15.4	-17	2.4	2.1
Feb	2006	293.8	279.6	0.3	-0.8	-12.9	-14.5	2.5	2.6
Mar	2009	370	381	7.5	7.2	-8.4	-8.4	2.8	2.7
Apr	2007	413.7	421.4	15	15.2	-0.4	-1.9	3	2.8
May	2010	423.7	423.8	21.6	21.8	6.8	7.2	3	2.7
Jun	2012	370.5	359.4	25.1	24.8	15	15.4	2.4	2.2
Jul	2007	340.6	330	27.2	26.9	20.1	20.4	2.2	2
Aug	2012	371.4	382.5	26.3	26.1	19.3	19.6	2	1.9
Sep	2010	341.2	336.3	21.1	21.3	13.1	12.7	2	1.9
Oct	2007	286	277.6	14.1	13.7	4.9	4.9	2	1.9
Nov	2012	239.4	249.5	5.1	4.4	-5.3	-6.4	2.3	2.2
Dec	2008	219.4	225.1	-1.2	-0.8	-13.2	-15	2.5	2.3

Table 5.7 Comparison between the 11-year average and selected month of TMMs in Shanghai.

Month	Years when TMMS are selected	Global solar radiation(W/m^2)		Dry-bulb temperature (℃)		Dew point temperature (℃)		Wind speed (m/s)	
		Daily average of 11 years	Daily average of selected months	Daily average of 11 years	Daily average of selected months	Daily average of 11 years	Daily average of selected months	Daily average of 11 years	Daily average of selected months
Jan	2016	242	229.3	4.9	4.5	-0.8	-0.7	2.7	2.6
Feb	2013	250.6	222.6	6.6	6.8	1.4	2.3	2.9	2.8
Mar	2013	342	351.3	10.7	11.1	4	3.9	3	2.9
Apr	2007	376.7	369.5	15.9	15.7	8.7	7.7	3.1	2.9
May	2010	385.6	377.1	21.3	20.8	14.1	13.9	3	3.3
Jun	2011	294.9	277	24.4	24.3	20	20.3	2.7	2.7
Jul	2012	372	391.9	29.3	29.7	23.4	23.2	3	3
Aug	2008	364.2	364.7	28.9	28.4	23.3	23.2	3.1	2.9
Sep	2014	333.3	310.2	24.7	24.2	19.3	20.2	2.8	2.9
Oct	2008	315.3	277.4	20.2	20.7	14	15.4	2.6	2.5
Nov	2007	240.3	264.5	13.9	13.9	8.1	6.8	2.5	2.5
Dec	2008	253.6	261.1	7.4	7.6	1.1	0.6	2.6	2.6

Table 5.8 Comparison between the 11-year average and selected month of TMMs in Guangzhou.

Month	Years when TMMS are selected	Global solar radiation(W/m^2)		Dry-bulb temperature (℃)		Dew point temperature (℃)		Wind speed (m/s)	
		Daily average of 11 years	Daily average of selected months	Daily average of 11 years	Daily average of selected months	Daily average of 11 years	Daily average of selected months	Daily average of 11 years	Daily average of selected months
Jan	2013	272.2	310.7	13.6	13.6	6.8	8.2	2.3	2.9
Feb	2015	245.9	270.6	16.2	17.8	10.9	11.4	2.2	2.4
Mar	2016	214.3	209.8	18.5	17.8	14.1	13.6	1.9	2.1
Apr	2014	241.1	237.9	22.7	23.7	18.6	19.9	1.9	2
May	2013	293.3	282.9	26.2	26.5	21.9	23.2	1.9	2
Jun	2012	321.9	341.2	28.3	27.7	24.2	24.4	2	2.3
Jul	2013	386.5	372.2	29.5	28.7	24.4	24.6	2	2.3
Aug	2008	381.6	367.2	29.3	29.3	24	23.6	1.8	1.7
Sep	2008	370.2	395.3	28.1	28.7	22.4	22.8	2	1.5
Oct	2015	369.5	362.6	25.4	25.7	17.9	19.1	2.1	2.5
Nov	2014	316.1	278.9	20.5	21.5	13.5	15.8	2.1	2.4
Dec	2006	302	330.2	15.5	16.1	7.7	7.6	2.3	1.4

Table 5.9 Comparison between the 11-year average and selected month of TMMs in Kunming.

Month	Years when TMMS are selected	Global solar radiation(W/m^2)		Dry-bulb temperature (℃)		Dew point temperature (℃)		Wind speed (m/s)	
		Daily average of 11 years	Daily average of selected months	Daily average of 11 years	Daily average of selected months	Daily average of 11 years	Daily average of selected months	Daily average of 11 years	Daily average of selected months
Jan	2012	399	438.6	9.3	10.2	1.9	1.2	3.8	3.7
Feb	2011	464.9	533.8	11.9	12.8	1.3	1.9	4.4	4.1
Mar	2012	472.6	473.3	15.1	14.7	3.3	3.4	4.5	3.9
Apr	2006	460.8	430.6	17.6	18.3	7.2	7.1	4.3	3.7
May	2011	415.4	414.6	19.4	19.3	11.6	12.1	3.9	2.8
Jun	2009	357.2	350.1	20.3	20.6	15.4	15.4	3.3	2.1
Jul	2014	344	344.8	20.2	19.4	16.3	16.8	2.7	3.2
Aug	2006	381.7	405.6	19.8	20.8	15.8	15.9	2.5	2.3
Sep	2006	347.7	351.6	18.5	18.5	14.4	14.3	2.6	2.4
Oct	2011	323.8	301.1	15.9	15.7	11.6	11.6	2.7	2.2
Nov	2013	377.3	389.5	12.3	11.5	6.9	6.4	3.3	4.5
Dec	2010	342.3	338.1	9.1	9.8	3.7	4.6	3.4	2.8

5.3.3 Atmospheric radiation data

The Atmospheric radiation (downward longwave radiation) which was mostly emitted by the gases composed in the atmosphere such as carbon dioxide, ozone and water vapor plays a crucial role in building passive cooling design, especially in the radiative cooling design, because the buildings can be cooled through the heat transfer from the building surface to the atmosphere. Therefore, the atmospheric radiation data is significant for the building thermal simulation. Zhang et al. [82] estimated the LW radiation based on the Philipps equations with cloud data in TMY in previous studies, however, the results of estimation were not validated since lacking measured LW radiation data and was also not included in the TMY. The LW radiations of 24 cities were calculated based on the new proposed model in Chapter 4 and were also added to the new TMY. The variations of the LW radiation in the new TMY were shown in Fig.5.4.

Comparing Fig.5.4 to Fig.5.5, the results showed that the LW radiation and dry-bulb temperature have a similar variation tendency, because the LW radiation values are mainly determined by the temperature. From Fig.5.7, it can be seen that the atmospheric pressure values are larger in the winter season than in the summer season, because more water vapor existing in the atmosphere during the summer season, which can be illustrated by humidity ratio variations in Fig.5.9.

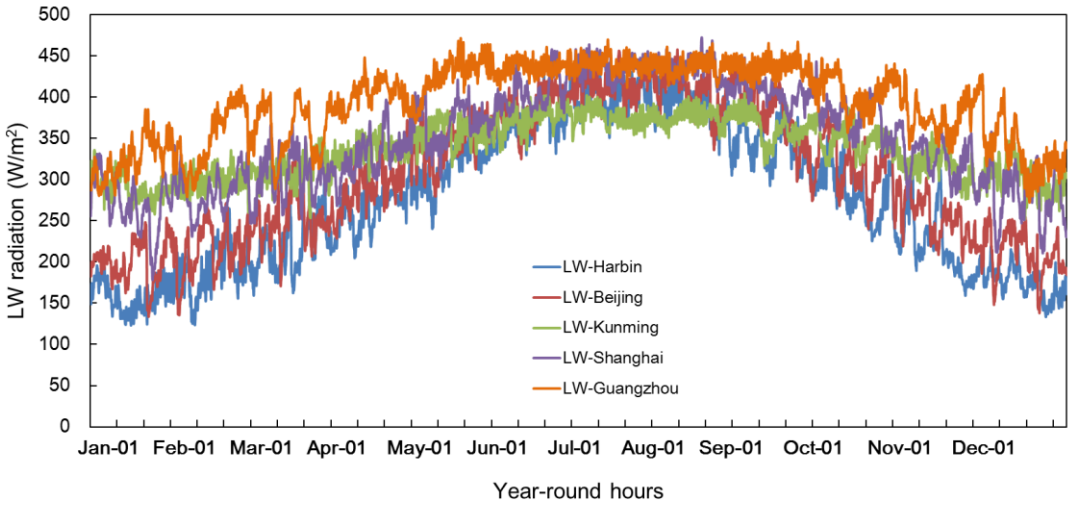

Fig.5.4 LW radiation variations of five representative cities for year-round hours (8760 hours).

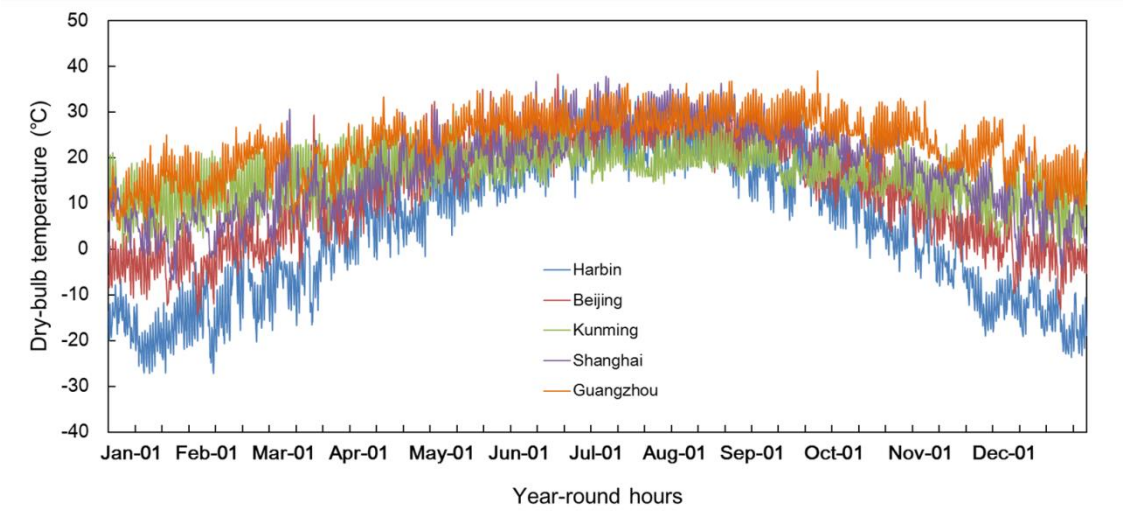

Fig.5.5 Dry-bulb temperature variations of five representative cities for year-round hours (8760 hours).

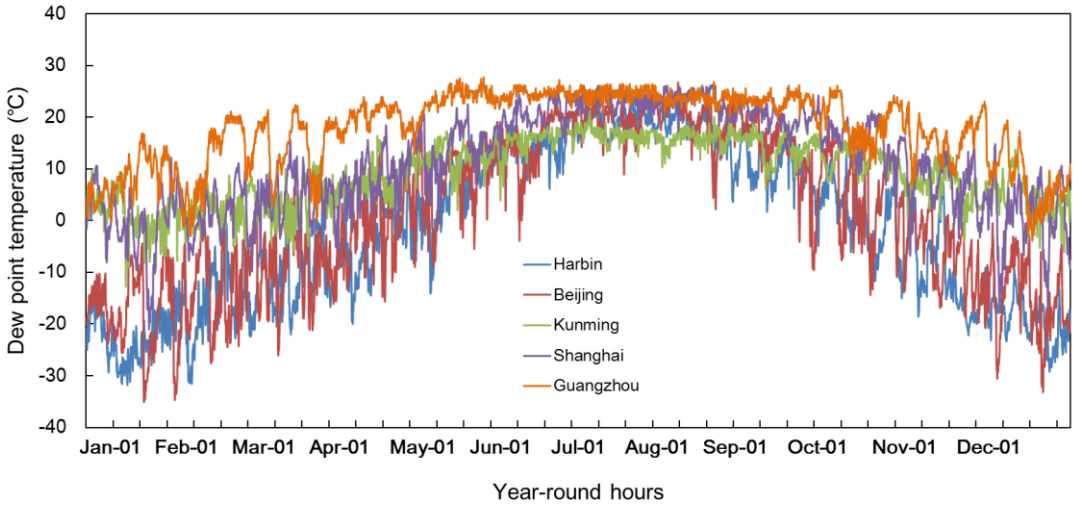

Fig.5.6 Dew point temperature variations of five representative cities for year-round hours (8760 hours).

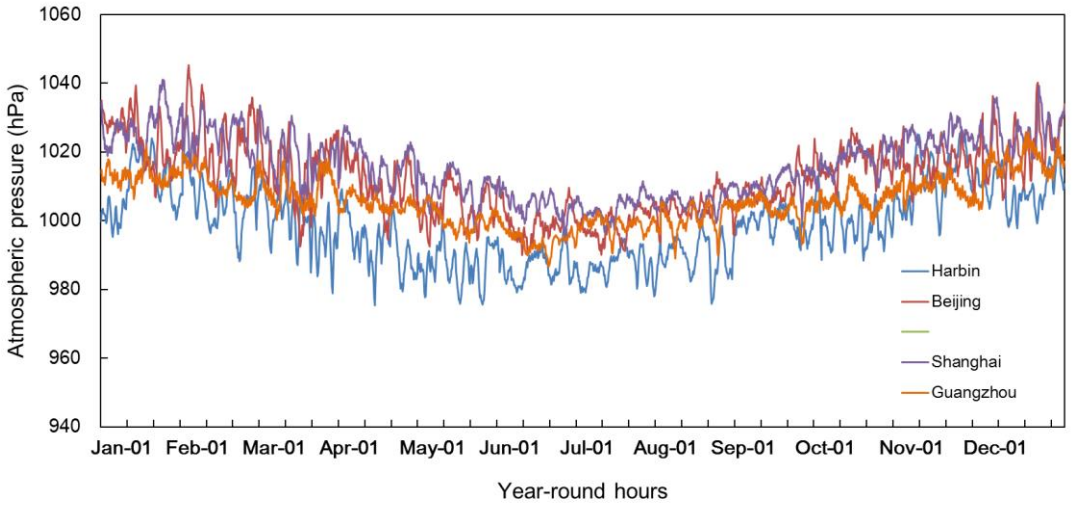

Fig.5.7 Atmospheric pressure variations of four representative cities for year-round hours (8760 hours).

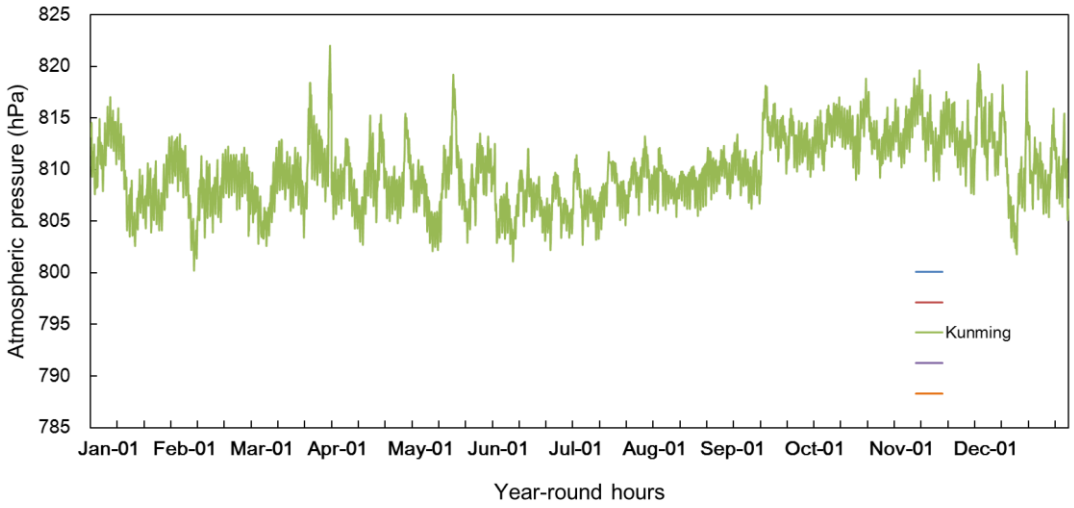

Fig.5.8 Atmospheric pressure variation of Kunming for year-round hours (8760 hours).

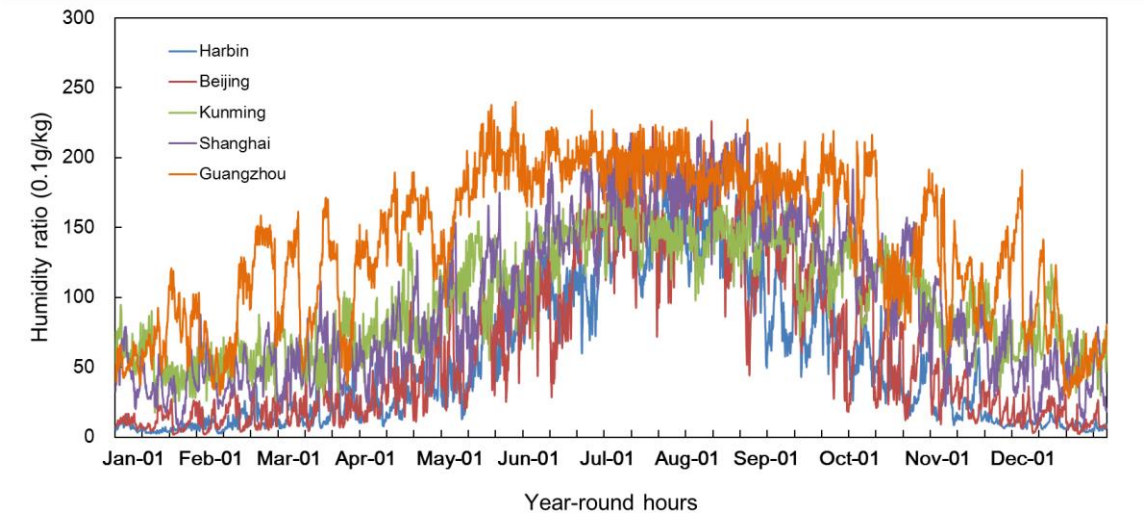

Fig.5.9 Humidity ratio variations of five representative cities for year-round hours (8760 hours).

5.3.4 Monthly average values of different meteorological elements

The monthly average values of dry-bulb temperature, dew point temperature, and wind speed were calculated from the new TMY for five representative cities as shown in Fig.5.10, Fig.5.11 and Fig.5.12. It can be seen that the temperature differences are particularly large in different building climate zones of China, which are one of the important indicators for the division of the building climate zones.

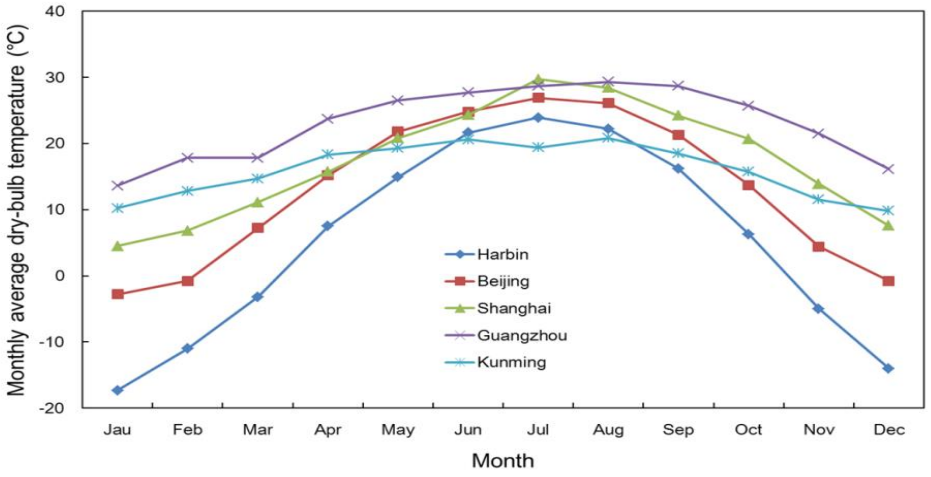

Fig.5.10 Monthly average dry-bulb temperature variations of five representative cities.

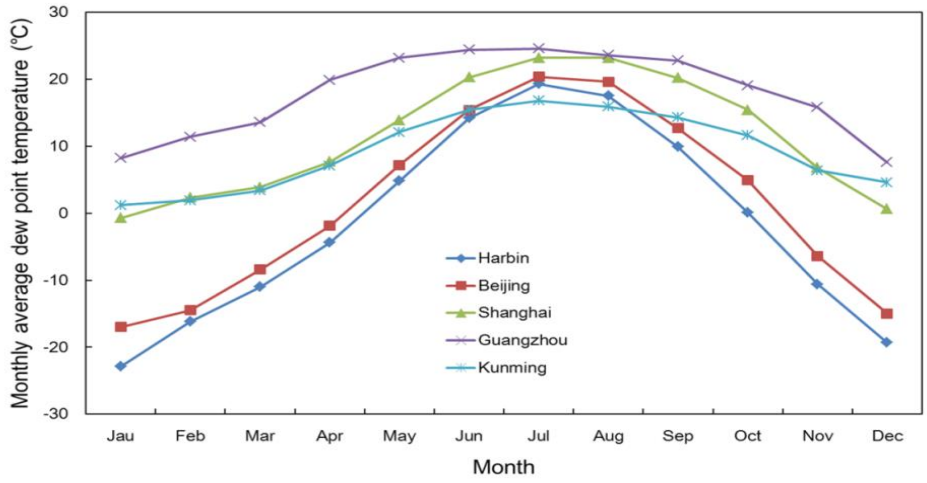

Fig.5.11 Monthly average dew point temperature variations of five representative cities.

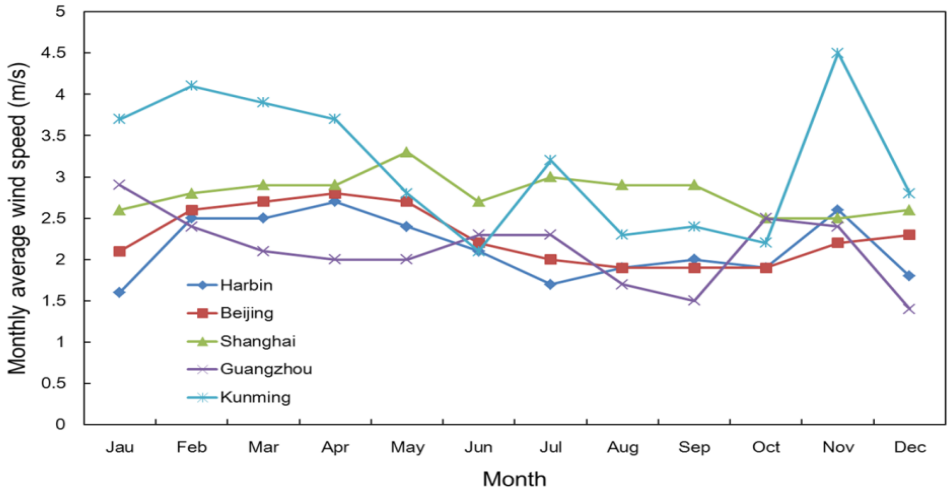

Fig.5.12 Monthly average wind speed variations of five representative cities.

5.3.5 Typical Meteorological Days (TMDs)

The Typical Meteorological Days (TMDs), which are defined as the monthly average values for each hour (24 hours for one month), can reflect the average conditions of each month. Compared to the TMY, the TMDs have many advantages such as fewer data records, since only one-day data records in each month. The TMDs only contains 288 data records for each location.

In this study, the TMDs were calculated for 24 locations of China using the same datasets developed for TMY from 2006 to 2016. The TMDs are composed by calculating the monthly average hourly values of the dry-bulb temperature, dew point temperature, relative humidity, humidity ratio, global horizontal solar radiation, direct normal solar radiation, diffuse solar radiation, wind direction, wind speed, cloud cover, atmospheric pressure, and atmospheric radiation, so they can be regarded as the representative day of each month for employing in various building simulations. The TMDs of five representative cities are attached in the Appendix.

5.4 Summary

New typical meteorological year (TMY) included 8760 data records for 24

locations of China was developed based on the proposed decomposition solar model in Chapter 2, the proposed atmospheric radiation model in Chapter 4, and the latest routine meteorological elements from 2006 to 2016, which is indispensable for building simulation. Several data processing methods were utilized for the development of TMY such as the separation of direct and diffuse solar radiation, the selection of typical meteorological months (TMMs), and the data smoothing connection. In addition, the typical meteorological days (TMDs) included 288 data records were also developed for 24 locations of China using the same datasets for developing TMY. The proposed TMY and TMD will be significant for studying on building thermal simulation and energy consumption simulation in Chinese locations.

Table 5.10 Data format of the TMY file for Beijing

MON	DAY	HOUR	LOCT	TEM	DEW	RH	X	TH	NR	DF	WD	WS	CC	AZ	HT	AP	SH	LW
1	1	1	0.7	-5.8	-20	32	7.5	0	0	0	1	2.5	0	999	0	1034.3	0	184.3
1	1	2	1.7	-6.1	-20	32	7.4	0	0	0	1	1.8	0	999	0	1034.6	0	183
1	1	3	2.7	-6.1	-20.2	32	7.3	0	0	0	1	1.8	0	999	0	1034.7	0	183
1	1	4	3.7	-6.4	-20	33	7.4	0	0	0	2	1.8	0	999	0	1034.7	0	182.7
1	1	5	4.7	-7.2	-19.4	37	7.8	0	0	0	2	1.8	0	999	0	1034.8	0	183
1	1	6	5.7	-8.1	-18.9	41	8.2	0	0	0	2	1.5	0	999	0	1034.9	0	182.6
1	1	7	6.7	-8.4	-18.7	43	8.3	0	0	0	1	1.2	0	999	0	1034.9	0	183
1	1	8	7.7	-7.8	-18.9	40	8.2	0	0	0	1	0.9	0	-56	3	1035	0.05	183.1
1	1	9	8.7	-6.2	-19.1	35	8	144	352	71	1	0.9	0	-46	12	1034.5	0.21	185.6
1	1	10	9.7	-4	-19.3	29	7.9	297	654	80	2	0.9	0	-33	19	1034	0.33	189.1
1	1	11	10.7	-1.7	-19.4	24	7.8	418	835	72	2	0.9	0	-20	24	1033.5	0.41	193.3
1	1	12	11.7	-0.1	-19.4	22	7.8	465	863	75	2	1.2	0	-5	27	1033	0.45	197.8
1	1	13	12.7	0.7	-19.3	21	7.9	437	794	86	8	1.5	0	11	26	1032.5	0.44	200
1	1	14	13.7	0.6	-18.9	21	8.2	344	636	99	8	1.8	0	26	23	1032	0.38	199.5
1	1	15	14.7	0.1	-18.4	23	8.6	220	457	90	8	1.8	0	39	17	1032.1	0.28	200.2
1	1	16	15.7	-0.6	-18	25	8.9	83	204	53	11	1.8	0	50	8	1032.1	0.15	199.7
1	1	17	16.7	-1.1	-17.8	27	9	0	0	0	11	1.8	0	999	0	1032.2	0	200
1	1	18	17.7	-1.6	-17.8	28	9	0	0	0	11	1.5	0	999	0	1032.2	0	198.9
1	1	19	18.7	-2.3	-17.7	29	9.1	0	0	0	9	1.2	0	999	0	1032.3	0	196.8
1	1	20	19.7	-3.3	-17.2	33	9.5	0	0	0	9	0.9	0	999	0	1032.3	0	196.7
1	1	21	20.7	-4.6	-16.4	39	10.1	0	0	0	9	0.9	0	999	0	1032.2	0	196.6
1	1	22	21.7	-5.8	-16.2	43	10.3	0	0	0	9	0.9	0	999	0	1032.1	0	194.7
1	1	23	22.7	-6.7	-16.1	47	10.4	0	0	0	9	0.9	0	999	0	1032	0	193.9
1	1	24	23.7	-7.5	-15.3	53	11.1	0	0	0	9	0.9	0	999	0	1031.9	0	194.8

CHAPTER 6

Conclusions and suggestions

6.1 Conclusions

Solar radiation and atmospheric radiation data, especially the hourly values, are very significant for a variety of applications in the building field. For example, solar radiation data are indispensable for building thermal simulation, air-conditioning design, as well as the photovoltaic (PV) systems. While the atmospheric radiation data are valuable for building radiative cooling design and the building simulation. However, the weather stations that measured solar radiation and atmospheric radiation are very few compared with those that measured routine meteorological elements such as temperature, relative humidity, and wind speed. Moreover, most weather stations can only provide daily values or monthly values of solar radiation; what's worse, the routine weather stations can't provide the measured values of atmospheric radiation in China, which will not meet the needs of various applications in building field. Therefore, developing the empirical models of solar radiation and atmospheric radiation using other routine meteorological elements (temperature, relative humidity, and sunshine duration) are necessary and significant for making up for the data deficiency.

To develop the solar radiation and atmospheric radiation data for building simulation in China, a series of related work were carried out in this study: 1)Two different hourly solar radiation models (decomposition model and sunshine duration based model) were proposed for all-sky conditions, which have good performance with high estimation accuracy. 2) The downward longwave radiation model (atmospheric radiation model) was established based on the temperature, water vapor pressure and relative humidity, and the distribution maps of downward longwave radiation and radiative cooling potential over parts of China were created, which are valuable for building simulation and building radiative cooling system design. 3) The new typical meteorological year (TMY) was developed for 24 locations of China based on the proposed decomposition solar model, the proposed atmospheric radiation model and the routine meteorological elements from 2006 - 2016, which is significant

for building thermal simulation and building energy consumption simulation.

The research background, research purpose, and research significance were stated in Chapter 1.

In Chapter 2, a new decomposition solar model which can divide the daily values of solar radiation into the hourly values was proposed using the hourly/daily radiation ratio for all-sky conditions. Moreover, two kinds of hourly solar radiation datasets (the frequency levels of 95% and 97.5%) are established for Chinese locations. The main conclusions from this study are as follows:

(1) Compared with the Zhang model, the proposed model is more accurate with the average of R^2, 0.90 and RMSE, 81.61 W/m^2. The proposed model also can estimate the hourly solar radiation better for all-sky conditions and wider locations compared with other existing decomposition models in China.

(2) The latest hourly global solar radiation dataset from 2006 to 2016 for the 17 locations was developed using the proposed model, which can be used to generate the Typical Meteorological Year (TMY).

(3) As an application of the new hourly solar radiation dataset, two kinds of datasets (frequency levels of 95% and 97.5%) for air-conditioning were developed, which can provide a valuable reference for air-conditioning design.

In Chapter 3, a new hourly solar model, which was different from the decomposition model, was proposed using the hourly sunshine duration for all-sky conditions. The hourly values of solar radiation are more useful than daily values for some specific applications; however, the existing solar models for estimating hourly values are much less than those for estimating daily values. Furthermore, most of the hourly solar models were developed only for clear-sky conditions, not for all-sky conditions. In the current empirical solar models, the daily sunshine duration parameter has been extensively studied and discussed such as Angstrom-Prescott equation; however, the hourly sunshine duration parameter was paid little attention. Therefore, the hourly sunshine duration was introduced and discussed, and then two existing hourly solar models: Nimiya model and Zhang model were analyzed

and improved for Beijing. The main conclusions of this study are as follows:

(1) The hourly sunshine duration parameter was very effective for estimating solar radiation under all-sky conditions, which should be considered more in future empirical solar models.

(2) The Nimiya model was modified by replacing the daily mean temperature with the three-hour temperature difference, the performance of which was better than the original Nimiya model for Beijing.

(3) The proposed model in this study had better performance with a higher correlation coefficient (0.956) and lower RMSE (84.59 W/m^2) compared with the modified Nimiya model for Beijing.

(4) The proposed model also performed very well for estimating the daily solar values by adding up the hourly values for each day.

In Chapter 4, new empirical models of downward longwave radiation (atmospheric radiation), which can be classified into four cases: all day, nighttime, daytimes with and without cloud modification factor, were developed based on the routine meteorological parameters (temperature, water vapor pressure and relative humidity) for all-sky conditions in China. Since the measured LW radiation data is not available in the meteorological stations, few studies have focused on the modeling of downward longwave radiation in China. As the application of the new proposed models in this study, the distribution maps of the downward longwave radiation and the radiative cooling potential were generated over China, which can provide a valuable reference for building radiative cooling design. The main conclusions of this study are as follows:

(1) For the all day, the proposed downward longwave radiation performs well with R^2 of 0.86 and RMSE of 30.26 W/m^2, which is more accurate than the Sridhar model under all-sky conditions for locations in China.

(2) For the daytime, if the hourly cloud data or the solar radiation data are available, the model with cloud modification factor is favorable, which is more accurate than the Crawford and Duchon model with R^2 of 0.87 and RMSE of 28.59 W/m^2;

otherwise, the model without cloud modification factor is recommended for simplicity with limited errors.

(3) For the nighttime, the proposed model was employed in calculating the radiative cooling potential of 351 locations in China, which can provide a valuable reference for the design of building radiative cooling system.

In Chapter 5, new typical meteorological year (TMY) for 24 locations of China was developed based on the proposed decomposition solar model (Chapter 2), the proposed atmospheric radiation model, and the routine meteorological elements such as temperature from 2006 - 2016. A series of data processing were conducted based on the statistical methods and the global solar radiation was separated into the direct normal and diffuse components using the Gompertz function. Five representative locations (Harbin, Beijing, Shanghai, Guangzhou and Kunming) were selected to compare and discuss. The main conclusions of this study are as follows:

(1) The hourly global solar radiation data was calculated using the proposed decomposition solar model, which has been proven to be more accurate than the original Zhang solar model.

(2) The atmospheric radiation data was calculated using the proposed downward longwave radiation model, which is a significant supplement to the TMY.

(3) The TMY of 24 locations for about the recent years was developed based on the routine meteorological elements from 2006 - 2016, as well as the statistical methods.

Chapter 6 makes some conclusions on this study, and gives suggestion for further studies.

6.2 Suggestions for further studies

This study also has some suggestions for further studies, which are listed as follows:

(1) For the new decomposition solar model in Chapter 2, it should be expanded to more locations.
(2) For the hourly sunshine duration solar model in Chapter 3, more hourly sunshine duration data for other locations should be collected to test the model performance.
(3) For the atmospheric radiation model in Chapter 4, one of our proposed models for the nighttime has no cloud parameter, which is where it needs to be improved. In addition, the applicability of our models for Southern China needs to be further verified.
(4) For the proposed TMY in Chapter 5, it should be expanded to more Chinese locations, and be compared with the existing TMY through calculating the building cooling and heating loads.

To study the impact of global warming on building energy consumption, future TMY such as the next 20 years, 50 years is indispensable. The simulated data generated from the global climate model (GCM) is one of the important data sources for developing future TMY. The BCC_CSM1.1(m) dataset is developed using the Beijing Climate Center Climate System Model and has future data records. Therefore, developing future TMY based on the BCC_CSM1.1(m) data will be worthy of future studies.

Publications

1. Kai Chang, and Qingyuan Zhang. “Improvement of the hourly global solar model and solar radiation for air-conditioning design in China.” Renewable energy 138 (2019): 1232-1238.

2. Kai Chang, and Qingyuan Zhang. “Modeling of downward longwave radiation and radiative cooling potential in China.” Journal of Renewable and Sustainable Energy 11, 066501 (2019); https://doi.org/10.1063/1.5117319

Acknowledgement

First of all, I would like to thank my supervisor, Prof. Zhang Qingyuan for his guidance and helps during my Ph.D. studies. His kindness, rich knowledge, rigorous and diligent attitude, and modesty will have a positive and profound impact on my future work and life. He always reminds me to cherish time and not to waste my life, and gives me valuable advice when I have problems in research. Without his care and guidance, I think I would not finish my studies smoothly.

I also wish to thank the graduation committee members: Prof. Sadohara Satoru, Prof. Narumi Daisuke, Prof. Tanaka Ineko, and Prof. Yoshida Satoshi for their valuable comments and suggestions. Special thanks are given to Prof. Tanaka Ineko for her care and guidance.

I am greatly appreciating the help from my friends in Japan, we spent too many happy days together and see too many beautiful sceneries together. I am also thankful to my friends in China and I will hardly forget her encouragement and company.

Finally, I am deeply grateful to my father, Chang Tao and my mother, Xiang Cuirong for their consistent support and understanding.

Chang Kai

Yokohama, Japan

2019.12.9

References:

[1] Hall, I.; Prairie, R.; Anderson, H.; Boes, E. Generation of Typical Meteorological Years for 26 SOLMET Stations; Technical Report SAND78-1601; Sandia National Laboratories: Albuquerque, NM, USA, 1978.

[2] Marion,W.; Urban, K. Users Manual for TMY2s-Typical Meteorological Years Derived from the 1961–1990 National Solar Radiation Data Base; Technical Report NREL/TP-463-7668; National Renewable Energy Laboratory: Golden, CO, USA, 1995.

[3] Wilcox, S.; Marion,W. User's Manual for TMY3 Data Sets; Technical Report NREL/TP-581-43156; National Renewable Energy Laboratory: Golden, CO, USA, 2008.

[4] Thevenard, Didier J., and Alfred P. Brunger. "The development of typical weather years for international locations: part I, algorithms." *Ashrae Transactions* 108 (2002): 376.

[5] Joe, Yu, Huang Fenxian, Donghyun Seo, and Moncef Krarti. "Development of 3012 IWEC2 Weather Files for International Locations (RP-1477)." *ASHRAE transactions* 120, no. 1 (2014).

[6] 松尾陽. (1974). 標準気象データに関する研究. *空気調和 衛生工学*, *48*, 603-625.

[7] 曽我和弘, 赤坂裕. "標準年気象データの作成法に関する研究: EA 法と SHASE 法の比較." *日本建築学会環境系論文集* 69, no. 581 (2004): 21-28.

[8] Pissimanis, D., G. Karras, V. Notaridou, and K. Gavra. "The generation of a ~~–t~~ypical meteorological year" for the city of Athens." *Solar Energy* 40, no. 5 (1988): 405-411.

[9] https://energyplus.net/weather/sources#TMY, accessed in 2019.12.01

[10] Bre, Facundo, and Victor D. Fachinotti. "Generation of typical meteorological years for the Argentine Littoral Region." *Energy and Buildings* 129 (2016): 432-444.

[11] Qingyuan, Zhang, Joe Huang, and Lang Siwei. "Development of typical year weather data for Chinese locations." *ASHRAE transactions* 108, no. 2 (2002):

1063-75.

[12] 张晴原. (2004). *中国建筑用标准气象数据库*. 机械工业出版社.

[13] Zhang, Qinyuan, and Hongxing Yang. "Typical meteorological database handbook for buildings." *China Achitecture & Building Press: Beijing, China* (2012).

[14] Bureau, China Meteorological. "China standard weather data for analyzing building thermal conditions." *Beijing, China: China Building Industry Publishing House* (2005).

[15]http://www.cma.gov.cn/en/aboutcma/brochure/201203/P020120319791316093320.pdf, accessed in 2019.12.01

[16] Chen, J. L., & Li, G. S. (2013). Estimation of monthly average daily solar radiation from measured meteorological data in Yangtze River Basin in China. International Journal of Climatology, 33(2), 487-498.

[17] Yaman, K., & Arslan, G. (2018, June). The impact of hourly solar radiation model on building energy analysis in different climatic regions of Turkey. In Building Simulation (Vol. 11, No. 3, pp. 483-495). Tsinghua University Press.

[18] Besharat, F., Dehghan, A. A., & Faghih, A. R. (2013). Empirical models for estimating global solar radiation: A review and case study. Renewable and Sustainable Energy Reviews, 21, 798-821.

[19] Prescott, J. A. (1940). Evaporation from a water surface in relation to solar radiation. Trans. Roy. Soc. S. Aust., 46, 114-118.

[20] Jain, S., & Jain, P. C. (1988). A comparison of the Angstrom-type correlations and the estimation of monthly average daily global irradiation. Solar Energy, 40(2), 93-98.

[21] Supit, I., & Van Kappel, R. R. (1998). A simple method to estimate global radiation. Solar Energy, 63(3), 147-160.

[22] Badescu, V. (1999). Correlations to estimate monthly mean daily solar global irradiation: application to Romania. Energy, 24(10), 883-893.

[23] Hargreaves, G. H., & Samani, Z. A. (1982). Estimating potential evapotranspiration. Journal of the Irrigation and Drainage Division, 108(3),

225-230.

[24] Bristow, K. L., & Campbell, G. S. (1984). On the relationship between incoming solar radiation and daily maximum and minimum temperature. Agricultural and Forest Meteorology, 31(2), 159-166.

[25] Allen, R. G. (1997). Self-calibrating method for estimating solar radiation from air temperature. Journal of Hydrologic engineering, 2(2), 56-67.

[26] Almorox, J. Y., & Hontoria, C. (2004). Global solar radiation estimation using sunshine duration in Spain. Energy Conversion and Management, 45(9-10), 1529-1535.

[27] Chen, R., Ersi, K., Yang, J., Lu, S., & Zhao, W. (2004). Validation of five global radiation models with measured daily data in China. Energy Conversion and Management, 45(11-12), 1759-1769.

[28] Wu, G., Liu, Y., & Wang, T. (2007). Methods and strategy for modeling daily global solar radiation with measured meteorological data–A case study in Nanchang station, China. Energy conversion and management, 48(9), 2447-2452.

[29] ASHRAE, ASHRAE handbook of fundamentals, Ventilation and infiltration. Atlanta, American Society of Heating, Refrigerating and Air-Conditioning Engineers, Inc., 2005.

[30] Nijegorodov, N. (1996). Improved ASHRAE model to predict hourly and daily solar radiation components in Botswana, Namibia, and Zimbabwe. Renewable energy, 9(1-4), 1270-1273.

[31] Machler, M. A., & Iqbal, M. (1985). A modification of the ASHRAE clear sky irradiation model. ASHRAE transactions, 91(1), 106-115.

[32] Parishwad, G. V., Bhardwaj, R. K., & Nema, V. K. (1997). Estimation of hourly solar radiation for India. Renewable Energy, 12(3), 303-313.

[33] Whillier, A. (1956). The determination of hourly values of total solar radiation from daily summations. Archiv für Meteorologie, Geophysik und Bioklimatologie, Serie B, 7(2), 197-204.

[34] Liu, B. Y., & Jordan, R. C. (1960). The interrelationship and characteristic

distribution of direct, diffuse and total solar radiation. Solar energy, 4(3), 1-19.

[35] Jain, P. C. (1984). Comparison of techniques for the estimation of daily global irradiation and a new technique for the estimation of hourly global irradiation (No. IC--84/9). International Centre for Theoretical Physics.

[36] Baig, A., Akhter, P., & Mufti, A. (1991). A novel approach to estimate the clear day global radiation. Renewable Energy, 1(1), 119-123.

[37] Newell, T. A. (1983). Simple models for hourly to daily radiation ratio correlations. Solar Energy, 31(3), 339-342.

[38] Kambezidis, H. D., Psiloglou, B. E., Karagiannis, D., Dumka, U. C., & Kaskaoutis, D. G. (2017). Meteorological Radiation Model (MRM v6. 1): Improvements in diffuse radiation estimates and a new approach for implementation of cloud products. Renewable and Sustainable Energy Reviews, 74, 616-637.

[39] Yao, W., Li, Z., Xiu, T., Lu, Y., & Li, X. (2015). New decomposition models to estimate hourly global solar radiation from the daily value. Solar Energy, 120, 87-99.

[40] Kim, K. H., Baltazar, J. C., & Haberl, J. S. (2014). Evaluation of meteorological base models for estimating hourly global solar radiation in Texas. Energy Procedia, 57, 1189-1198.

[41] Kim, K. H., Oh, J. K. W., & Jeong, W. (2016). Study on solar radiation models in South Korea for improving office building energy performance analysis. Sustainability, 8(6), 589.

[42] Seo, D., & Krarti, M. (2007). Impact of Solar Models on Building Energy Analysis for Tropical Sites. ASHRAE Transactions, 113(1).

[43] https://www.ncdc.noaa.gov/isd/data-access, accessed in 2019.12.01

[44] http://data.cma.cn/data/cdcdetail/dataCode/RADI_MUL_CHN_DAY.html, accessed in 2019.12.01

[45] Sungur, C. (2009). Multi-axes sun-tracking system with PLC control for photovoltaic panels in Turkey. Renewable Energy, 34(4), 1119-1125.

[46] Despotovic, M., Nedic, V., Despotovic, D., & Cvetanovic, S. (2015). Review and

statistical analysis of different global solar radiation sunshine models. Renewable and Sustainable Energy Reviews, 52, 1869-1880.

[47] Benson, M. A. (1958). Characteristics of frequency curves based on a theoretical 1,000-year record (No. 58-13). US Dept. of the Interior, Geological Survey, Water Resources Division,.

[48] Zhang, Q. (2006). Development of the typical meteorological database for Chinese locations. Energy and buildings, 38(11), 1320-1326.

[49] Zhang, J., Zhao, L., Deng, S., Xu, W., & Zhang, Y. (2017). A critical review of the models used to estimate solar radiation. Renewable and Sustainable Energy Reviews, 70, 314-329.

[50] Shen, P. (2017). Impacts of climate change on US building energy use by using downscaled hourly future weather data. Energy and Buildings, 134, 61-70.

[51] Mousavi Maleki, Seyed Abbas, H. Hizam, and Chandima Gomes. "Estimation of hourly, daily and monthly global solar radiation on inclined surfaces: Models re-visited." *Energies* 10, no. 1 (2017): 134.

[52] Despotovic, Milan, et al. "Review and statistical analysis of different global solar radiation sunshine models." Renewable and Sustainable Energy Reviews 52 (2015): 1869-1880.

[53] Angstrom, Anders. "Solar and terrestrial radiation. Report to the international commission for solar research on actinometric investigations of solar and atmospheric radiation." Quarterly Journal of the Royal Meteorological Society 50.210 (1924): 121-126.

[54] Handbook, ASHRAE Fundamentals. "American Society of Heating." Refrigerating and Air Conditioning Engineers, Atlanta (2005).

[55] Ineichen, Pierre, and Richard Perez. "A new airmass independent formulation for the Linke turbidity coefficient." Solar Energy 73.3 (2002): 151-157.

[56] Rigollier, Christelle, Olivier Bauer, and Lucien Wald. "On the clear sky model of the ESRA—European Solar Radiation Atlas—with respect to the Heliosat method." Solar energy 68.1 (2000): 33-48.

[57] Nimiya, H., H. Akasaka, and Y. Matsuo. "A method to estimate the hourly

downward atmospheric radiation using AMeDAS data." *TRANSACTIONS-SOCIETY OF HEATING AIR CONDITIONING AND SANITARY ENGINEERS OF JAPAN* (1996): 133-144.

[58] Yao, Wanxiang, et al. "Evaluation of global solar radiation models for Shanghai, China." *Energy conversión and management* 84 (2014): 597-612.

[59] Chang, Kai, and Qingyuan Zhang. "Improvement of the hourly global solar model and solar radiation for air-conditioning design in China." Renewable energy 138 (2019): 1232-1238.

[60] http://data.cma.cn/en, accessed in 2019.12.01

[61] Duffie, J. A., Beckman, W. A., & Worek, W. M. (1994). Solar engineering of thermal processes.

[62] Antonanzas-Torres, F., R. Urraca, J. Polo, O. Perpiñán-Lamigueiro, and R. Escobar. "Clear sky solar irradiance models: A review of seventy models." *Renewable and Sustainable Energy Reviews* 107 (2019): 374-387.

[63] Iziomon, MOSES G., H. E. L. M. U. T. Mayer, and A. N. D. R. E. A. S. Matzarakis. "Downward atmospheric longwave irradiance under clear and cloudy skies: Measurement and parameterization." Journal of Atmospheric and Solar-Terrestrial Physics 65.10 (2003): 1107-1116.

[64] Vall, S., & Castell, A. (2017). Radiative cooling as low-grade energy source: a literature review. Renewable and Sustainable Energy Reviews, 77, 803-820.

[65] Li, Mengying, Yuanjie Jiang, and Carlos FM Coimbra. "On the determination of downward long-wave irradiance under all-sky conditions." Solar Energy 144 (2017): 40-48.

[66] Goforth, Mark A., George W. Gilchrist, and Joseph D. Sirianni. "Cloud effects on thermal downwelling sky radiance." Thermosense XXIV. Vol. 4710. International Society for Optics and Photonics, 2002.

[67] Wang, Kaicun, and Robert E. Dickinson. "Global atmospheric downward longwave radiation at the surface from ground‐based observations, satellite retrievals, and reanalyses." Reviews of Geophysics 51.2 (2013): 150-185.

[68] Evangelisti, Luca, Claudia Guattari, and Francesco Asdrubali. "On the sky

temperature models and their influence on buildings energy performance: A critical review." Energy and Buildings 183 (2019): 607-625.

[69] Kneizys, Francis X., et al. Users guide to LOWTRAN 7. No. AFGL-TR-88-0177. AIR FORCE GEOPHYSICS LAB HANSCOM AFB MA, 1988.

[70] Snell, Hilary E., et al. "Validation of FASE (FASCODE for the environment) and MODTRAN3: Updates and comparisons with clear-sky measurements." Passive Infrared Remote Sensing of Clouds and the Atmosphere III. Vol. 2578. International Society for Optics and Photonics, 1995.

[71] Masiri, I., et al. "A technique for mapping downward longwave radiation using satellite and ground-based data in the tropics." Renewable energy 103 (2017): 171-179.

[72] Brunt, David. "Notes on radiation in the atmosphere. I." Quarterly Journal of the Royal Meteorological Society 58.247 (1932): 389-420.

[73] Elsasser, Walter M. "Heat transfer by infrared radiation in the atmosphere." Harvard Meteor. Studies 6 (1942): 107.

[74] Swinbank, W. CQJR. "Long‐wave radiation from clear skies." Quarterly Journal of the Royal Meteorological Society 89.381 (1963): 339-348.

[75] Idso, Sherwood B., and Ray D. Jackson. "Thermal radiation from the atmosphere." Journal of Geophysical Research 74.23 (1969): 5397-5403.

[76] Idso, Sherwood B. "A set of equations for full spectrum and 8‐to 14‐μm and 10.5‐to 12.5‐μm thermal radiation from cloudless skies." Water resources research 17.2 (1981): 295-304.

[77] Centeno, Melchor. "New formulae for the equivalent night sky emissivity." Solar Energy 28.6 (1982): 489-498.

[78] Berdahl, Paul, and Richard Fromberg. "The thermal radiance of clear skies." Solar Energy 29.4 (1982): 299-314.

[79] Brutsaert, Wilfried. "On a derivable formula for long‐wave radiation from clear skies." Water Resources Research 11.5 (1975): 742-744.

[80] Crawford, Todd M., and Claude E. Duchon. "An improved parameterization for estimating effective atmospheric emissivity for use in calculating daytime

downwelling longwave radiation." Journal of Applied Meteorology 38.4 (1999): 474-480.

[81] Wang, Jiao, et al. "Estimation of surface longwave radiation over the Tibetan plateau region using MODIS data for cloud-free skies." IEEE Journal of Selected Topics in Applied Earth Observations and Remote Sensing 7.9 (2014): 3695-3703.

[82] Qingyuan, Zhang, and Liu Yu. "Potentials of passive cooling for passive design of residential buildings in China." Energy Procedia 57 (2014): 1726-1732.

[83] https://db.cger.nies.go.jp/asiafluxdb/?page_id=15, accessed in 2019.12.01

[84] Kumar, Ravinder, and L. Umanand. "Estimation of global radiation using clearness index model for sizing photovoltaic system." Renewable energy 30.15 (2005): 2221-2233.

[85] Sridhar, V., and Ronald L. Elliott. "On the development of a simple downwelling longwave radiation scheme." Agricultural and Forest Meteorology 112.3-4 (2002): 237-243.

[86] Zhai, Yao, et al. "Scalable-manufactured randomized glass-polymer hybrid metamaterial for daytime radiative cooling." Science 355.6329 (2017): 1062-1066.

[87] Li, Mengying, Hannah B. Peterson, and Carlos FM Coimbra. "Radiative cooling resource maps for the contiguous United States." Journal of Renewable and Sustainable Energy 11.3 (2019): 036501.

[88] Kasten, Fritz, and Andrew T. Young. "Revised optical air mass tables and approximation formula." Applied optics 28.22 (1989): 4735-4738.

[89] Ineichen, Pierre. "Conversion function between the Linke turbidity and the atmospheric water vapor and aerosol content." Solar Energy 82.11 (2008): 1095-1097.

[90] Inman, Rich H., James G. Edson, and Carlos FM Coimbra. "Impact of local broadband turbidity estimation on forecasting of clear sky direct normal irradiance." Solar Energy 117 (2015): 125-138.

[91] http://www.soda-pro.com/help/general-knowledge/linke-turbidity-factor,

accessed in 2019.12.01

[92] Sousa, Joana. "Energy simulation software for buildings: review and comparison." In *International Workshop on Information Technology for Energy Applicatons-IT4Energy, Lisabon*. 2012.

[93] Wang, Haojie, and Qingyan Chen. "Impact of climate change heating and cooling energy use in buildings in the United States." *Energy and Buildings* 82 (2014): 428-436.

[94] Said, S. A. M., and H. M. Kadry. "Generation of representative weather—year data for Saudi Arabia." Applied Energy 48, no. 2 (1994): 131-136.

[95] Thevenard, Didier J., and Alfred P. Brunger. "The development of typical weather years for international locations: Part II, production/Discussion." ASHRAE Transactions 108 (2002): 480.

[96] El-Sebaii, A. A., F. S. Al-Hazmi, A. A. Al-Ghamdi, and Saud Jameel Yaghmour. "Global, direct and diffuse solar radiation on horizontal and tilted surfaces in Jeddah, Saudi Arabia." Applied energy 87, no. 2 (2010): 568-576.

[97] Zhang, Q., C. Lou, and H. X. Yang. "A new method to separate horizontal solar radiation into direct and diffuse components." (2004).

[98] Bilguun BUYANTOGTOKH, Qingyuan ZHANG. "DEVELOPMENT OF SOLAR MODEL AND TYPICAL METEOROLOGICAL YEAR FOR ULAANBAATAR, MONGOLIA", Journal of Environmental Engineering (Transactions of AIJ), 2017

[99] Zhang, Qingyuan. "Climatic zoning for the thermal design of residences in China based on heating degree-days and cooling degree-hours." *Journal of Asian Architecture and Building Engineering* 4, no. 2 (2005): 533-539.

[100] Yang, Liu, Joseph C. Lam, and Jiaping Liu. "Analysis of typical meteorological years in different climates of China." Energy Conversion and Management 48, no. 2 (2007): 654-668.

Appendix Typical Meteorological Days (TMDs)

Abbreviations:

TEM: dry-bulb temperature (℃)

DEW: dew point temperature (℃)

RH: relative humidity (%)

X: humidity ratio (0.1g/kg)

TH: global horizontal solar radiation (W/m^2)

NR: direct normal solar radiation (W/m^2)

DF: diffuse solar radiation (W/m^2)

WD: wind direction

WS: wind speed (m/s)

CC: cloud cover

AP: atmospheric pressure (hPa)

LW: atmospheric radiation (W/m^2)

Harbin

HOUR	TEM	DEW	RH	X	TH	NR	DF	WD	WS	CC	AP	LW
						January						
1	-19.2	-22.7	74	6.6	0	0	0	9	1.5	3	1008.9	158
2	-19.5	-23	74	6.4	0	0	0	9	1.5	4	1008.9	156.8
3	-19.7	-23.2	74	6.4	0	0	0	9	1.5	4	1008.9	155.9
4	-20	-23.5	74	6.2	0	0	0	8	1.5	3	1008.9	154.8
5	-20.4	-23.9	74	6.1	0	0	0	8	1.5	3	1009	153.3
6	-20.9	-24.1	75	6	0	0	0	8	1.6	4	1009	152.2
7	-20.9	-24.1	76	6	0	0	0	8	1.6	4	1009	152.2
8	-20.3	-23.6	75	6.2	49	138	33	8	1.6	4	1009.1	154.2
9	-19	-22.6	73	6.7	154	324	76	8	1.9	5	1008.9	158.4
10	-17.1	-21.4	69	7.3	230	365	108	9	2.1	5	1008.8	164
11	-15.1	-20.4	65	8	267	353	130	9	2.4	5	1008.7	169.5
12	-13.6	-19.7	61	8.4	302	457	121	9	2.5	5	1008.5	173.2
13	-12.9	-19.6	58	8.5	287	513	102	10	2.6	4	1008.3	174.6
14	-12.9	-19.7	57	8.4	216	484	79	10	2.7	4	1008.2	174.1
15	-13.4	-19.9	59	8.3	118	421	45	10	2.5	4	1008.3	172.8
16	-14.2	-20.1	62	8.1	19	75	14	10	2.2	4	1008.5	171.2
17	-15	-20.3	65	8	0	0	0	10	1.9	4	1008.7	169.8
18	-15.7	-20.5	67	7.8	0	0	0	10	1.9	4	1008.8	168.4
19	-16.2	-20.7	69	7.7	0	0	0	9	1.8	4	1009	167.1
20	-16.6	-21	69	7.5	0	0	0	9	1.7	4	1009.1	165.8
21	-17.1	-21.3	70	7.4	0	0	0	9	1.7	3	1009.1	164.5
22	-17.6	-21.6	72	7.2	0	0	0	8	1.6	3	1009.1	163.1
23	-18.2	-21.9	73	7	0	0	0	8	1.6	3	1009.1	161.3
24	-18.7	-22.3	74	6.8	0	0	0	8	1.5	3	1009.1	159.7
						February						
1	-14.6	-19.1	70	9.4	0	0	0	9	1.7	4	1005.6	174.7
2	-15	-19.5	70	9.3	0	0	0	9	1.7	4	1005.6	173.3
3	-15.4	-19.8	70	9.1	0	0	0	9	1.7	4	1005.6	171.8
4	-15.8	-20.1	70	8.9	0	0	0	8	1.7	4	1005.7	170.3
5	-16.2	-20.3	71	8.7	0	0	0	8	1.7	3	1005.8	169.1
6	-16.4	-20.4	72	8.6	0	0	0	8	1.8	4	1005.9	168.8
7	-16.2	-20.1	72	8.7	29	89	20	9	1.9	4	1005.9	169.7
8	-15.2	-19.6	70	9	123	257	68	9	2	4	1006	172.3
9	-13.6	-18.9	66	9.4	244	384	113	9	2.3	4	1005.8	176.3
10	-11.7	-18.1	60	10	338	445	142	10	2.7	5	1005.6	181.3
11	-9.8	-17.4	55	10.6	390	457	161	10	3	5	1005.4	186.1
12	-8.4	-17	51	10.9	434	561	147	10	3.1	5	1005.2	189.5
13	-7.6	-16.8	49	11.1	421	622	124	11	3.3	5	1005	191.3
14	-7.5	-16.8	49	11.1	347	611	102	11	3.4	5	1004.8	191.7
15	-7.8	-16.8	50	11.2	243	608	69	11	3.1	5	1004.9	191.2
16	-8.4	-16.8	52	11.2	99	416	37	10	2.7	5	1005	190.3
17	-9.1	-16.8	55	11.2	3	3	3	10	2.4	5	1005.2	189.1
18	-9.9	-16.9	58	11.1	0	0	0	10	2.2	4	1005.3	187.7
19	-10.7	-17	61	10.9	0	0	0	9	2	4	1005.4	186.1
20	-11.5	-17.3	64	10.8	0	0	0	9	1.9	4	1005.5	184.4
21	-12.2	-17.6	65	10.6	0	0	0	9	1.8	4	1005.5	182.7
22	-12.8	-17.9	67	10.3	0	0	0	9	1.8	4	1005.5	180.8
23	-13.4	-18.3	68	10	0	0	0	9	1.8	3	1005.5	178.8
24	-13.9	-18.6	69	9.8	0	0	0	9	1.7	4	1005.4	177.3

Harbin

HOUR	TEM	DEW	RH	X	TH	NR	DF	WD	WS	CC	AP	LW
						March						
1	-5.2	-10.8	67	18.3	0	0	0	9	2.1	4	1000.3	215.5
2	-5.8	-11	69	18.1	0	0	0	9	2.1	5	1000.2	213.9
3	-6.4	-11.3	70	17.8	0	0	0	9	2.1	5	1000.3	212
4	-6.8	-11.6	71	17.5	0	0	0	9	2.1	4	1000.4	210.6
5	-6.9	-11.6	71	17.3	0	0	0	9	2.1	4	1000.4	210.3
6	-6.5	-11.4	70	17.5	26	71	20	9	2.3	5	1000.5	211.5
7	-5.6	-11.1	67	18	119	277	62	9	2.5	5	1000.6	214
8	-4.4	-10.8	63	18.4	236	329	117	9	2.6	5	1000.7	217.1
9	-2.9	-10.6	58	18.7	366	428	156	9	3	5	1000.5	220.1
10	-1.5	-10.6	53	18.7	463	483	181	10	3.3	6	1000.3	222.8
11	-0.3	-10.6	48	18.6	508	481	204	10	3.7	6	1000.1	225.1
12	0.6	-10.7	46	18.5	548	569	186	10	3.7	6	999.8	226.7
13	1.1	-10.7	44	18.5	529	603	166	11	3.8	6	999.5	227.9
14	1.4	-10.7	44	18.6	453	592	143	11	3.9	6	999.3	228.6
15	1.4	-10.7	44	18.6	352	610	102	11	3.6	6	999.4	228.6
16	1	-10.7	45	18.7	215	588	60	10	3.3	6	999.6	228
17	0.4	-10.6	47	18.8	58	290	25	10	3	6	999.7	226.9
18	-0.4	-10.4	50	19	0	0	0	10	2.7	6	999.9	225.6
19	-1.4	-10.3	54	19.1	0	0	0	10	2.4	5	1000	224.2
20	-2.3	-10.2	58	19.3	0	0	0	10	2.1	5	1000.2	222.8
21	-3	-10.2	61	19.3	0	0	0	10	2.1	4	1000.2	221.6
22	-3.6	-10.3	62	19.1	0	0	0	9	2.1	4	1000.1	220.2
23	-4.1	-10.4	64	18.8	0	0	0	9	2.1	4	1000.1	218.9
24	-4.5	-10.5	65	18.7	0	0	0	9	2.1	4	1000.1	217.9
						April						
1	4.6	-4	58	30.8	0	0	0	9	2.3	5	995.2	258
2	3.9	-4	60	30.8	0	0	0	9	2.3	5	995.2	256.5
3	3.2	-4.1	63	30.8	0	0	0	9	2.3	5	995.3	254.8
4	2.7	-4.1	65	30.6	0	0	0	9	2.3	5	995.4	253.6
5	2.8	-4	64	30.6	20	68	15	9	2.3	5	995.5	254.2
6	3.7	-3.8	61	31.1	106	237	60	9	2.6	5	995.6	256.7
7	5.2	-3.6	57	31.6	228	300	120	9	3	5	995.7	260.6
8	6.9	-3.5	51	31.9	335	305	180	9	3.3	5	995.8	264.9
9	8.5	-3.8	46	31.6	448	358	224	9	3.6	6	995.5	268.2
10	9.8	-4.2	41	30.8	528	388	255	10	4	6	995.3	270.2
11	10.7	-4.7	38	29.9	568	388	275	10	4.3	7	995	271.3
12	11.3	-5.1	36	29.2	586	421	268	10	4.3	7	994.7	271.9
13	11.8	-5.3	35	28.7	558	435	247	10	4.2	7	994.4	272.4
14	12.1	-5.5	34	28.5	492	437	212	10	4.2	7	994.2	273
15	12.2	-5.5	34	28.5	399	448	164	10	4	7	994.3	273.2
16	11.9	-5.4	35	28.7	280	454	109	10	3.8	7	994.5	272.6
17	11.2	-5.2	37	29.2	145	433	55	10	3.6	7	994.6	271.5
18	10.2	-4.8	40	29.9	27	154	16	10	3.2	6	994.8	270
19	9.1	-4.3	44	30.7	0	0	0	9	2.7	6	994.9	268.2
20	7.9	-3.9	48	31.5	0	0	0	9	2.3	5	995.1	266.4
21	7	-3.7	52	31.9	0	0	0	9	2.3	5	995.1	264.7
22	6.2	-3.7	54	31.8	0	0	0	9	2.3	5	995.1	263.1
23	5.8	-3.7	55	31.5	0	0	0	9	2.3	5	995	261.8
24	5.4	-3.7	56	31.6	0	0	0	9	2.3	5	995	261.1

Harbin

HOUR	TEM	DEW	RH	X	TH	NR	DF	WD	WS	CC	AP	LW
						May						
1	12.8	5.5	66	60.2	0	0	0	8	2.1	6	990.6	312.5
2	12.1	5.5	68	60.1	0	0	0	8	2.1	6	990.6	310.6
3	11.4	5.4	71	59.9	0	0	0	8	2.2	6	990.7	308.7
4	11	5.5	72	60	0	0	0	8	2.2	6	990.8	307.8
5	11.2	5.7	72	60.6	58	118	41	8	2.2	6	990.9	309.1
6	12.2	6	69	61.8	164	191	104	8	2.5	6	991	312.4
7	13.6	6.2	64	62.7	269	221	166	9	2.9	6	991.1	317
8	15.3	6.1	59	62.6	361	234	224	9	3.2	6	991.2	321.5
9	16.7	5.7	53	61.3	467	289	267	9	3.4	6	991	324.4
10	17.8	5.2	49	59.5	542	322	294	9	3.6	7	990.7	326
11	18.6	4.7	46	57.9	575	320	315	9	3.8	7	990.4	326.8
12	19.1	4.4	43	56.9	592	346	312	9	3.8	7	990.2	327.5
13	19.6	4.2	42	56.3	567	354	292	9	3.8	7	989.9	328.5
14	20	4.1	41	55.7	509	358	257	9	3.8	7	989.6	329.4
15	20.2	3.9	40	55.2	430	369	209	9	3.6	7	989.7	329.5
16	20	3.7	40	54.9	324	373	151	9	3.4	7	989.9	328.5
17	19.4	3.8	42	55.2	205	370	90	9	3.2	7	990	326.7
18	18.5	4.1	45	56.2	83	330	36	9	2.9	7	990.1	324.5
19	17.2	4.6	49	57.8	0	0	0	8	2.5	7	990.3	322.4
20	16	5.2	54	59.7	0	0	0	8	2.2	6	990.4	320.6
21	15	5.5	59	61.2	0	0	0	8	2.1	6	990.4	319.3
22	14.3	5.7	62	61.7	0	0	0	8	2.1	6	990.4	317.8
23	13.9	5.7	63	61.5	0	0	0	8	2.1	6	990.5	316.5
24	13.5	5.7	64	61.4	0	0	0	8	2.1	6	990.5	315.4
						June						
1	18.7	13.8	76	103.3	0	0	0	8	1.6	6	989.1	361.7
2	18.2	13.8	78	103	0	0	0	8	1.6	6	989.1	360
3	17.7	13.8	80	102.9	0	0	0	8	1.6	6	989.2	358.6
4	17.6	13.9	81	103.4	1	1	1	7	1.7	6	989.4	358.4
5	17.9	14.1	80	104.6	79	115	57	7	1.7	6	989.5	360.2
6	18.8	14.3	77	106.1	181	163	123	7	2	6	989.6	363.7
7	20.1	14.4	72	107.2	284	187	188	8	2.2	6	989.7	368.1
8	21.6	14.4	66	107.4	373	192	249	8	2.5	7	989.8	372.7
9	22.8	14.3	61	106.7	480	246	296	8	2.7	7	989.6	376.2
10	23.8	14	58	105.2	559	288	324	8	2.9	7	989.3	378.4
11	24.4	13.7	55	103.5	596	295	343	8	3	7	989.1	379.7
12	24.9	13.5	53	101.9	621	321	340	8	3	7	988.8	380.3
13	25.3	13.3	51	100.6	605	339	318	9	3	7	988.5	380.9
14	25.6	13.1	50	99.7	548	346	284	9	3	7	988.3	381.4
15	25.7	13	50	99	469	356	234	9	2.9	7	988.4	381.4
16	25.5	12.9	50	98.9	363	358	175	8	2.8	7	988.4	380.5
17	24.9	13	52	99.4	242	343	115	8	2.7	7	988.5	378.8
18	24	13.2	55	100.6	123	315	58	8	2.4	7	988.6	376.4
19	22.9	13.5	59	102.4	13	47	10	8	2.1	7	988.7	373.7
20	21.8	13.9	64	104.3	0	0	0	8	1.8	7	988.7	371.2
21	20.8	14.1	68	105.8	0	0	0	8	1.8	6	988.8	369.2
22	20.1	14.2	71	106.3	0	0	0	7	1.8	6	988.8	367.4
23	19.6	14.2	73	105.9	0	0	0	7	1.8	6	988.9	365.7
24	19.2	14.1	75	105.5	0	0	0	7	1.7	6	988.9	364.5

Harbin

HOUR	TEM	DEW	RH	X	TH	NR	DF	WD	WS	CC	AP	LW
July												
1	21.1	18.3	85	137.1	0	0	0	7	1.4	6	988	387.5
2	20.6	18.2	87	136.1	0	0	0	7	1.4	6	988	385.6
3	20.1	18.1	89	135.4	0	0	0	7	1.5	6	988.1	383.8
4	19.9	18.1	89	135.1	0	0	0	7	1.5	6	988.2	382.9
5	20.2	18.2	88	135.7	51	69	41	7	1.6	6	988.4	384.2
6	21	18.4	85	137.3	149	126	108	7	1.8	6	988.5	387.3
7	22.2	18.6	81	139.2	247	157	173	8	2	7	988.6	391.7
8	23.5	18.7	76	140.4	334	166	233	8	2.2	7	988.7	396.3
9	24.6	18.7	71	140.5	445	226	281	8	2.4	7	988.5	399.7
10	25.4	18.6	67	139.7	526	262	314	8	2.5	7	988.3	401.9
11	25.9	18.4	65	138.7	557	254	343	8	2.7	8	988.2	403.2
12	26.3	18.3	63	137.9	588	287	341	8	2.7	8	988	404.2
13	26.7	18.3	62	137.4	578	312	321	9	2.8	8	987.8	405.2
14	27	18.2	60	137.1	524	310	290	9	2.9	8	987.6	406.1
15	27.1	18.2	60	136.6	454	328	238	9	2.7	8	987.7	406.4
16	27	18.2	61	136.6	353	336	177	8	2.6	7	987.8	405.8
17	26.4	18.3	63	137.3	230	308	117	8	2.4	7	987.9	404.3
18	25.6	18.5	66	138.8	110	259	58	8	2.1	7	987.9	402.3
19	24.6	18.7	71	140.7	9	19	8	8	1.8	7	988	399.9
20	23.6	18.8	76	142.1	0	0	0	8	1.5	6	988.1	397.3
21	22.8	18.9	79	142.4	0	0	0	8	1.5	6	988.1	395
22	22.2	18.8	82	141.4	0	0	0	7	1.4	6	988.1	392.9
23	21.8	18.6	83	139.9	0	0	0	7	1.4	6	988.1	391
24	21.5	18.5	84	138.5	0	0	0	7	1.4	6	988.1	389.4
August												
1	19.9	17.4	86	129.2	0	0	0	8	1.4	5	991.6	379.8
2	19.3	17.2	88	128	0	0	0	8	1.4	6	991.6	377.6
3	18.7	17	90	126.7	0	0	0	8	1.4	6	991.7	375.1
4	18.4	16.9	91	125.6	0	0	0	8	1.5	6	991.8	373.6
5	18.6	16.9	90	125.8	19	22	16	8	1.5	6	991.9	374.6
6	19.5	17.2	87	127.6	105	110	78	8	1.7	6	992	377.9
7	20.8	17.5	82	130.5	209	150	147	8	2	6	992.1	383
8	22.3	17.8	76	132.7	303	164	211	8	2.2	6	992.2	388.8
9	23.7	17.8	71	133.1	420	238	261	8	2.3	7	992	392.9
10	24.6	17.6	66	131.8	512	294	289	8	2.5	7	991.8	395.4
11	25.3	17.3	63	129.8	556	306	311	8	2.7	7	991.6	396.5
12	25.8	17.1	60	128.1	587	350	303	8	2.7	7	991.4	397.1
13	26.1	16.9	59	127	570	380	278	9	2.8	7	991.2	397.8
14	26.4	16.8	58	126.4	507	371	248	9	2.8	7	991	398.5
15	26.5	16.8	57	126	428	391	197	9	2.7	7	991.1	398.5
16	26.2	16.8	58	126	318	405	138	8	2.5	7	991.2	397.6
17	25.5	16.9	61	126.8	183	359	82	8	2.4	7	991.4	395.6
18	24.5	17.1	65	128.3	53	179	31	8	2.1	6	991.5	392.9
19	23.3	17.4	71	129.8	0	0	0	8	1.8	6	991.6	389.8
20	22.1	17.5	76	130.8	0	0	0	8	1.5	6	991.7	386.7
21	21.1	17.5	81	130.7	0	0	0	8	1.5	5	991.7	384.1
22	20.6	17.4	83	130	0	0	0	7	1.4	5	991.7	382.2
23	20.3	17.4	84	129.2	0	0	0	7	1.4	5	991.7	381
24	20.1	17.3	85	128.6	0	0	0	7	1.4	5	991.7	380

Harbin

HOUR	TEM	DEW	RH	X	TH	NR	DF	WD	WS	CC	AP	LW
September												
1	13.2	9.5	80	78.6	0	0	0	8	1.5	5	997.6	329.2
2	12.6	9.4	82	77.7	0	0	0	8	1.5	5	997.6	327.1
3	11.9	9.2	84	76.8	0	0	0	8	1.5	5	997.7	324.7
4	11.5	9	85	75.9	0	0	0	8	1.6	5	997.9	323
5	11.5	9.1	85	75.9	0	0	0	8	1.6	5	998	323.3
6	12.3	9.3	83	77.3	53	88	41	8	1.8	5	998.1	326.1
7	13.6	9.8	78	79.7	164	186	107	9	2	5	998.3	331
8	15.3	10.1	72	81.6	262	207	168	9	2.2	5	998.4	336.6
9	17	10.1	65	82	387	307	209	9	2.4	5	998.1	341.2
10	18.4	9.7	59	80.6	480	373	232	9	2.7	6	997.9	344.2
11	19.6	9.2	54	78.3	518	378	250	9	2.9	6	997.6	345.8
12	20.3	8.7	50	76.2	559	471	228	9	2.9	6	997.3	346.6
13	20.9	8.4	48	74.7	535	502	204	10	2.9	6	997.1	347.2
14	21.1	8.2	46	73.9	460	495	175	10	2.9	6	996.8	347.5
15	21.1	8.2	46	73.8	361	512	128	10	2.6	6	996.9	347.3
16	20.7	8.3	48	74.4	229	501	79	9	2.3	6	997.1	346.2
17	19.7	8.6	51	75.7	78	283	36	9	2	6	997.3	344.1
18	18.4	9	57	77.3	0	0	0	9	1.9	6	997.4	341.5
19	16.9	9.4	63	78.6	0	0	0	9	1.7	5	997.6	338.3
20	15.4	9.6	70	79.2	0	0	0	9	1.6	5	997.7	335.1
21	14.4	9.5	74	79	0	0	0	9	1.5	5	997.7	332.2
22	13.8	9.4	76	78.3	0	0	0	8	1.5	5	997.8	330.3
23	13.5	9.3	77	77.7	0	0	0	8	1.5	5	997.8	329.2
24	13.3	9.3	78	77.4	0	0	0	8	1.5	5	997.8	328.4
October												
1	4.5	-0.5	72	39.9	0	0	0	9	1.7	5	1001.3	270.5
2	4	-0.6	73	39.4	0	0	0	9	1.7	5	1001.3	268.8
3	3.5	-0.8	75	39	0	0	0	9	1.7	5	1001.4	267.2
4	3.1	-1	76	38.6	0	0	0	8	1.8	5	1001.6	265.9
5	3.1	-1	76	38.4	0	0	0	8	1.8	5	1001.7	265.8
6	3.5	-0.8	75	38.8	14	23	12	8	1.9	5	1001.8	267.3
7	4.4	-0.4	72	39.8	92	162	61	9	2.1	5	1002	270.3
8	5.8	-0.2	67	40.6	184	200	117	9	2.3	5	1002.1	274.1
9	7.3	-0.2	61	40.9	287	282	160	9	2.6	5	1001.8	277.4
10	8.8	-0.5	55	40.5	363	334	186	10	2.9	6	1001.6	280.2
11	10.2	-0.9	49	39.7	394	344	200	10	3.2	6	1001.3	282.5
12	11.2	-1.3	45	38.8	422	436	180	10	3.3	6	1001	284
13	11.8	-1.5	43	38.3	389	466	154	10	3.3	5	1000.7	284.8
14	11.8	-1.6	43	38.1	313	462	121	10	3.3	5	1000.5	284.6
15	11.3	-1.5	44	38.1	211	463	77	10	2.9	5	1000.6	283.4
16	10.4	-1.4	47	38.5	83	322	34	9	2.4	6	1000.8	281.6
17	9.3	-1.1	51	39	4	4	4	9	1.9	6	1001	279.4
18	8.3	-0.9	55	39.5	0	0	0	9	1.8	5	1001.1	277.5
19	7.3	-0.7	59	39.8	0	0	0	9	1.8	5	1001.3	275.6
20	6.4	-0.7	63	39.9	0	0	0	9	1.7	4	1001.5	273.9
21	5.8	-0.7	65	39.8	0	0	0	9	1.7	4	1001.5	272.4
22	5.3	-0.7	67	39.6	0	0	0	8	1.6	4	1001.5	271.3
23	4.9	-0.7	69	39.3	0	0	0	8	1.6	4	1001.5	270.4
24	4.6	-0.7	70	39.2	0	0	0	8	1.7	4	1001.5	269.7

Harbin

HOUR	TEM	DEW	RH	X	TH	NR	DF	WD	WS	CC	AP	LW
November												
1	-6.2	-10.6	73	19.1	0	0	0	9	2.1	5	1004.4	215.2
2	-6.4	-10.7	73	18.9	0	0	0	9	2	5	1004.4	214.4
3	-6.7	-10.8	74	18.8	0	0	0	9	2.1	5	1004.5	213.7
4	-6.9	-11	75	18.7	0	0	0	9	2.1	5	1004.6	212.9
5	-7.2	-11	76	18.5	0	0	0	9	2.1	5	1004.7	212.3
6	-7.2	-11	76	18.5	0	0	0	9	2.2	5	1004.8	212.3
7	-7	-10.8	76	18.7	29	64	23	9	2.2	5	1004.8	213.3
8	-6.2	-10.6	73	19.1	102	159	68	9	2.3	5	1004.9	215.2
9	-5.1	-10.3	68	19.4	193	252	112	9	2.6	5	1004.7	217.6
10	-3.7	-10.2	63	19.6	261	307	138	10	2.8	6	1004.4	220.3
11	-2.4	-10.2	58	19.7	290	316	152	10	3.1	6	1004.2	222.8
12	-1.4	-10.3	54	19.7	310	407	136	10	3.1	6	1004	224.6
13	-0.9	-10.4	52	19.6	277	445	111	10	3.2	6	1003.7	225.3
14	-1	-10.5	52	19.4	196	407	82	10	3.2	6	1003.5	224.8
15	-1.5	-10.5	54	19.3	95	337	42	10	2.9	6	1003.6	223.6
16	-2.3	-10.5	57	19.3	10	28	8	10	2.6	6	1003.8	222.1
17	-3.1	-10.4	60	19.3	0	0	0	10	2.2	6	1004	220.7
18	-3.8	-10.4	62	19.3	0	0	0	10	2.3	5	1004.1	219.5
19	-4.3	-10.5	64	19.2	0	0	0	10	2.3	5	1004.3	218.4
20	-4.7	-10.6	66	19	0	0	0	10	2.3	5	1004.4	217.4
21	-5.1	-10.7	67	19	0	0	0	10	2.2	5	1004.4	216.5
22	-5.5	-10.7	69	19	0	0	0	9	2.2	5	1004.4	215.8
23	-5.9	-10.7	71	18.9	0	0	0	9	2.1	4	1004.4	215.2
24	-6.2	-10.8	72	18.8	0	0	0	9	2.1	5	1004.4	214.5
December												
1	-15.7	-19	76	9.3	0	0	0	9	1.7	5	1006	174
2	-15.9	-19.2	76	9.2	0	0	0	9	1.7	5	1006	173.1
3	-16	-19.3	76	9.1	0	0	0	9	1.7	5	1006	172.6
4	-16.2	-19.5	77	9	0	0	0	9	1.7	5	1006	171.8
5	-16.6	-19.7	77	8.9	0	0	0	9	1.7	5	1006.1	170.7
6	-16.9	-19.9	78	8.7	0	0	0	9	1.7	5	1006.1	169.9
7	-16.9	-19.8	78	8.8	0	0	0	9	1.8	5	1006.1	170
8	-16.4	-19.5	78	9	45	107	32	9	1.9	5	1006.1	171.6
9	-15.4	-18.8	75	9.4	136	253	77	9	2.1	6	1006	174.6
10	-14	-18.1	72	9.9	200	290	107	9	2.3	6	1005.8	178.6
11	-12.5	-17.4	68	10.5	226	276	126	9	2.5	6	1005.7	182.6
12	-11.4	-17	64	10.8	248	370	116	9	2.6	6	1005.5	185.3
13	-10.8	-16.9	62	10.9	224	413	95	10	2.6	6	1005.3	186.4
14	-10.9	-17	62	10.9	151	364	68	10	2.7	5	1005.1	186
15	-11.4	-17.1	64	10.8	55	221	31	10	2.5	5	1005.3	184.9
16	-12.1	-17.2	67	10.6	0	0	0	9	2.3	5	1005.5	183.6
17	-12.8	-17.4	69	10.5	0	0	0	9	2.1	6	1005.7	182.3
18	-13.3	-17.5	72	10.4	0	0	0	9	2	5	1005.8	181.3
19	-13.7	-17.7	73	10.2	0	0	0	9	1.9	5	1006	180.2
20	-14	-18	73	10	0	0	0	9	1.9	5	1006.1	178.9
21	-14.4	-18.2	73	9.9	0	0	0	9	1.8	5	1006.1	177.7
22	-14.8	-18.5	74	9.7	0	0	0	9	1.8	4	1006.1	176.5
23	-15.2	-18.7	75	9.4	0	0	0	9	1.8	4	1006.1	175.2
24	-15.6	-19	76	9.3	0	0	0	9	1.7	5	1006.1	173.9

Beijing

HOUR	TEM	DEW	RH	X	TH	NR	DF	WD	WS	CC	AP	LW
January												
1	-5.1	-14.6	52	13.3	0	0	0	8	2.1	5	1025.5	202.8
2	-5.4	-14.8	52	13.1	0	0	0	8	2.1	5	1025.6	201.8
3	-5.6	-14.9	52	13	0	0	0	8	2.1	5	1025.6	201
4	-5.8	-15.1	52	12.9	0	0	0	7	2.1	4	1025.7	200.1
5	-6.2	-15.2	53	12.6	0	0	0	7	2.1	4	1025.8	199
6	-6.5	-15.3	54	12.5	0	0	0	7	2.1	4	1025.9	198
7	-6.6	-15.4	54	12.4	0	0	0	7	2.2	5	1026	197.7
8	-6.1	-15.4	52	12.4	15	31	12	7	2.2	5	1026.1	198.4
9	-4.9	-15.4	47	12.4	125	268	66	7	2.4	5	1025.8	200.4
10	-3.2	-15.5	42	12.4	250	426	102	8	2.7	5	1025.5	203.3
11	-1.4	-15.7	37	12.3	342	503	124	8	2.9	5	1025.2	206.5
12	0	-16	33	12.1	403	584	125	8	3	5	1024.7	208.8
13	0.9	-16.2	30	11.9	393	568	126	8	3	5	1024.3	209.9
14	1.2	-16.5	29	11.7	319	464	125	8	3	5	1023.8	210
15	1.2	-16.5	29	11.6	229	404	98	8	2.9	5	1024	209.6
16	0.8	-16.4	31	11.7	109	268	58	9	2.7	5	1024.2	209.1
17	0.1	-16.1	32	12	13	28	11	9	2.6	6	1024.4	208.4
18	-0.8	-15.7	35	12.3	0	0	0	9	2.4	5	1024.7	207.7
19	-1.7	-15.3	39	12.7	0	0	0	9	2.3	5	1024.9	207
20	-2.6	-14.9	42	13.1	0	0	0	9	2.1	5	1025.1	206.5
21	-3.2	-14.6	46	13.5	0	0	0	9	2.1	5	1025.2	206.2
22	-3.7	-14.5	48	13.6	0	0	0	8	2.1	4	1025.3	205.7
23	-4.2	-14.5	49	13.6	0	0	0	8	2	4	1025.4	205
24	-4.6	-14.5	51	13.5	0	0	0	8	2.1	4	1025.5	204
February												
1	-2.1	-12.1	51	16.9	0	0	0	7	2.1	5	1022	216.6
2	-2.6	-12.2	53	16.8	0	0	0	7	2.1	5	1022.1	215.6
3	-2.9	-12.2	54	16.8	0	0	0	7	2	5	1022.2	214.7
4	-3.2	-12.3	55	16.7	0	0	0	7	2	5	1022.3	213.9
5	-3.6	-12.2	56	16.6	0	0	0	7	2	5	1022.3	213.4
6	-3.8	-12.1	57	16.6	0	0	0	7	2	5	1022.5	213.4
7	-3.7	-12	57	16.7	0	0	0	6	2	5	1022.6	213.9
8	-2.9	-12.2	54	16.6	56	127	37	6	2.1	5	1022.8	214.8
9	-1.5	-12.6	47	16.1	190	339	90	6	2.4	6	1022.4	216
10	0.3	-13.2	40	15.4	328	474	124	8	2.8	6	1022	217.9
11	2	-13.8	35	14.9	420	516	153	8	3.1	6	1021.7	220.2
12	3.4	-14.1	31	14.5	487	585	156	8	3.2	6	1021.2	222.2
13	4.2	-14.3	29	14.4	481	568	160	8	3.2	6	1020.7	223.7
14	4.6	-14.3	28	14.3	408	471	164	8	3.3	6	1020.2	224.6
15	4.8	-14.2	28	14.4	318	432	134	8	3.3	6	1020.3	225.3
16	4.7	-14.1	29	14.7	195	350	92	9	3.2	6	1020.4	225.5
17	4.2	-13.8	30	15	57	135	39	9	3.2	6	1020.5	224.9
18	3.3	-13.4	33	15.4	0	0	0	9	2.9	6	1020.7	224.1
19	2.1	-12.9	36	15.9	0	0	0	8	2.7	6	1020.9	223
20	1.1	-12.4	40	16.5	0	0	0	8	2.4	5	1021.1	222
21	0.3	-12.2	44	17	0	0	0	8	2.4	5	1021.3	221.2
22	-0.3	-12.1	46	17.2	0	0	0	8	2.3	5	1021.4	220.4
23	-0.8	-12	47	17.1	0	0	0	8	2.2	5	1021.6	219.4
24	-1.3	-12	49	17.1	0	0	0	8	2.2	5	1021.7	218.4

Beijing

HOUR	TEM	DEW	RH	X	TH	NR	DF	WD	WS	CC	AP	LW
						March						
1	4.9	-7.6	45	24.1	0	0	0	8	2.3	5	1016.6	246.5
2	4.2	-7.6	48	24.2	0	0	0	8	2.2	5	1016.8	244.9
3	3.5	-7.6	50	24.2	0	0	0	8	2.2	5	1016.9	243.3
4	2.9	-7.6	52	24.2	0	0	0	7	2.1	5	1017	242.1
5	2.7	-7.5	53	24.2	0	0	0	7	2	5	1017.2	241.9
6	2.8	-7.3	53	24.4	0	0	0	7	2	5	1017.3	242.7
7	3.4	-7.3	51	24.5	46	114	31	7	2.1	5	1017.5	244.2
8	4.5	-7.5	47	24.4	161	272	85	7	2.2	5	1017.7	246.2
9	6	-7.9	42	23.7	318	410	137	7	2.5	6	1017.3	248.1
10	7.6	-8.5	36	22.9	458	503	173	8	2.8	6	1016.9	250.2
11	9.1	-9.1	32	22.1	543	513	205	8	3.1	6	1016.5	252.5
12	10.3	-9.5	29	21.5	608	575	205	8	3.3	6	1016	254.5
13	11.2	-9.7	27	21.2	601	574	203	9	3.5	6	1015.4	256.6
14	11.9	-9.9	26	21.1	526	508	202	9	3.6	6	1014.9	258.2
15	12.3	-9.9	25	21	437	501	166	9	3.7	6	1014.9	259.2
16	12.4	-9.9	25	21.1	303	441	124	9	3.7	6	1014.8	259.3
17	12	-9.8	26	21.3	145	292	76	9	3.8	6	1014.8	258.5
18	11.1	-9.4	28	21.7	23	48	19	9	3.5	6	1015	257.1
19	10	-8.9	30	22.4	0	0	0	8	3.1	6	1015.1	255.5
20	8.9	-8.4	34	23.3	0	0	0	8	2.8	5	1015.3	254
21	7.9	-8	37	24.1	0	0	0	8	2.7	5	1015.5	252.9
22	7.1	-7.8	39	24.4	0	0	0	8	2.6	5	1015.8	251.7
23	6.5	-7.6	41	24.4	0	0	0	8	2.6	5	1016	250.3
24	5.9	-7.5	43	24.6	0	0	0	8	2.5	5	1016.2	249.3
						April						
1	12.2	0.5	49	44.2	0	0	0	7	2.3	6	1010.3	292.7
2	11.3	0.6	52	44.4	0	0	0	7	2.1	6	1010.4	290.8
3	10.4	0.6	56	44.6	0	0	0	7	2	6	1010.6	288.6
4	9.8	0.7	58	44.6	0	0	0	7	1.9	5	1010.7	287
5	9.7	0.7	58	44.5	0	0	0	7	1.8	5	1010.9	286.9
6	10.2	0.8	57	44.6	25	43	21	7	2	5	1011.1	288.1
7	11.3	0.7	53	44.7	130	223	76	7	2.3	6	1011.3	290.8
8	12.7	0.5	48	44.4	269	310	139	7	2.5	6	1011.5	294
9	14.2	0.1	43	43.6	432	425	188	7	2.8	6	1011	297
10	15.7	-0.4	39	42.5	561	481	225	8	3.1	6	1010.6	299.9
11	17	-0.9	35	41.3	625	457	265	8	3.4	7	1010.2	302.1
12	18	-1.3	32	40.2	677	490	271	8	3.6	7	1009.7	304.2
13	18.9	-1.7	30	39.3	669	496	264	9	3.9	7	1009.2	306
14	19.6	-1.9	28	38.7	599	455	257	9	4.1	6	1008.7	307.6
15	20	-1.9	27	38.5	508	448	218	9	4.1	7	1008.8	308.7
16	20	-1.9	27	38.6	372	399	169	9	4.2	7	1008.8	308.8
17	19.4	-1.7	29	39.1	213	293	114	9	4.3	7	1008.9	307.6
18	18.5	-1.4	31	39.8	69	146	46	9	3.9	7	1009	305.5
19	17.3	-1	34	40.8	0	0	0	9	3.4	6	1009.1	303
20	16.1	-0.5	37	42.2	0	0	0	9	3	6	1009.2	300.8
21	15.2	-0.1	41	43.6	0	0	0	9	2.9	6	1009.4	299.3
22	14.4	0.2	43	44.3	0	0	0	8	2.8	6	1009.6	298
23	13.8	0.4	45	44.4	0	0	0	8	2.6	5	1009.8	296.9
24	13.2	0.6	47	44.9	0	0	0	8	2.5	5	1009.9	296

Beijing

HOUR	TEM	DEW	RH	X	TH	NR	DF	WD	WS	CC	AP	LW
						May						
1	18.6	7.8	54	72	0	0	0	7	2.2	6	1004.5	337.8
2	17.6	8	58	72.4	0	0	0	7	2	6	1004.7	335.5
3	16.6	8.1	61	72.6	0	0	0	7	1.9	6	1004.9	332.7
4	15.9	8	64	72.3	0	0	0	7	1.9	6	1005.1	330.6
5	15.9	7.9	64	71.7	0	0	0	7	1.8	6	1005.3	330.4
6	16.7	7.9	60	71.5	66	107	48	7	2.1	6	1005.5	332.2
7	18.1	7.8	55	71.4	201	267	112	7	2.3	6	1005.7	336.1
8	19.8	7.6	50	70.7	344	344	172	7	2.6	6	1005.9	341
9	21.5	7.2	44	69.4	503	445	214	7	2.9	6	1005.5	345
10	22.9	6.7	40	67.5	614	477	252	8	3.1	7	1005.2	348.1
11	24	6.2	37	65.7	650	413	305	8	3.4	7	1004.8	350.4
12	24.9	5.8	34	64.1	694	447	308	8	3.6	7	1004.4	352.4
13	25.7	5.5	32	63	682	461	295	9	3.9	7	1004	354.3
14	26.3	5.3	31	62.2	614	424	284	9	4.1	7	1003.6	356
15	26.6	5.2	30	61.8	529	416	244	9	4.2	7	1003.6	356.8
16	26.6	5.2	31	61.9	403	372	196	9	4.2	7	1003.6	356.5
17	26.1	5.4	32	62.6	256	282	142	9	4.3	7	1003.6	355.2
18	25.2	5.8	34	64	121	201	75	9	3.8	7	1003.6	353.1
19	24	6.2	37	65.9	15	27	13	8	3.4	7	1003.6	350.7
20	22.8	6.7	40	67.8	0	0	0	8	2.9	6	1003.7	347.9
21	21.7	7	44	69.5	0	0	0	8	2.8	6	1003.8	345.5
22	20.8	7.3	47	70.4	0	0	0	8	2.7	6	1004	343.2
23	20.1	7.5	49	70.8	0	0	0	8	2.6	6	1004.2	341.5
24	19.5	7.7	51	71.7	0	0	0	8	2.4	6	1004.3	340.3
						June						
1	22.4	15.5	68	115	0	0	0	6	1.8	7	1000.9	379.8
2	21.7	15.6	71	115.2	0	0	0	6	1.6	7	1001	377.6
3	20.9	15.7	74	115.4	0	0	0	6	1.6	7	1001.2	375.6
4	20.4	15.7	76	115.5	0	0	0	5	1.6	7	1001.4	374.3
5	20.4	15.7	76	115.6	0	0	0	5	1.6	7	1001.5	374.4
6	21	15.8	74	115.8	66	65	53	5	1.8	7	1001.7	376.1
7	22.1	15.7	69	115.8	172	151	120	6	2	7	1001.8	379.3
8	23.4	15.6	64	115.4	287	201	188	6	2.2	7	1002	383.3
9	24.8	15.4	59	114.4	423	273	246	6	2.3	7	1001.7	387.1
10	26	15.1	55	113	529	328	288	6	2.4	7	1001.3	390.4
11	27	14.8	51	111.3	580	315	327	6	2.4	8	1001	393
12	27.8	14.5	48	109.6	615	331	338	6	2.7	8	1000.7	395
13	28.6	14.3	46	108	609	332	333	7	2.9	8	1000.3	396.9
14	29.1	14	44	106.6	562	309	320	7	3.1	8	999.9	398.3
15	29.5	13.8	43	105.5	493	310	277	7	3.1	8	999.9	399
16	29.4	13.8	43	105.2	385	285	220	7	3.2	8	999.9	398.8
17	29	13.9	45	106	255	212	162	7	3.2	8	999.9	397.5
18	28.2	14.2	47	107.7	134	151	92	7	3	8	1000	395.6
19	27.2	14.6	50	110.1	30	43	26	7	2.8	8	1000	393.1
20	26.1	15	55	112.6	0	0	0	7	2.5	8	1000	390.5
21	25.1	15.3	58	114.5	0	0	0	7	2.4	7	1000.1	388.3
22	24.3	15.5	62	115.4	0	0	0	7	2.2	7	1000.3	386.1
23	23.7	15.6	64	115.7	0	0	0	7	2.1	7	1000.5	384.2
24	23.1	15.7	66	116.2	0	0	0	7	2	7	1000.6	382.7

Beijing

HOUR	TEM	DEW	RH	X	TH	NR	DF	WD	WS	CC	AP	LW
July												
1	25.1	20.4	77	155.2	0	0	0	6	1.8	7	999.5	409.1
2	24.5	20.4	79	155.1	0	0	0	6	1.7	8	999.6	407.1
3	23.9	20.4	82	154.8	0	0	0	6	1.6	8	999.8	405.2
4	23.5	20.4	84	154.5	0	0	0	5	1.6	7	999.9	403.9
5	23.5	20.4	84	154.5	0	0	0	5	1.5	7	1000.1	403.8
6	23.9	20.4	82	154.8	44	37	38	5	1.6	8	1000.2	405.3
7	24.7	20.4	78	155.1	141	122	103	5	1.7	8	1000.4	407.9
8	25.8	20.4	74	155	244	170	168	5	1.9	8	1000.5	411.4
9	26.9	20.3	69	154.2	371	232	231	5	2	8	1000.3	414.6
10	27.9	20.1	65	152.9	473	282	279	6	2.1	8	1000.1	417.5
11	28.9	19.9	61	151.4	530	276	319	6	2.2	8	999.8	420.1
12	29.6	19.8	58	150	574	287	339	6	2.4	8	999.6	422.4
13	30.3	19.6	56	148.7	576	294	336	7	2.6	8	999.3	424.3
14	30.8	19.5	54	147.6	531	275	319	7	2.8	8	999	425.8
15	31	19.4	53	146.8	463	262	281	7	2.9	8	999	426.4
16	31	19.3	53	146.6	361	237	225	7	2.9	8	999	426
17	30.5	19.4	55	147.3	239	177	162	7	3	8	999	424.5
18	29.8	19.6	57	149	121	118	88	7	2.8	8	999	422.6
19	28.9	19.9	61	151.4	25	31	22	7	2.5	8	999	420.2
20	27.9	20.2	65	153.8	0	0	0	7	2.2	8	999.1	417.9
21	27.1	20.4	69	155.5	0	0	0	7	2.1	8	999.2	415.9
22	26.5	20.5	71	156.2	0	0	0	6	2	7	999.3	414.2
23	26.1	20.5	73	156.2	0	0	0	6	1.9	7	999.5	412.6
24	25.6	20.5	75	156.3	0	0	0	6	1.8	7	999.5	411.3
August												
1	23.9	20	79	150.8	0	0	0	7	1.5	7	1003.5	403.4
2	23.4	19.9	82	150.1	0	0	0	7	1.5	7	1003.6	401.4
3	22.9	19.8	84	149.1	0	0	0	7	1.5	7	1003.7	399.4
4	22.5	19.7	85	147.7	0	0	0	7	1.5	7	1003.9	397.8
5	22.5	19.6	84	146.9	0	0	0	7	1.5	7	1004	397.3
6	22.9	19.6	82	147	17	15	16	7	1.6	7	1004.2	398.4
7	23.7	19.7	79	147.7	114	123	83	6	1.7	7	1004.3	401.1
8	24.9	19.7	74	148	229	178	153	6	1.8	7	1004.5	404.9
9	26.2	19.5	69	146.9	379	274	215	6	2	7	1004.3	408.5
10	27.4	19.2	63	144.6	506	345	261	6	2.1	7	1004.1	411.8
11	28.5	18.8	58	141.9	569	332	304	6	2.3	7	1003.8	414.2
12	29.3	18.5	55	139.3	618	367	314	6	2.4	7	1003.6	415.8
13	29.8	18.3	53	137.5	611	366	312	7	2.6	7	1003.3	417
14	30.2	18.1	51	136.6	550	324	302	7	2.7	7	1003	418
15	30.4	18.1	51	136.5	472	316	258	7	2.8	7	1003	418.6
16	30.2	18.2	52	137.6	356	285	203	7	2.9	7	1003	418.6
17	29.7	18.5	54	139.7	214	193	140	7	2.9	7	1003.1	417.5
18	28.8	18.9	57	142.7	85	104	64	7	2.6	7	1003.1	415.6
19	27.7	19.3	62	145.8	8	7	7	7	2.3	7	1003.2	413
20	26.5	19.6	67	148	0	0	0	7	2	7	1003.2	410.2
21	25.7	19.7	71	149.2	0	0	0	7	1.9	7	1003.3	407.9
22	25.1	19.8	74	149.4	0	0	0	7	1.8	7	1003.5	406.2
23	24.7	19.8	75	149.4	0	0	0	7	1.7	7	1003.6	404.9
24	24.3	19.8	77	149.5	0	0	0	7	1.6	7	1003.6	403.8

Beijing

HOUR	TEM	DEW	RH	X	TH	NR	DF	WD	WS	CC	AP	LW
September												
1	18.6	14.2	77	105.2	0	0	0	7	1.5	6	1010.5	362.9
2	18	14.2	80	104.9	0	0	0	7	1.4	6	1010.6	361.1
3	17.5	14.1	82	104.3	0	0	0	7	1.4	6	1010.8	359.3
4	17.1	13.9	83	103.2	0	0	0	7	1.5	6	1011	357.6
5	17.1	13.7	82	102.1	0	0	0	7	1.5	6	1011.2	356.7
6	17.4	13.6	80	101.6	0	0	0	7	1.7	6	1011.4	357.1
7	18.1	13.6	77	101.7	77	108	56	6	1.8	6	1011.6	359
8	19.3	13.5	72	101.7	185	198	118	6	2	6	1011.8	362.3
9	20.7	13.3	66	101	327	310	176	6	2.1	6	1011.5	365.7
10	22.1	13	60	99.4	449	381	217	7	2.2	6	1011.2	368.8
11	23.4	12.6	54	97	514	376	253	7	2.3	7	1010.9	371.4
12	24.3	12.1	50	94.5	561	409	261	7	2.4	7	1010.5	373.1
13	25.1	11.7	47	92.3	548	411	255	7	2.6	7	1010.2	374.2
14	25.5	11.5	45	90.8	480	367	240	7	2.7	7	1009.8	375
15	25.7	11.4	45	90.3	392	347	198	7	2.7	7	1009.9	375.3
16	25.5	11.5	46	91.1	266	293	145	7	2.7	7	1010	375.2
17	24.8	11.9	48	93.1	129	173	84	7	2.7	7	1010	374.1
18	23.7	12.5	53	96.1	30	42	25	7	2.4	7	1010.1	372.5
19	22.4	13.1	59	99.2	0	0	0	7	2.1	7	1010.2	370.2
20	21.2	13.6	65	101.8	0	0	0	7	1.8	6	1010.3	367.9
21	20.2	13.9	69	103.4	0	0	0	7	1.7	6	1010.4	366.2
22	19.6	14	72	103.8	0	0	0	7	1.6	6	1010.5	364.8
23	19.3	14	73	103.8	0	0	0	7	1.5	6	1010.6	363.8
24	18.9	14	75	103.9	0	0	0	7	1.5	6	1010.7	362.8
October												
1	11.6	6.1	72	62.6	0	0	0	6	1.5	6	1016.2	311.7
2	11	5.9	74	61.9	0	0	0	6	1.4	6	1016.3	309.8
3	10.5	5.7	75	61	0	0	0	6	1.5	6	1016.5	307.7
4	10.2	5.4	75	60	0	0	0	6	1.5	5	1016.6	305.8
5	10.1	5.3	75	59.3	0	0	0	6	1.5	5	1016.8	305.2
6	10.3	5.4	75	59.5	0	0	0	6	1.6	5	1017	306
7	11	5.5	72	60.3	31	57	24	6	1.7	5	1017.2	308.2
8	12.2	5.4	67	60.3	126	182	79	6	1.8	6	1017.4	310.7
9	13.6	5	60	59	257	305	132	6	2	6	1017	312.9
10	15.2	4.4	53	57	373	393	168	7	2.3	6	1016.6	314.9
11	16.6	3.8	47	55.3	437	404	198	7	2.6	6	1016.3	317.2
12	17.7	3.4	44	54.4	481	456	199	7	2.7	6	1015.8	319.5
13	18.5	3.3	41	54.2	461	448	194	7	2.8	6	1015.3	321.7
14	18.9	3.4	41	54.3	380	370	183	7	2.9	6	1014.9	323.2
15	19	3.4	41	54.5	286	343	141	7	2.8	6	1015	323.6
16	18.6	3.6	42	55.1	161	258	89	8	2.6	6	1015.2	322.9
17	17.8	3.9	45	56.3	46	86	33	8	2.4	6	1015.3	321.3
18	16.6	4.5	49	58	0	0	0	8	2.2	6	1015.5	319.8
19	15.3	5.1	55	60	0	0	0	7	1.9	6	1015.7	318.1
20	14.1	5.6	61	61.5	0	0	0	7	1.7	6	1015.9	316.4
21	13.2	5.7	65	62.2	0	0	0	7	1.7	5	1016	314.7
22	12.6	5.7	67	62.1	0	0	0	7	1.7	5	1016.1	313.2
23	12.3	5.7	68	61.6	0	0	0	7	1.6	5	1016.3	312.1
24	11.8	5.7	70	61.4	0	0	0	7	1.6	5	1016.4	310.9

Beijing

HOUR	TEM	DEW	RH	X	TH	NR	DF	WD	WS	CC	AP	LW
November												
1	2.9	-4.5	63	30	0	0	0	7	1.8	5	1020.4	252.8
2	2.5	-4.6	65	29.7	0	0	0	7	1.8	5	1020.5	251.6
3	2.2	-4.7	65	29.5	0	0	0	7	1.8	5	1020.6	250.6
4	2	-4.9	65	29.1	0	0	0	7	1.8	5	1020.6	249.5
5	1.8	-5	66	28.7	0	0	0	7	1.8	4	1020.7	248.8
6	1.7	-4.9	66	28.7	0	0	0	7	1.9	5	1020.9	248.8
7	2	-4.8	66	29	0	0	0	7	2	5	1021	249.6
8	2.8	-4.8	62	29.1	63	120	43	7	2.1	5	1021.1	251.3
9	4.1	-5.1	56	28.7	175	262	95	7	2.4	5	1020.7	253.2
10	5.8	-5.5	49	28	285	383	127	7	2.6	6	1020.4	255.7
11	7.5	-6	43	27.2	355	435	148	7	2.9	6	1020	258.3
12	8.8	-6.4	39	26.6	396	498	148	7	2.9	6	1019.6	260.4
13	9.5	-6.6	37	26.3	370	476	144	8	3	6	1019.2	261.7
14	9.6	-6.6	37	26.3	286	373	134	8	3.1	5	1018.8	262
15	9.4	-6.5	37	26.5	188	301	97	8	2.9	6	1019	261.4
16	8.7	-6.3	39	26.9	76	165	49	8	2.7	6	1019.2	260.4
17	7.9	-6	42	27.4	0	0	0	8	2.5	6	1019.5	259.3
18	7	-5.6	46	28.1	0	0	0	8	2.4	6	1019.7	258.2
19	6.1	-5.2	49	28.8	0	0	0	8	2.2	5	1019.9	257.3
20	5.3	-5	53	29.3	0	0	0	8	2.1	5	1020.2	256.3
21	4.6	-4.9	56	29.7	0	0	0	8	2	5	1020.2	255.4
22	4.1	-4.8	58	29.7	0	0	0	7	2	5	1020.3	254.4
23	3.7	-4.8	59	29.5	0	0	0	7	1.9	4	1020.4	253.4
24	3.2	-4.8	61	29.5	0	0	0	7	1.9	5	1020.4	252.3
December												
1	-3.1	-12.3	54	16.3	0	0	0	8	2.2	5	1023.3	214
2	-3.4	-12.4	54	16.2	0	0	0	8	2.2	5	1023.3	213.3
3	-3.6	-12.5	55	16.1	0	0	0	8	2.2	5	1023.4	212.5
4	-3.8	-12.7	55	15.9	0	0	0	8	2.2	4	1023.4	211.4
5	-4.1	-12.9	55	15.6	0	0	0	8	2.2	4	1023.5	210.3
6	-4.4	-12.9	56	15.4	0	0	0	8	2.2	5	1023.6	209.5
7	-4.4	-13	56	15.4	0	0	0	7	2.3	5	1023.7	209.5
8	-3.8	-13	53	15.3	20	45	16	7	2.4	5	1023.7	210.4
9	-2.6	-13.2	48	15.2	128	272	68	7	2.7	6	1023.4	212.1
10	-0.9	-13.5	42	15	239	411	100	8	2.9	6	1023.1	214.6
11	0.9	-13.8	37	14.7	314	467	122	8	3.2	6	1022.8	217.5
12	2.2	-14.1	33	14.4	366	552	120	8	3.3	6	1022.4	219.6
13	3	-14.3	31	14.2	349	542	118	9	3.3	6	1022	220.7
14	3.1	-14.4	31	14.1	270	432	112	9	3.4	5	1021.6	220.7
15	2.8	-14.3	31	14.2	174	354	81	9	3.2	5	1021.9	220.1
16	2.1	-14.1	33	14.4	59	166	37	8	2.9	5	1022.1	219.2
17	1.3	-13.7	36	14.8	0	0	0	8	2.7	6	1022.3	218.4
18	0.4	-13.3	40	15.3	0	0	0	8	2.5	5	1022.6	217.9
19	-0.3	-12.9	43	15.7	0	0	0	8	2.3	5	1022.8	217.6
20	-1	-12.6	46	16	0	0	0	8	2.2	5	1023.1	217.1
21	-1.5	-12.5	48	16.3	0	0	0	8	2.2	5	1023.2	216.4
22	-2	-12.5	50	16.3	0	0	0	8	2.1	5	1023.2	215.7
23	-2.4	-12.5	51	16.2	0	0	0	8	2.1	4	1023.3	214.8
24	-2.8	-12.5	52	16.1	0	0	0	8	2.1	5	1023.3	214

Shanghai

HOUR	TEM	DEW	RH	X	TH	NR	DF	WD	WS	CC	AP	LW
						January						
1	3.6	-0.5	75	38	0	0	0	8	2.3	6	1027.1	267.9
2	3.5	-0.6	76	37.9	0	0	0	8	2.3	6	1027	267.5
3	3.3	-0.7	76	37.8	0	0	0	8	2.3	6	1027.1	266.8
4	3.1	-0.8	76	37.5	0	0	0	8	2.3	6	1027.2	266.2
5	2.9	-0.7	78	37.5	0	0	0	8	2.3	6	1027.3	265.9
6	2.8	-0.6	79	37.7	0	0	0	8	2.3	6	1027.4	266.2
7	3	-0.4	79	38.2	0	0	0	8	2.4	6	1027.6	267.1
8	3.5	-0.4	77	38.5	79	167	51	8	2.4	7	1027.8	268.4
9	4.3	-0.4	72	38.5	188	290	98	8	2.7	7	1027.5	269.7
10	5.4	-0.7	66	38.1	308	421	127	9	3	7	1027.2	271.1
11	6.4	-1	61	37.5	365	425	155	9	3.3	7	1026.9	272.4
12	7.1	-1.2	58	36.9	397	449	161	9	3.3	7	1026.5	273.1
13	7.4	-1.4	56	36.5	347	376	162	8	3.4	7	1026.1	273.1
14	7.4	-1.5	56	36.2	241	225	148	8	3.4	7	1025.7	272.8
15	7.2	-1.5	57	36.2	159	194	101	8	3.3	7	1025.9	272.2
16	6.8	-1.4	58	36.4	87	161	58	7	3.1	7	1026.2	271.6
17	6.3	-1.3	61	36.7	10	9	10	7	3	7	1026.4	271
18	5.8	-1	63	37.1	0	0	0	7	2.8	7	1026.6	270.6
19	5.3	-0.8	66	37.5	0	0	0	7	2.7	6	1026.9	270.3
20	4.9	-0.6	69	37.9	0	0	0	7	2.5	6	1027.2	270.1
21	4.6	-0.5	71	38.3	0	0	0	7	2.5	6	1027.1	270
22	4.4	-0.4	72	38.4	0	0	0	7	2.4	6	1027.1	269.7
23	4.2	-0.4	73	38.4	0	0	0	7	2.4	6	1027.1	269.3
24	4	-0.4	74	38.5	0	0	0	7	2.3	6	1027.1	269.1
						February						
1	5.4	1.6	77	44.4	0	0	0	8	2.4	6	1024	279.6
2	5.2	1.6	78	44.4	0	0	0	8	2.4	7	1023.9	279.2
3	5	1.5	79	44.3	0	0	0	8	2.4	7	1024	278.7
4	4.8	1.5	79	44.2	0	0	0	7	2.4	6	1024.1	278.3
5	4.7	1.5	80	44.1	0	0	0	7	2.4	6	1024.2	278.2
6	4.7	1.6	81	44.4	0	0	0	7	2.5	7	1024.4	278.7
7	4.9	1.8	81	44.9	25	45	21	8	2.5	7	1024.5	279.7
8	5.4	1.9	79	45.3	100	211	59	8	2.6	7	1024.7	281.1
9	6.2	1.8	74	45.3	222	318	108	8	2.8	7	1024.4	282.3
10	7.2	1.7	70	45	334	439	139	7	3.1	7	1024.1	283.8
11	8.1	1.4	65	44.6	386	426	167	7	3.4	7	1023.8	285.2
12	8.7	1.2	62	44.1	424	451	179	7	3.5	7	1023.4	286
13	9.1	1	61	43.6	390	398	182	7	3.6	7	1023	286.3
14	9.1	0.9	60	43.3	293	261	176	7	3.7	7	1022.6	286
15	9	0.8	60	43	215	231	134	7	3.5	7	1022.8	285.3
16	8.6	0.8	61	42.9	118	183	78	7	3.4	7	1023	284.3
17	8.1	0.9	63	43	35	54	28	7	3.3	7	1023.2	283.3
18	7.5	1.1	66	43.3	0	0	0	7	3.1	7	1023.4	282.4
19	7	1.3	69	43.6	0	0	0	6	3	7	1023.6	281.7
20	6.5	1.4	71	44	0	0	0	6	2.8	7	1023.8	281.3
21	6.2	1.5	73	44.4	0	0	0	6	2.7	7	1023.8	281
22	5.9	1.6	74	44.4	0	0	0	6	2.6	6	1023.9	280.7
23	5.8	1.6	75	44.4	0	0	0	6	2.5	6	1023.9	280.3
24	5.6	1.6	76	44.5	0	0	0	6	2.4	6	1023.8	280.2

Shanghai

HOUR	TEM	DEW	RH	X	TH	NR	DF	WD	WS	CC	AP	LW
						March						
1	8.9	4.4	74	54	0	0	0	7	2.5	6	1020.4	298.2
2	8.6	4.4	76	54	0	0	0	7	2.4	6	1020.3	297.5
3	8.3	4.3	77	53.9	0	0	0	7	2.4	6	1020.4	296.6
4	8.1	4.3	78	53.8	0	0	0	7	2.4	6	1020.5	296
5	8	4.3	78	53.9	0	0	0	7	2.4	6	1020.7	296.1
6	8.3	4.5	78	54.3	0	0	0	7	2.6	6	1020.9	297.2
7	8.9	4.6	76	54.9	96	239	51	7	2.8	6	1021.1	299
8	9.7	4.6	72	55.1	203	308	98	7	2.9	6	1021.3	301
9	10.7	4.4	67	54.7	362	454	144	7	3.2	6	1021	302.6
10	11.7	4.1	62	53.7	481	537	169	8	3.4	6	1020.7	304
11	12.6	3.7	58	52.6	522	488	206	8	3.7	6	1020.4	305.1
12	13.3	3.3	55	51.7	563	487	223	8	3.7	6	1020	305.8
13	13.7	3.2	53	51.2	519	425	232	7	3.8	6	1019.6	306.4
14	13.8	3.1	53	51.1	394	293	223	7	3.9	6	1019.2	306.7
15	13.7	3.2	53	51.3	300	260	175	7	3.7	7	1019.3	306.6
16	13.3	3.3	55	51.7	179	218	112	6	3.6	7	1019.5	305.9
17	12.7	3.5	57	52.2	80	119	57	6	3.5	7	1019.6	304.8
18	11.9	3.7	60	52.7	0	0	0	6	3.3	7	1019.8	303.5
19	11.1	4	64	53.2	0	0	0	6	3.1	6	1020.1	302.1
20	10.5	4.1	67	53.7	0	0	0	6	3	6	1020.3	300.9
21	10	4.2	69	54.2	0	0	0	6	2.8	6	1020.3	300.3
22	9.7	4.3	71	54.3	0	0	0	7	2.7	6	1020.3	299.8
23	9.5	4.4	72	54.3	0	0	0	7	2.6	6	1020.3	299.5
24	9.3	4.5	73	54.5	0	0	0	7	2.5	6	1020.3	299.4
						April						
1	13.8	9	75	74.5	0	0	0	7	2.4	6	1014.9	328.6
2	13.4	9.1	76	74.6	0	0	0	7	2.3	6	1014.9	327.7
3	13	9.1	78	74.6	0	0	0	7	2.2	6	1015	326.8
4	12.8	9.1	79	74.6	0	0	0	7	2.2	6	1015.2	326.3
5	12.9	9.2	79	74.8	0	0	0	7	2.1	6	1015.3	326.9
6	13.3	9.3	78	75.5	46	108	31	7	2.4	6	1015.5	328.5
7	14.1	9.4	75	76.2	178	336	80	7	2.8	6	1015.7	330.9
8	15.1	9.4	70	76.2	306	406	131	7	3.1	6	1015.9	333.5
9	16.2	9.1	65	75.4	472	518	175	7	3.3	6	1015.6	335.6
10	17.3	8.7	61	74	582	563	204	8	3.5	6	1015.4	337.2
11	18.1	8.4	57	72.7	593	463	256	8	3.7	6	1015.1	338.5
12	18.7	8.1	55	71.7	620	454	271	8	3.8	6	1014.8	339.4
13	19	8	53	71.3	564	422	264	7	3.9	6	1014.4	340.2
14	19.2	8	53	71.2	446	295	258	7	4	6	1014.1	340.5
15	19.1	7.9	53	71.1	349	264	208	7	3.9	6	1014.2	340.1
16	18.8	7.9	54	71.2	223	207	144	6	3.8	6	1014.3	339
17	18.1	8	56	71.5	100	120	73	6	3.7	7	1014.4	337.2
18	17.3	8.2	59	71.9	12	8	11	6	3.5	6	1014.6	335.2
19	16.4	8.4	62	72.7	0	0	0	6	3.2	6	1014.8	333.4
20	15.6	8.7	66	73.6	0	0	0	6	3	6	1015	332
21	15	8.8	69	74.3	0	0	0	6	2.9	6	1014.9	331.2
22	14.7	8.9	71	74.5	0	0	0	6	2.8	6	1014.9	330.5
23	14.5	9	72	74.5	0	0	0	6	2.7	6	1014.9	330.1
24	14.3	9.1	73	74.8	0	0	0	6	2.6	6	1014.8	329.9

Shanghai

HOUR	TEM	DEW	RH	X	TH	NR	DF	WD	WS	CC	AP	LW
						May						
1	19.3	14.6	75	106.5	0	0	0	7	2.4	6	1010	365.9
2	18.9	14.6	77	106.9	0	0	0	7	2.4	6	1010	365.2
3	18.5	14.7	79	106.9	0	0	0	7	2.3	6	1010.1	364.2
4	18.2	14.6	80	106.8	0	0	0	7	2.2	6	1010.3	363.5
5	18.4	14.7	80	106.8	0	0	0	7	2.2	6	1010.5	363.9
6	18.9	14.8	78	107.3	91	190	57	7	2.5	6	1010.7	365.6
7	19.8	14.8	74	107.7	227	350	104	7	2.8	7	1010.9	368.4
8	20.9	14.7	69	107.2	358	422	154	7	3	7	1011.1	371.4
9	22.1	14.4	64	105.7	526	523	196	7	3.2	7	1010.8	373.8
10	23	14	60	103.8	626	553	224	7	3.4	7	1010.6	375.6
11	23.7	13.7	57	102.1	621	436	283	7	3.6	7	1010.4	377
12	24.2	13.5	55	101.2	630	425	298	7	3.7	7	1010.1	377.8
13	24.4	13.4	54	100.9	571	395	286	6	3.8	7	1009.9	378.5
14	24.5	13.4	54	100.8	452	279	274	6	3.8	6	1009.6	378.6
15	24.4	13.3	54	100.6	372	262	226	6	3.8	7	1009.7	378.2
16	24.1	13.3	55	100.4	258	214	168	6	3.7	7	1009.8	376.9
17	23.5	13.4	57	100.5	128	120	95	6	3.7	7	1009.9	375
18	22.7	13.5	60	101.1	34	37	29	6	3.4	7	1010	372.8
19	21.8	13.7	63	102.2	0	0	0	6	3.1	6	1010.2	370.7
20	21	14	67	103.6	0	0	0	6	2.9	6	1010.3	369
21	20.4	14.2	70	105	0	0	0	6	2.8	6	1010.3	368
22	20	14.3	72	105.6	0	0	0	6	2.7	6	1010.2	367.3
23	19.8	14.4	73	106	0	0	0	6	2.6	6	1010.2	367
24	19.6	14.6	74	106.9	0	0	0	6	2.5	6	1010.1	367.1
						June						
1	23	20	84	149.4	0	0	0	6	2.2	8	1005.4	400.2
2	22.7	20	85	149.5	0	0	0	6	2.1	8	1005.3	399.6
3	22.5	19.9	86	149.2	0	0	0	6	2.1	8	1005.5	398.7
4	22.3	19.9	87	148.9	0	0	0	6	2	8	1005.6	398.1
5	22.4	19.9	86	149.1	0	0	0	6	2	8	1005.8	398.6
6	22.8	20	85	150	74	117	53	6	2.2	8	1005.9	400
7	23.4	20.2	83	151.1	174	182	111	6	2.5	8	1006.1	402.4
8	24.1	20.3	80	152.1	260	210	166	6	2.7	8	1006.3	405
9	24.8	20.3	77	152.4	374	248	231	6	2.8	8	1006.1	407.4
10	25.4	20.2	74	152	449	272	274	6	3	8	1005.9	409.3
11	26	20.1	72	151.1	459	219	311	6	3.1	8	1005.8	410.7
12	26.4	20	70	150.2	475	208	328	6	3.3	8	1005.6	411.6
13	26.6	19.9	69	149.5	441	227	297	6	3.4	8	1005.3	412.2
14	26.8	19.8	68	149.1	362	189	261	6	3.5	8	1005.1	412.4
15	26.7	19.8	68	149	296	153	219	6	3.5	8	1005.2	412
16	26.4	19.9	69	149	210	152	153	6	3.4	8	1005.3	411
17	25.9	19.9	71	149.3	115	98	89	6	3.4	8	1005.3	409.5
18	25.3	20	74	149.7	48	46	40	6	3.2	8	1005.5	407.6
19	24.7	20	76	150.1	0	0	0	6	2.9	8	1005.6	405.8
20	24.1	20	79	150.3	0	0	0	6	2.7	8	1005.7	404.2
21	23.8	20.1	80	150.4	0	0	0	6	2.6	8	1005.7	403.1
22	23.5	20	81	150.2	0	0	0	6	2.4	7	1005.6	402.4
23	23.4	20	82	150.2	0	0	0	6	2.3	7	1005.6	401.9
24	23.3	20.1	83	150.7	0	0	0	6	2.2	7	1005.5	401.9

Shanghai

HOUR	TEM	DEW	RH	X	TH	NR	DF	WD	WS	CC	AP	LW
						July						
1	27.7	23.5	79	185.5	0	0	0	7	2.4	6	1004.1	431.2
2	27.4	23.5	80	185.2	0	0	0	7	2.3	6	1004	430.1
3	27.1	23.4	81	184.7	0	0	0	7	2.2	6	1004.1	429
4	26.9	23.4	82	184.5	0	0	0	7	2.2	6	1004.3	428.4
5	27	23.5	82	185	0	0	0	7	2.1	7	1004.4	428.8
6	27.4	23.6	80	186	83	146	57	7	2.4	7	1004.6	430.5
7	28.1	23.6	78	186.8	215	256	121	8	2.7	7	1004.8	433.1
8	29	23.6	74	186.7	329	275	188	8	3	7	1005	436.2
9	29.9	23.5	70	185.6	485	353	247	8	3.2	7	1004.8	439.1
10	30.8	23.3	66	183.7	588	376	294	8	3.4	7	1004.6	441.5
11	31.4	23.2	63	182.1	598	293	350	8	3.6	7	1004.4	443.3
12	31.8	23.1	62	181.1	602	261	370	8	3.7	7	1004.2	444.4
13	31.9	23.1	61	181	555	257	346	7	3.8	7	1003.9	445
14	31.9	23.1	62	181.3	457	197	316	7	3.8	7	1003.7	445.1
15	31.7	23.1	62	181.6	370	168	264	7	3.7	7	1003.8	444.5
16	31.4	23.1	63	181.6	268	170	189	7	3.6	7	1003.8	443.2
17	30.9	23.2	65	181.8	156	122	116	7	3.5	7	1003.9	441.3
18	30.2	23.2	68	182.2	60	60	49	7	3.2	7	1004.1	439.1
19	29.6	23.3	70	182.9	0	0	0	6	3	7	1004.2	436.9
20	29	23.4	73	183.9	0	0	0	6	2.8	6	1004.4	435
21	28.5	23.4	75	184.7	0	0	0	6	2.7	6	1004.3	433.8
22	28.3	23.5	76	185.2	0	0	0	7	2.6	6	1004.3	433.1
23	28.1	23.5	77	185.6	0	0	0	7	2.5	6	1004.3	432.6
24	28	23.5	78	185.8	0	0	0	7	2.5	6	1004.2	432.3
						August						
1	27.6	23.5	79	185.4	0	0	0	7	2.5	6	1005.9	430.6
2	27.3	23.5	80	185.6	0	0	0	7	2.4	6	1005.7	429.8
3	27	23.5	82	185.6	0	0	0	7	2.3	6	1005.9	428.9
4	26.9	23.5	82	185.5	0	0	0	6	2.3	6	1006	428.4
5	26.9	23.5	82	185.8	0	0	0	6	2.2	6	1006.1	428.8
6	27.3	23.6	81	186.4	49	90	37	6	2.5	6	1006.3	430.2
7	28	23.7	78	186.9	198	273	108	7	2.8	6	1006.4	432.6
8	28.8	23.6	74	186.6	325	295	180	7	3.1	6	1006.6	435.5
9	29.6	23.5	71	185.2	478	378	234	7	3.2	7	1006.4	437.8
10	30.3	23.3	67	183	579	412	275	6	3.3	7	1006.2	439.7
11	30.9	23.1	65	180.8	589	333	324	6	3.5	7	1006.1	441
12	31.3	23	63	179.3	601	296	350	6	3.6	7	1005.8	441.7
13	31.4	22.9	62	178.8	557	280	336	6	3.8	7	1005.6	442
14	31.3	22.9	62	178.8	457	208	310	6	3.9	7	1005.3	441.7
15	31	22.9	63	178.9	361	178	252	6	3.8	7	1005.4	440.5
16	30.6	22.9	65	179.1	255	170	179	6	3.8	7	1005.5	438.9
17	30	23	67	179.6	135	118	101	6	3.7	7	1005.6	436.9
18	29.4	23	70	180.3	33	33	28	6	3.5	7	1005.8	435
19	28.8	23.1	72	181	0	0	0	6	3.3	6	1006	433.2
20	28.3	23.2	74	181.6	0	0	0	6	3.1	6	1006.2	431.7
21	28	23.2	76	182.2	0	0	0	6	2.9	6	1006.2	430.9
22	27.8	23.3	77	182.7	0	0	0	6	2.7	6	1006.2	430.5
23	27.7	23.3	78	183.3	0	0	0	6	2.6	6	1006.2	430.4
24	27.6	23.4	78	184	0	0	0	6	2.5	6	1006	430.3

Shanghai

HOUR	TEM	DEW	RH	X	TH	NR	DF	WD	WS	CC	AP	LW
September												
1	23.5	19.6	79	146.2	0	0	0	6	2.1	7	1011.9	400.4
2	23.3	19.6	81	146.4	0	0	0	6	2	7	1011.8	399.7
3	23	19.6	82	146.3	0	0	0	6	2	7	1012	399
4	22.9	19.6	82	146.1	0	0	0	6	2	6	1012.1	398.5
5	22.9	19.7	82	146.3	0	0	0	6	2.1	6	1012.3	398.9
6	23.3	19.7	81	147	16	21	14	6	2.3	6	1012.5	400.2
7	23.8	19.8	79	147.8	153	286	79	6	2.7	7	1012.7	402.3
8	24.6	19.8	76	147.7	277	328	139	6	2.9	7	1012.9	404.5
9	25.3	19.7	72	146.4	421	388	198	6	3.1	7	1012.6	406.3
10	26	19.4	68	144.4	512	386	246	5	3.3	7	1012.4	407.5
11	26.5	19.2	66	142.7	507	289	297	5	3.5	8	1012.2	408.3
12	26.8	19.1	64	141.7	518	280	309	5	3.6	7	1011.9	408.8
13	26.9	19	63	141.3	474	283	281	6	3.6	7	1011.6	409
14	26.8	19	64	141	381	220	251	6	3.7	7	1011.4	408.5
15	26.6	18.9	64	140.4	303	192	202	6	3.6	7	1011.6	407.4
16	26.2	18.8	65	139.9	193	191	127	5	3.5	7	1011.8	405.7
17	25.7	18.8	67	139.9	84	117	60	5	3.5	7	1011.9	404
18	25.2	18.9	69	140.7	0	0	0	5	3.2	7	1012.2	402.8
19	24.7	19.1	72	142	0	0	0	5	3	6	1012.4	401.8
20	24.3	19.3	74	143.2	0	0	0	5	2.8	6	1012.7	401.2
21	24	19.3	76	144	0	0	0	5	2.6	6	1012.6	400.6
22	23.8	19.4	77	144.2	0	0	0	6	2.5	6	1012.5	400.2
23	23.7	19.4	77	144.3	0	0	0	6	2.3	6	1012.5	400
24	23.6	19.4	78	144.7	0	0	0	6	2.2	6	1012.4	399.8
October												
1	18.8	14.5	76	105.4	0	0	0	7	1.9	6	1018.3	364.3
2	18.5	14.4	78	105.2	0	0	0	7	1.8	7	1018.2	363.3
3	18.2	14.4	79	104.9	0	0	0	7	1.8	6	1018.4	362.4
4	18	14.4	80	104.7	0	0	0	6	1.8	6	1018.6	361.8
5	18.1	14.4	80	104.8	0	0	0	6	1.9	6	1018.8	362.1
6	18.4	14.6	79	105.7	0	0	0	6	2.1	6	1019	363.7
7	19.1	14.7	76	106.8	109	246	59	6	2.4	6	1019.3	366.1
8	20	14.7	72	106.9	227	313	114	6	2.7	6	1019.5	368.7
9	20.9	14.5	68	105.7	372	394	166	6	2.9	7	1019.2	370.3
10	21.6	14.1	64	103.3	466	422	204	6	3.1	7	1018.9	371.2
11	22.2	13.7	60	100.8	478	340	248	6	3.3	7	1018.6	371.4
12	22.6	13.4	58	98.8	486	332	258	6	3.4	7	1018.2	371.5
13	22.8	13.2	56	97.6	433	312	238	6	3.5	7	1017.9	371.2
14	22.7	13.1	56	97.1	325	229	203	6	3.5	7	1017.5	370.6
15	22.4	13	57	97	230	187	151	6	3.4	7	1017.7	369.4
16	21.9	13.1	59	97.3	122	144	86	6	3.2	7	1017.9	368.1
17	21.3	13.3	62	98.3	27	29	23	6	3	7	1018.1	366.9
18	20.8	13.5	64	99.7	0	0	0	6	2.8	6	1018.4	366.1
19	20.3	13.8	67	101.3	0	0	0	5	2.6	6	1018.7	365.7
20	19.8	14	70	102.6	0	0	0	5	2.4	6	1018.9	365.3
21	19.5	14.2	72	103.4	0	0	0	5	2.3	6	1018.9	364.8
22	19.2	14.2	73	103.8	0	0	0	6	2.2	6	1018.8	364.3
23	19.1	14.3	74	103.9	0	0	0	6	2.1	6	1018.8	364
24	18.9	14.3	75	104.1	0	0	0	6	2	6	1018.7	363.6

Shanghai

HOUR	TEM	DEW	RH	X	TH	NR	DF	WD	WS	CC	AP	LW
November												
1	12.6	8.6	78	73.1	0	0	0	8	2.1	6	1022.1	323.9
2	12.3	8.5	78	72.6	0	0	0	8	2.1	6	1022.1	322.9
3	12.1	8.3	79	72	0	0	0	8	2.1	6	1022.2	321.7
4	11.9	8.2	79	71.4	0	0	0	7	2.1	6	1022.3	320.8
5	11.8	8.3	80	71.5	0	0	0	7	2.1	5	1022.5	320.9
6	11.9	8.6	81	72.6	0	0	0	7	2.2	6	1022.7	322.3
7	12.4	8.9	80	74.2	45	91	33	8	2.2	6	1022.9	324.7
8	13.2	9.1	77	75.1	132	201	80	8	2.3	6	1023.1	327.3
9	14.1	8.9	72	74.6	254	293	133	8	2.6	7	1022.8	328.9
10	15.1	8.4	66	72.9	353	376	162	8	3	7	1022.5	329.7
11	15.9	7.9	61	70.7	386	361	187	8	3.3	7	1022.2	330
12	16.5	7.4	58	69.1	395	366	191	8	3.3	7	1021.8	330
13	16.7	7.2	57	68.2	336	321	177	8	3.3	7	1021.4	329.8
14	16.6	7.1	57	68	233	206	150	8	3.3	7	1020.9	329.2
15	16.2	7.2	58	68.1	141	162	95	8	3.1	7	1021.2	328.4
16	15.7	7.4	60	68.5	69	93	53	7	2.8	7	1021.4	327.4
17	15.1	7.6	63	69.1	0	0	0	7	2.6	7	1021.7	326.4
18	14.6	7.8	66	69.9	0	0	0	7	2.5	7	1021.9	325.7
19	14.1	8	68	70.6	0	0	0	7	2.4	6	1022.2	325.1
20	13.6	8.1	71	71	0	0	0	7	2.3	6	1022.5	324.4
21	13.2	8.2	73	71.3	0	0	0	7	2.3	6	1022.5	323.8
22	12.9	8.2	74	71.4	0	0	0	7	2.2	6	1022.4	323.2
23	12.7	8.3	75	71.6	0	0	0	7	2.2	5	1022.4	323
24	12.5	8.3	77	71.8	0	0	0	7	2.1	6	1022.3	322.8
December												
1	6.1	1.6	74	44.9	0	0	0	9	2.2	6	1025.6	281.3
2	5.9	1.5	75	44.6	0	0	0	9	2.2	6	1025.5	280.6
3	5.7	1.4	75	44.4	0	0	0	9	2.2	6	1025.6	279.8
4	5.5	1.3	75	44	0	0	0	9	2.2	5	1025.7	279
5	5.3	1.2	76	43.7	0	0	0	9	2.2	5	1025.8	278.4
6	5.3	1.4	77	43.9	0	0	0	9	2.3	5	1026	278.7
7	5.4	1.6	77	44.5	9	9	8	9	2.4	6	1026.2	279.8
8	6.1	1.7	75	45	98	200	59	9	2.5	6	1026.4	281.6
9	7	1.6	70	45	226	346	106	9	2.8	6	1026.1	283.3
10	8.2	1.4	64	44.5	343	477	129	9	3.2	6	1025.8	285
11	9.3	1	58	43.7	389	473	152	9	3.5	6	1025.5	286.4
12	10	0.7	55	42.9	414	504	152	9	3.5	6	1025.1	287.1
13	10.3	0.4	53	42.3	354	421	153	9	3.5	6	1024.7	287
14	10.2	0.3	53	41.9	236	252	140	9	3.5	6	1024.3	286.2
15	9.8	0.2	54	41.6	144	187	92	9	3.2	6	1024.5	285
16	9.3	0.2	56	41.6	62	93	47	8	2.9	6	1024.8	283.8
17	8.8	0.4	58	42	0	0	0	8	2.7	6	1025	282.9
18	8.2	0.7	61	42.6	0	0	0	8	2.6	6	1025.3	282.5
19	7.7	1	64	43.3	0	0	0	8	2.4	6	1025.5	282.3
20	7.2	1.2	67	43.9	0	0	0	8	2.3	6	1025.8	282.1
21	6.8	1.3	69	44.2	0	0	0	8	2.3	5	1025.8	281.6
22	6.5	1.3	71	44.3	0	0	0	8	2.2	5	1025.8	281.1
23	6.3	1.3	72	44.1	0	0	0	8	2.2	5	1025.8	280.7
24	6.1	1.3	73	44.1	0	0	0	8	2.2	5	1025.7	280.2

Guangzhou

HOUR	TEM	DEW	RH	X	TH	NR	DF	WD	WS	CC	AP	LW
January												
1	12	7	73	66.7	0	0	0	9	2.1	8	1015.1	316.1
2	11.8	6.9	74	66.2	0	0	0	9	2.2	8	1015.2	315.1
3	11.6	6.8	74	65.7	0	0	0	9	2.1	8	1015.3	314.2
4	11.4	6.6	74	65.2	0	0	0	9	2.1	7	1015.5	313.3
5	11.1	6.6	75	64.8	0	0	0	9	2.1	7	1015.6	312.3
6	10.8	6.5	77	64.6	0	0	0	9	2.1	8	1015.8	311.5
7	10.7	6.5	77	64.6	0	0	0	9	2.1	8	1016	311.1
8	11.1	6.5	75	64.6	47	59	38	9	2.1	8	1016.3	312
9	12	6.4	71	64.6	144	142	99	9	2.2	8	1015.9	314
10	13.4	6.4	65	64.7	275	262	153	8	2.4	8	1015.5	317.5
11	14.8	6.4	60	64.9	376	326	192	8	2.6	7	1015.1	321.5
12	15.9	6.5	57	65.2	446	379	209	8	2.6	7	1014.6	325
13	16.7	6.5	55	65.5	444	372	213	9	2.6	7	1014	327.5
14	17.1	6.6	54	65.7	375	290	210	9	2.6	7	1013.5	329.1
15	17.3	6.6	53	65.8	302	270	170	9	2.5	7	1013.6	329.7
16	17.2	6.7	54	66	196	240	111	10	2.5	7	1013.7	329.5
17	16.7	6.8	56	66.5	80	151	52	10	2.4	7	1013.8	328.4
18	15.8	7	59	67.4	0	0	0	10	2.4	7	1014	326.6
19	14.7	7.3	64	68.4	0	0	0	10	2.3	7	1014.2	324.6
20	13.8	7.6	68	69.2	0	0	0	10	2.2	7	1014.4	323
21	13.2	7.7	71	69.6	0	0	0	10	2.1	7	1014.5	321.7
22	12.8	7.6	72	69.2	0	0	0	9	2.1	7	1014.7	320.5
23	12.6	7.4	73	68.4	0	0	0	9	2.1	7	1014.9	319.2
24	12.3	7.3	73	67.8	0	0	0	9	2.1	7	1014.9	318
February												
1	14.7	11	79	87.9	0	0	0	8	1.9	8	1012.3	339.6
2	14.5	10.9	80	87.4	0	0	0	8	1.9	8	1012.4	338.6
3	14.3	10.8	81	87	0	0	0	8	1.9	8	1012.6	337.8
4	14.1	10.7	81	86.5	0	0	0	8	1.9	8	1012.7	336.9
5	13.9	10.7	82	86	0	0	0	8	1.8	8	1012.8	336.1
6	13.7	10.7	83	85.9	0	0	0	8	1.8	8	1013.1	335.6
7	13.7	10.7	83	86	0	0	0	7	1.8	8	1013.3	335.5
8	14	10.7	81	86.3	41	40	35	7	1.8	9	1013.5	336.5
9	14.8	10.7	77	86.7	129	89	100	7	2	9	1013.2	338.6
10	16	10.7	73	87.1	244	164	167	8	2.2	9	1012.8	341.7
11	17.1	10.7	68	87.4	336	215	216	8	2.4	8	1012.5	345.2
12	18.1	10.8	65	87.5	402	254	243	8	2.4	8	1012	348.1
13	18.8	10.8	62	87.4	402	254	247	9	2.5	8	1011.5	350.2
14	19.2	10.8	61	87.2	350	199	235	9	2.6	8	1011	351.5
15	19.4	10.7	60	86.9	296	202	194	9	2.6	8	1011.1	351.9
16	19.3	10.7	60	86.8	205	193	130	9	2.6	8	1011.1	351.7
17	18.9	10.8	62	87.1	94	122	66	9	2.5	8	1011.1	350.6
18	18.1	10.9	65	87.8	14	16	13	9	2.4	8	1011.2	348.8
19	17.2	11.1	69	88.8	0	0	0	9	2.3	8	1011.3	346.8
20	16.4	11.3	73	89.8	0	0	0	9	2.2	8	1011.5	345.3
21	15.9	11.4	76	90.5	0	0	0	9	2.1	8	1011.6	344.3
22	15.6	11.4	78	90.4	0	0	0	8	2	8	1011.8	343.5
23	15.3	11.3	78	89.7	0	0	0	8	1.9	8	1012	342.4
24	15.1	11.2	79	89.2	0	0	0	8	1.9	8	1012.1	341.5

Guangzhou

HOUR	TEM	DEW	RH	X	TH	NR	DF	WD	WS	CC	AP	LW
						March						
1	17.2	14.3	84	106.9	0	0	0	8	1.7	8	1010.1	359.6
2	16.9	14.2	85	106.3	0	0	0	8	1.7	9	1010.1	358.6
3	16.7	14.1	85	105.6	0	0	0	8	1.7	8	1010.3	357.6
4	16.6	14	86	105	0	0	0	8	1.7	8	1010.4	356.8
5	16.4	14	86	104.6	0	0	0	8	1.7	8	1010.5	356.2
6	16.3	14	87	104.7	0	0	0	8	1.7	8	1010.8	355.9
7	16.4	14.1	87	105	17	15	16	7	1.6	9	1011.1	356.4
8	16.8	14.1	84	105.2	54	52	46	7	1.6	9	1011.4	357.6
9	17.6	14	80	105.2	144	84	116	7	1.8	9	1011.1	359.5
10	18.6	13.9	76	105.1	245	146	179	7	2	9	1010.8	362.1
11	19.6	13.9	72	105.1	319	175	226	7	2.2	9	1010.5	364.9
12	20.3	13.9	69	105.2	364	186	254	7	2.3	9	1010.1	367.1
13	20.8	13.9	68	105.3	360	188	253	8	2.4	9	1009.6	368.6
14	21.1	13.9	67	105.4	318	156	236	8	2.4	9	1009.1	369.5
15	21.2	13.9	67	105.3	259	140	194	8	2.4	9	1009.1	369.9
16	21.1	13.8	67	105.3	179	138	131	8	2.4	9	1009.1	369.6
17	20.8	13.9	68	105.4	91	95	70	8	2.4	9	1009.1	368.7
18	20.2	14	71	106	32	39	28	8	2.2	9	1009.2	367.2
19	19.4	14.2	74	107	0	0	0	7	2	8	1009.3	365.6
20	18.7	14.5	78	108.1	0	0	0	7	1.9	8	1009.4	364.4
21	18.2	14.6	80	108.9	0	0	0	7	1.8	8	1009.6	363.6
22	17.9	14.6	82	108.9	0	0	0	8	1.8	8	1009.7	362.9
23	17.7	14.6	82	108.5	0	0	0	8	1.7	8	1009.9	362.1
24	17.5	14.5	83	108.2	0	0	0	8	1.7	8	1010	361.5
						April						
1	21.3	18.7	86	139.4	0	0	0	7	1.6	8	1006.3	390.1
2	21.1	18.6	86	138.6	0	0	0	7	1.6	9	1006.4	388.8
3	20.8	18.5	87	137.6	0	0	0	7	1.5	8	1006.6	387.6
4	20.6	18.4	87	136.7	0	0	0	7	1.5	8	1006.7	386.6
5	20.5	18.3	88	136.4	0	0	0	7	1.5	8	1006.9	386.1
6	20.5	18.4	88	136.9	0	0	0	7	1.5	8	1007.1	386.3
7	20.7	18.5	87	137.7	44	39	37	7	1.6	9	1007.4	387.3
8	21.2	18.5	85	138.2	97	68	81	7	1.6	9	1007.6	389.1
9	22	18.5	81	138.3	198	98	159	7	1.8	9	1007.3	391.2
10	22.9	18.4	77	137.9	301	151	223	7	2	9	1007	393.7
11	23.8	18.4	73	137.5	372	169	271	7	2.2	9	1006.7	396.3
12	24.4	18.4	71	137.5	415	166	303	7	2.3	9	1006.3	398.4
13	24.9	18.4	69	137.6	402	162	299	8	2.3	9	1005.9	400
14	25.2	18.4	68	137.8	349	127	275	8	2.4	9	1005.5	401.1
15	25.3	18.4	68	137.8	287	114	228	8	2.4	9	1005.5	401.4
16	25.2	18.4	69	137.9	204	121	155	7	2.4	9	1005.5	401.2
17	24.8	18.4	70	138.3	110	89	86	7	2.3	9	1005.5	400.1
18	24.2	18.6	73	139	40	43	34	7	2.2	9	1005.6	398.5
19	23.5	18.7	76	140.1	0	0	0	7	2.1	8	1005.7	396.7
20	22.8	18.9	79	141.3	0	0	0	7	1.9	8	1005.7	395.3
21	22.4	19	82	142	0	0	0	7	1.8	8	1005.8	394.2
22	22.1	19	83	142	0	0	0	7	1.8	8	1006	393.5
23	21.8	18.9	84	141.5	0	0	0	7	1.7	8	1006.1	392.6
24	21.6	18.9	85	141.1	0	0	0	7	1.7	8	1006.2	391.8

Guangzhou

HOUR	TEM	DEW	RH	X	TH	NR	DF	WD	WS	CC	AP	LW
						May						
1	24.6	22	86	170.4	0	0	0	6	1.6	8	1002.5	414.4
2	24.4	21.9	87	169.7	0	0	0	6	1.5	8	1002.5	413.3
3	24.1	21.8	87	168.9	0	0	0	6	1.5	8	1002.7	412.2
4	23.9	21.7	88	168.2	0	0	0	6	1.4	8	1002.8	411.3
5	23.9	21.7	88	168.2	0	0	0	6	1.4	8	1003	411.4
6	24.1	21.8	88	169.1	0	0	0	6	1.5	8	1003.2	412.2
7	24.5	22	86	170.5	69	67	56	6	1.6	8	1003.4	413.9
8	25.1	22.1	84	171.8	148	101	115	6	1.7	8	1003.6	416.5
9	26	22.1	80	172.6	269	129	202	6	1.9	8	1003.3	419.3
10	26.9	22.1	76	172.7	382	174	271	7	2	8	1003	422.4
11	27.7	22	73	172.3	451	174	322	7	2.2	8	1002.8	425.2
12	28.4	22	70	171.7	491	173	352	7	2.2	8	1002.4	427.2
13	28.8	21.9	68	171	476	180	341	7	2.3	8	1002.1	428.4
14	29	21.8	68	170.3	416	144	316	7	2.4	8	1001.7	428.9
15	29	21.7	67	169.5	338	124	261	7	2.4	8	1001.7	428.5
16	28.7	21.7	68	169	246	135	184	7	2.4	8	1001.7	427.4
17	28.2	21.7	70	168.9	147	104	113	7	2.4	8	1001.8	425.4
18	27.5	21.7	73	169.2	59	64	47	7	2.3	8	1001.8	423
19	26.7	21.8	77	169.9	0	0	0	6	2.1	8	1001.9	420.5
20	26	21.9	80	170.7	0	0	0	6	2	8	1001.9	418.7
21	25.5	22	82	171.4	0	0	0	6	1.9	8	1002.1	417.6
22	25.3	22.1	83	171.7	0	0	0	6	1.8	8	1002.2	417
23	25.1	22.1	84	171.7	0	0	0	6	1.7	7	1002.3	416.6
24	25	22.1	85	171.6	0	0	0	6	1.6	7	1002.3	415.9
						June						
1	26.8	24.3	86	195.6	0	0	0	6	1.5	8	999	431.9
2	26.6	24.2	87	194.9	0	0	0	6	1.4	8	999.1	431
3	26.3	24.2	88	194.2	0	0	0	6	1.4	8	999.2	429.8
4	26.2	24.1	89	193.9	0	0	0	5	1.4	8	999.3	429.1
5	26.1	24.2	89	194.5	0	0	0	5	1.4	8	999.5	429.4
6	26.3	24.3	89	196.1	0	0	0	5	1.5	8	999.6	430.5
7	26.8	24.5	88	197.9	88	82	69	6	1.6	8	999.8	432.6
8	27.5	24.6	85	199.2	185	108	142	6	1.7	8	999.9	435.6
9	28.4	24.6	80	199.2	315	142	232	6	1.9	8	999.7	438.5
10	29.4	24.5	76	198	429	174	304	7	2.2	8	999.4	441.3
11	30.1	24.3	72	196.2	490	162	360	7	2.4	8	999.2	443.4
12	30.6	24.2	70	194.4	517	155	383	7	2.4	8	998.9	444.4
13	30.8	24	69	193.1	489	181	349	7	2.5	8	998.6	444.7
14	30.8	24	69	192.2	445	164	326	7	2.6	8	998.4	444.5
15	30.7	23.9	69	191.7	374	148	276	7	2.5	8	998.4	443.9
16	30.4	23.9	70	191.6	278	157	199	7	2.5	8	998.4	442.9
17	30	23.9	72	191.9	179	120	133	7	2.4	8	998.5	441.4
18	29.4	24	74	192.5	78	72	62	7	2.3	8	998.5	439.4
19	28.7	24.1	77	193.5	0	0	0	6	2.1	8	998.6	437.2
20	28	24.2	81	194.5	0	0	0	6	2	8	998.7	435.6
21	27.6	24.3	83	195.4	0	0	0	6	1.9	8	998.7	434.4
22	27.4	24.3	84	195.9	0	0	0	6	1.8	7	998.8	433.8
23	27.2	24.3	85	196.2	0	0	0	6	1.7	7	998.9	433.5
24	27.1	24.3	85	196.4	0	0	0	6	1.6	7	999	433.1

Guangzhou

HOUR	TEM	DEW	RH	X	TH	NR	DF	WD	WS	CC	AP	LW
July												
1	27.9	24.5	83	198.4	0	0	0	6	1.7	7	998.9	436.4
2	27.5	24.5	84	197.6	0	0	0	6	1.6	7	999	435.1
3	27.2	24.4	85	196.7	0	0	0	6	1.5	7	999.1	433.7
4	27	24.4	86	196.2	0	0	0	6	1.4	7	999.2	432.8
5	27	24.4	87	196.9	0	0	0	6	1.4	7	999.3	433
6	27.2	24.6	86	198.8	0	0	0	6	1.5	7	999.5	434.3
7	27.7	24.7	84	200.8	97	105	73	6	1.7	7	999.6	436.8
8	28.5	24.8	81	201.7	221	150	157	6	1.8	7	999.8	439.9
9	29.5	24.7	76	200.7	373	205	247	6	2	8	999.5	442.8
10	30.5	24.5	71	198.4	503	250	314	7	2.2	8	999.3	445.4
11	31.3	24.3	67	195.8	575	238	370	7	2.3	8	999.1	447.7
12	31.9	24.2	65	193.9	613	226	405	7	2.4	8	998.8	449.2
13	32.3	24.1	63	192.8	592	237	385	8	2.4	8	998.5	450.1
14	32.4	24	63	192.1	538	203	368	8	2.5	8	998.2	450.6
15	32.4	23.9	63	191.4	449	177	317	8	2.5	8	998.2	450.2
16	32.1	23.9	64	191.1	341	186	232	7	2.5	8	998.2	449.1
17	31.6	23.9	66	191.7	220	151	156	7	2.6	8	998.2	447.5
18	30.9	24.1	69	193.4	97	90	75	7	2.4	8	998.3	445.3
19	30.1	24.3	72	195.7	0	0	0	6	2.2	8	998.3	443.2
20	29.4	24.5	76	197.8	0	0	0	6	2	7	998.4	441.3
21	28.8	24.6	79	199	0	0	0	6	2	7	998.5	440
22	28.5	24.6	80	199.1	0	0	0	6	1.9	7	998.6	438.9
23	28.3	24.6	81	198.8	0	0	0	6	1.9	6	998.8	438.2
24	28.1	24.6	81	198.6	0	0	0	6	1.8	7	998.8	437.4
August												
1	27.5	24.3	83	195.3	0	0	0	7	1.5	7	998.8	434
2	27.2	24.2	85	194.9	0	0	0	7	1.4	7	998.9	432.8
3	26.8	24.2	86	193.9	0	0	0	7	1.4	7	999	431.4
4	26.6	24.1	86	193.1	0	0	0	6	1.4	7	999.1	430.2
5	26.5	24.1	87	193.1	0	0	0	6	1.4	7	999.2	430.1
6	26.7	24.2	87	194.3	0	0	0	6	1.4	7	999.4	431
7	27.2	24.3	85	196	82	105	62	6	1.5	7	999.5	433.1
8	28	24.4	82	197	208	182	138	6	1.6	7	999.6	436.4
9	29.1	24.4	77	196.5	371	253	223	6	1.7	7	999.4	439.7
10	30.2	24.2	71	194.7	510	306	290	7	1.9	7	999.2	443
11	31.2	24	67	192.4	580	274	351	7	2.1	8	999	446
12	31.9	23.8	64	190.3	620	259	384	7	2.2	8	998.7	447.8
13	32.3	23.7	62	188.6	589	247	375	8	2.4	8	998.4	448.9
14	32.5	23.5	61	187	519	199	357	8	2.5	8	998.1	449.2
15	32.5	23.4	61	185.7	439	192	301	8	2.4	8	998.1	448.6
16	32.2	23.4	62	185.1	336	223	215	7	2.4	8	998.1	447.3
17	31.7	23.4	64	186	204	171	138	7	2.3	8	998.2	445.5
18	30.9	23.6	67	188.2	74	88	56	7	2.2	8	998.2	443.3
19	30	23.9	71	191.1	0	0	0	6	2	7	998.3	440.9
20	29.1	24.1	75	193.7	0	0	0	6	1.9	7	998.4	438.9
21	28.5	24.2	78	195	0	0	0	6	1.8	7	998.5	437.4
22	28.2	24.3	80	195.3	0	0	0	6	1.7	7	998.6	436.2
23	28	24.3	81	195.1	0	0	0	6	1.6	7	998.7	435.5
24	27.7	24.3	82	195.1	0	0	0	6	1.5	7	998.8	434.7

Guangzhou

HOUR	TEM	DEW	RH	X	TH	NR	DF	WD	WS	CC	AP	LW
September												
1	26.5	22.6	80	177	0	0	0	7	1.7	7	1002.2	423.1
2	26.2	22.5	81	176.3	0	0	0	7	1.7	7	1002.3	421.8
3	25.9	22.4	82	175.4	0	0	0	7	1.7	7	1002.4	420.5
4	25.7	22.4	83	174.5	0	0	0	7	1.7	7	1002.6	419.4
5	25.5	22.3	83	174.2	0	0	0	7	1.6	7	1002.7	418.9
6	25.6	22.4	83	174.8	0	0	0	7	1.7	7	1003	419.3
7	25.9	22.5	82	175.8	60	78	47	7	1.8	7	1003.2	420.8
8	26.7	22.5	79	176.4	187	167	126	7	1.9	7	1003.4	423.6
9	27.7	22.5	74	176.2	353	254	211	7	2	7	1003.1	426.9
10	28.9	22.4	69	175.2	504	340	266	7	2.2	7	1002.8	430.6
11	30	22.3	65	173.9	586	340	315	7	2.4	7	1002.5	434
12	30.8	22.2	62	172.8	632	340	342	7	2.4	7	1002.1	436.4
13	31.2	22.1	60	171.9	599	310	342	7	2.4	8	1001.7	437.9
14	31.4	22	59	171	510	237	328	7	2.4	8	1001.3	438.4
15	31.4	22	59	170.1	413	218	269	7	2.4	8	1001.4	438
16	31.1	21.9	60	169.7	293	217	186	7	2.4	8	1001.5	436.9
17	30.6	22	62	170.3	154	154	105	7	2.4	7	1001.6	435
18	29.8	22.2	65	172	31	36	26	7	2.2	7	1001.7	432.6
19	28.8	22.4	70	174.3	0	0	0	7	2.1	7	1001.9	430.1
20	27.9	22.6	74	176.3	0	0	0	7	1.9	7	1002	427.9
21	27.4	22.6	77	177.3	0	0	0	7	1.8	7	1002.1	426.3
22	27	22.7	78	177.4	0	0	0	7	1.8	7	1002.2	425.2
23	26.8	22.6	79	177.1	0	0	0	7	1.7	7	1002.3	424.4
24	26.6	22.6	79	176.7	0	0	0	7	1.7	7	1002.3	423.5
October												
1	23.5	18.4	74	137	0	0	0	8	1.7	7	1007.4	395.2
2	23.2	18.3	75	136.1	0	0	0	8	1.7	7	1007.5	393.7
3	23	18.1	76	135	0	0	0	8	1.7	7	1007.7	392.4
4	22.7	18	76	133.8	0	0	0	7	1.7	6	1007.9	391
5	22.5	17.9	76	132.9	0	0	0	7	1.7	6	1008.2	390
6	22.5	17.9	76	132.5	0	0	0	7	1.8	6	1008.4	389.7
7	22.8	17.9	75	132.6	39	53	32	7	1.9	6	1008.7	390.6
8	23.5	17.9	72	132.7	165	157	112	7	2	6	1009	393
9	24.7	17.8	67	132.3	331	251	198	7	2.2	6	1008.6	396.4
10	26.1	17.7	62	131.6	487	348	251	6	2.4	6	1008.2	400.6
11	27.3	17.6	57	130.9	579	377	286	6	2.6	6	1007.8	404.7
12	28.3	17.5	54	130.3	629	403	300	6	2.6	7	1007.3	407.9
13	28.9	17.5	52	129.8	592	372	297	7	2.5	7	1006.8	409.9
14	29.1	17.4	51	129.1	488	289	281	7	2.5	7	1006.3	410.6
15	29.1	17.3	51	128.4	380	257	227	7	2.5	7	1006.5	410.3
16	28.8	17.3	52	128.3	245	229	148	7	2.5	7	1006.6	409.1
17	28.2	17.4	54	129.4	98	135	68	7	2.5	6	1006.8	407.1
18	27.2	17.7	58	131.6	2	1	2	7	2.3	6	1007	404.8
19	26.1	18.1	63	134.4	0	0	0	8	2.1	6	1007.2	402.4
20	25.1	18.4	68	136.7	0	0	0	8	1.9	6	1007.4	400.3
21	24.5	18.5	71	137.8	0	0	0	8	1.8	6	1007.5	398.8
22	24.1	18.5	72	137.8	0	0	0	7	1.8	6	1007.5	397.6
23	23.9	18.4	73	137.1	0	0	0	7	1.7	6	1007.6	396.5
24	23.7	18.3	73	136.3	0	0	0	7	1.7	6	1007.6	395.4

Guangzhou

HOUR	TEM	DEW	RH	X	TH	NR	DF	WD	WS	CC	AP	LW
November												
1	18.8	13.9	75	105.3	0	0	0	8	1.8	7	1011.1	362.3
2	18.4	13.8	76	104.6	0	0	0	8	1.8	7	1011.1	360.9
3	18.2	13.6	76	103.9	0	0	0	8	1.8	7	1011.3	359.7
4	18	13.5	76	102.8	0	0	0	8	1.8	6	1011.5	358.4
5	17.8	13.3	77	101.7	0	0	0	8	1.9	6	1011.7	357.2
6	17.7	13.3	77	101.3	0	0	0	8	1.9	6	1012	356.8
7	17.9	13.3	76	101.4	17	23	15	8	2	7	1012.3	357.4
8	18.6	13.3	73	101.7	108	133	76	8	2	7	1012.5	359.4
9	19.7	13.3	68	101.6	251	227	152	8	2.2	7	1012.1	362.5
10	21.1	13.2	63	101.4	396	339	198	7	2.3	6	1011.6	366.5
11	22.5	13.1	58	101.2	490	385	227	7	2.5	6	1011.2	370.7
12	23.5	13.1	55	101.1	541	425	236	7	2.5	6	1010.6	374.1
13	24.1	13.1	53	101.1	511	394	237	7	2.5	6	1010.1	376.3
14	24.3	13.1	53	100.9	414	299	227	7	2.5	7	1009.5	377
15	24.3	13.1	53	100.6	307	257	179	7	2.4	7	1009.7	376.6
16	23.9	13.1	54	100.7	176	201	110	8	2.3	7	1010	375.3
17	23.1	13.3	57	101.8	53	78	42	8	2.3	6	1010.2	373.5
18	22.2	13.6	61	103.7	0	0	0	8	2.2	6	1010.4	371.6
19	21.1	14	66	105.8	0	0	0	8	2	6	1010.7	369.7
20	20.2	14.3	70	107.3	0	0	0	8	1.9	6	1010.9	367.9
21	19.6	14.3	73	107.7	0	0	0	8	1.9	6	1011	366.5
22	19.3	14.2	74	106.9	0	0	0	7	1.9	6	1011.1	365.1
23	19.2	14	74	105.7	0	0	0	7	1.8	6	1011.1	363.7
24	18.9	13.8	74	104.7	0	0	0	7	1.8	6	1011.2	362.3
December												
1	13.8	8.2	71	71.9	0	0	0	8	2	7	1014.1	325.3
2	13.5	8	71	71.2	0	0	0	8	2.1	7	1014.2	323.9
3	13.3	7.9	72	70.6	0	0	0	8	2.1	7	1014.3	322.9
4	13.1	7.7	72	70	0	0	0	8	2.2	7	1014.5	321.8
5	12.8	7.6	72	69.3	0	0	0	8	2.2	6	1014.7	320.6
6	12.6	7.6	73	69	0	0	0	8	2.2	6	1014.9	319.8
7	12.6	7.6	73	69	0	0	0	8	2.2	7	1015.1	319.7
8	13.1	7.5	71	68.9	72	102	54	8	2.1	7	1015.3	320.9
9	14.3	7.4	65	68.8	196	227	118	8	2.3	7	1014.9	323.3
10	15.8	7.2	59	68.5	344	371	162	7	2.5	6	1014.4	327.1
11	17.3	7.1	54	68.3	449	438	190	7	2.7	6	1014	331.3
12	18.5	7.1	51	68.3	512	483	199	7	2.7	6	1013.4	334.7
13	19.2	7.1	49	68.4	488	446	205	8	2.7	6	1012.9	337.1
14	19.5	7.2	48	68.4	395	334	204	8	2.7	6	1012.3	338.2
15	19.5	7.2	48	68.4	302	308	160	8	2.6	6	1012.5	338.2
16	19.2	7.2	50	68.6	181	255	102	9	2.6	6	1012.7	337.5
17	18.5	7.5	52	69.4	56	114	40	9	2.6	6	1012.9	336
18	17.5	7.8	56	70.6	0	0	0	9	2.4	6	1013.1	334.2
19	16.3	8.3	61	72.2	0	0	0	9	2.2	6	1013.4	332.3
20	15.3	8.6	66	73.4	0	0	0	9	2.1	6	1013.6	330.8
21	14.7	8.7	69	74	0	0	0	9	2.1	6	1013.7	329.6
22	14.3	8.6	70	73.6	0	0	0	8	2	6	1013.9	328.4
23	14.1	8.4	70	72.7	0	0	0	8	2	6	1014	327.1
24	13.9	8.2	71	71.9	0	0	0	8	2	6	1014.1	325.7

Kunming

HOUR	TEM	DEW	RH	X	TH	NR	DF	WD	WS	CC	AP	LW
January												
1	6.9	2.8	76	58.6	0	0	0	9	2.8	5	811.9	287.4
2	6.6	2.9	78	58.7	0	0	0	9	2.7	5	811.9	286.7
3	6.3	2.9	80	58.9	0	0	0	9	2.7	5	811.7	286.2
4	6	2.9	82	58.9	0	0	0	9	2.6	5	811.6	285.5
5	5.4	2.8	84	58.4	0	0	0	9	2.5	5	811.4	284.1
6	4.8	2.6	86	57.6	0	0	0	9	2.6	5	811.7	282.1
7	4.4	2.5	88	57.2	0	0	0	9	2.6	6	812	280.9
8	4.8	2.6	86	57.5	0	0	0	9	2.6	6	812.4	282.1
9	6	2.8	80	58.4	112	294	54	9	3.1	6	812.8	285.3
10	8	3	72	59.3	319	615	86	9	3.7	6	813.2	290
11	10	2.8	64	58.8	494	734	112	9	4.2	6	813.6	294.7
12	11.7	2.3	56	56.8	638	862	112	9	4.7	6	812.6	297.1
13	13	1.4	49	53.6	678	872	118	9	5.2	6	811.6	297.7
14	14	0.6	44	50.7	606	723	149	9	5.7	5	810.6	297.6
15	14.7	0	41	48.7	509	619	152	9	5.8	5	810.1	297.7
16	15	-0.2	40	48	367	484	140	10	5.8	5	809.7	297.9
17	14.7	-0.1	41	48.5	187	287	97	10	5.9	5	809.2	297.4
18	13.7	0.3	44	49.6	42	59	34	10	5.1	5	809.7	295.5
19	12.2	0.8	49	51.2	0	0	0	9	4.4	5	810.1	292.9
20	10.7	1.3	55	53	0	0	0	9	3.7	4	810.6	290.6
21	9.5	1.9	61	55	0	0	0	9	3.4	4	811.1	289.7
22	8.7	2.3	66	56.7	0	0	0	9	3.2	4	811.5	289.4
23	8.1	2.7	70	57.8	0	0	0	9	2.9	4	811.9	289.1
24	7.5	2.8	74	58.4	0	0	0	9	2.9	4	811.9	288.4
February												
1	9.3	2.6	65	57.8	0	0	0	10	3.2	4	810.8	291.9
2	8.9	2.6	67	57.7	0	0	0	10	3	4	810.8	290.7
3	8.6	2.5	68	57.5	0	0	0	10	3	4	810.6	289.9
4	8.3	2.4	69	57.2	0	0	0	10	2.9	4	810.4	288.8
5	7.6	2.4	71	57	0	0	0	10	2.8	4	810.1	287.1
6	6.7	2.4	75	56.8	0	0	0	10	2.8	4	810.5	285.1
7	6.2	2.4	78	56.8	0	0	0	9	2.7	4	810.8	284.1
8	6.6	2.4	76	57	8	7	8	9	2.7	4	811.2	285.1
9	8.2	2.4	69	56.8	174	391	74	9	3.6	4	811.5	288.3
10	10.5	2.1	59	56.2	433	796	79	9	4.4	5	811.8	293.2
11	12.9	1.7	50	54.6	639	921	89	9	5.3	5	812.1	298.5
12	14.8	1.1	43	52.3	787	988	91	9	5.8	5	811.2	301.7
13	16	0.4	39	49.8	813	926	113	10	6.2	5	810.3	303
14	16.8	-0.2	36	47.7	701	692	183	10	6.7	5	809.4	303.4
15	17.4	-0.6	33	46.4	584	552	205	10	6.7	5	808.8	303.8
16	17.7	-0.8	33	45.9	437	442	187	10	6.7	5	808.2	304.3
17	17.5	-0.7	33	46.1	256	296	136	10	6.8	5	807.7	303.7
18	16.6	-0.5	35	46.8	94	140	65	10	6.1	5	808.1	301.8
19	15.3	-0.1	39	47.9	0	0	0	9	5.3	5	808.6	298.8
20	13.9	0.4	43	49.6	0	0	0	9	4.6	4	809	296.2
21	12.7	1	48	51.7	0	0	0	9	4.2	4	809.6	295
22	11.8	1.6	53	54	0	0	0	9	3.9	4	810.1	294.5
23	10.9	2.1	57	55.9	0	0	0	9	3.5	3	810.7	294.1
24	10.1	2.4	61	57.1	0	0	0	9	3.4	3	810.7	293.2

Kunming

HOUR	TEM	DEW	RH	X	TH	NR	DF	WD	WS	CC	AP	LW
						March						
1	12.5	4.3	60	65.3	0	0	0	9	3.3	5	810.8	306.1
2	12	4.2	61	65.1	0	0	0	9	3.1	5	810.8	304.7
3	11.7	4.2	63	64.9	0	0	0	9	3.1	5	810.6	303.6
4	11.3	4.2	64	65	0	0	0	10	3	5	810.4	302.5
5	10.7	4.2	67	65.2	0	0	0	10	2.9	5	810.1	301.3
6	10	4.3	70	65.6	0	0	0	10	2.9	5	810.6	300.1
7	9.8	4.4	71	65.9	0	0	0	9	2.9	5	811	299.8
8	10.4	4.4	69	65.9	55	97	39	9	2.8	5	811.4	301.4
9	12	4.3	62	65.4	251	386	110	9	3.7	5	811.6	304.8
10	14.2	4	53	64.2	502	672	129	10	4.7	5	811.9	309.8
11	16.4	3.5	45	62.2	691	769	152	10	5.6	5	812.1	314.8
12	18.1	2.9	39	59.7	828	820	162	10	6	6	811.2	317.9
13	19.2	2.3	36	57.3	836	743	200	10	6.4	6	810.3	319.5
14	20	1.8	33	55.6	704	506	278	10	6.8	6	809.5	320.2
15	20.5	1.5	31	54.6	599	411	282	10	6.8	6	808.8	320.9
16	20.7	1.4	31	54.3	464	344	241	10	6.7	6	808.2	321.5
17	20.5	1.5	32	54.5	288	249	170	10	6.7	6	807.5	321
18	19.7	1.7	34	55.2	129	138	91	10	6	6	808	318.9
19	18.4	2	37	56.4	3	1	3	10	5.3	5	808.4	315.7
20	17	2.5	41	58.2	0	0	0	10	4.6	5	808.8	312.8
21	15.8	3.1	46	60.4	0	0	0	10	4.2	5	809.5	311.2
22	14.8	3.6	50	62.7	0	0	0	9	3.8	5	810.1	310.3
23	14	4.1	54	64.5	0	0	0	9	3.5	4	810.8	309.4
24	13.2	4.4	57	65.7	0	0	0	9	3.4	5	810.8	308.4
						April						
1	15	8	65	84.4	0	0	0	9	3.2	5	810.2	327
2	14.5	7.9	67	84.1	0	0	0	9	3	5	810.1	325.4
3	14	7.8	68	83.6	0	0	0	9	2.9	5	809.9	323.8
4	13.6	7.8	70	83.4	0	0	0	9	2.9	5	809.7	322.5
5	13.2	7.9	72	83.9	0	0	0	9	2.8	5	809.6	321.8
6	12.9	8.1	74	85	0	0	0	9	2.8	5	810	321.9
7	13.1	8.3	74	86.1	9	7	8	9	2.8	5	810.4	323.2
8	14	8.3	71	86.4	136	237	75	9	2.8	6	810.8	325.8
9	15.5	8.1	64	85.5	356	464	140	9	3.6	6	811	329.2
10	17.4	7.7	56	83.4	585	645	169	9	4.5	6	811.1	333.1
11	19.2	7.3	49	80.9	742	689	201	9	5.3	6	811.2	337.2
12	20.6	6.8	44	78.7	838	698	224	9	5.5	6	810.5	340
13	21.6	6.5	41	77	812	603	265	10	5.8	7	809.8	342.1
14	22.2	6.2	39	75.8	688	421	316	10	6	7	809	343.4
15	22.6	6.1	37	75	581	327	314	10	6	7	808.4	344.2
16	22.7	6	37	74.5	451	263	273	10	6	7	807.8	344.2
17	22.4	5.9	38	74.3	286	178	195	10	6	7	807.2	342.9
18	21.6	5.9	40	74.5	138	102	105	10	5.5	7	807.5	340.2
19	20.4	6.1	43	75.2	16	10	15	9	5	6	807.9	336.7
20	19.1	6.4	47	76.7	0	0	0	9	4.5	6	808.2	333.5
21	17.9	6.9	52	78.8	0	0	0	9	4.2	6	808.9	331.5
22	17	7.3	56	81.1	0	0	0	9	3.9	5	809.6	330.4
23	16.3	7.7	60	83.1	0	0	0	9	3.5	5	810.3	329.7
24	15.6	8	63	84.7	0	0	0	9	3.4	5	810.2	329

Kunming

HOUR	TEM	DEW	RH	X	TH	NR	DF	WD	WS	CC	AP	LW
						May						
1	17.3	11.9	72	110.9	0	0	0	9	3.2	6	809.2	349.1
2	16.8	11.9	75	110.8	0	0	0	9	3.1	7	809.1	347.7
3	16.3	11.9	76	110.8	0	0	0	9	3	7	809	346.3
4	15.9	11.9	79	111	0	0	0	9	2.9	6	808.8	345.4
5	15.6	12.1	80	111.9	0	0	0	9	2.9	6	808.7	345.2
6	15.6	12.2	81	113.1	0	0	0	9	2.9	6	809.1	345.9
7	15.9	12.4	80	114.2	31	47	26	9	3	7	809.5	347.3
8	16.7	12.4	77	114.5	170	227	97	9	3.1	7	809.8	349.6
9	17.8	12.3	72	113.7	357	370	166	9	3.5	7	809.9	352.2
10	19.2	12	65	112.2	540	489	207	8	3.9	7	810	355.2
11	20.5	11.8	60	110.2	662	508	250	8	4.3	7	810.1	358.3
12	21.6	11.5	55	108.5	747	525	278	8	4.5	7	809.5	360.9
13	22.6	11.2	52	107	746	478	309	9	4.7	7	808.9	363.2
14	23.3	11.1	50	105.8	666	362	342	9	4.9	7	808.3	365.1
15	23.8	10.9	48	104.9	583	304	328	9	5	7	807.7	366.1
16	23.9	10.8	47	104.2	457	260	276	9	5	7	807.1	366.4
17	23.6	10.7	48	104	298	176	205	9	5.1	7	806.5	365.1
18	22.9	10.8	50	104.1	159	110	120	9	4.7	7	806.7	362.7
19	21.8	10.9	54	105	36	27	32	9	4.4	7	806.9	359.5
20	20.6	11.2	58	106.5	0	0	0	9	4.1	6	807.2	356.5
21	19.6	11.4	62	108.3	0	0	0	9	3.9	6	807.9	354.5
22	18.9	11.7	66	109.8	0	0	0	9	3.7	6	808.6	353
23	18.3	11.9	68	110.9	0	0	0	9	3.5	6	809.2	351.9
24	17.8	12	71	111.7	0	0	0	9	3.4	6	809.2	351
						June						
1	18.6	15.5	83	139.6	0	0	0	8	2.8	8	807.6	367.7
2	18.2	15.5	85	139.3	0	0	0	8	2.8	8	807.6	366.7
3	17.9	15.4	86	138.8	0	0	0	8	2.7	8	807.4	365.7
4	17.7	15.4	87	138.5	0	0	0	9	2.7	8	807.3	364.9
5	17.5	15.4	87	138.5	0	0	0	9	2.7	8	807.1	364.5
6	17.5	15.4	88	139	0	0	0	9	2.7	8	807.4	364.5
7	17.6	15.5	88	139.7	30	35	25	9	2.8	8	807.7	365.3
8	18.1	15.6	86	140.5	137	107	101	9	2.8	8	808	367
9	18.9	15.7	82	140.9	279	173	188	9	3.1	8	808.1	369.4
10	20	15.7	77	140.8	422	245	256	8	3.4	8	808.2	372.3
11	21	15.6	72	140.2	532	271	311	8	3.7	8	808.3	375.2
12	22	15.5	68	139.3	618	299	353	8	3.8	8	807.8	377.6
13	22.7	15.3	65	138.5	639	302	368	8	4	8	807.4	379.6
14	23.4	15.3	62	137.9	593	254	369	8	4.1	8	806.9	381.4
15	23.8	15.2	61	137.7	528	218	345	8	4.1	8	806.4	382.8
16	24	15.2	60	137.8	425	189	292	8	4.1	8	805.8	383.3
17	23.8	15.2	61	137.9	287	123	218	8	4.2	8	805.3	382.5
18	23.1	15.2	63	137.7	156	70	129	8	3.9	8	805.5	380.3
19	22.2	15.2	67	137.6	45	27	40	8	3.6	8	805.7	377.3
20	21.2	15.2	70	137.7	0	0	0	8	3.4	8	805.9	374.2
21	20.4	15.3	74	138.2	0	0	0	8	3.2	7	806.5	372.1
22	19.8	15.4	77	138.8	0	0	0	8	3.1	7	807.2	370.7
23	19.4	15.5	79	139.4	0	0	0	8	2.9	7	807.8	369.8
24	19	15.5	81	139.9	0	0	0	8	2.9	7	807.7	369

Kunming

HOUR	TEM	DEW	RH	X	TH	NR	DF	WD	WS	CC	AP	LW
July												
1	18.7	16.4	87	147.7	0	0	0	8	2.4	8	807.9	372
2	18.4	16.4	88	147.1	0	0	0	8	2.4	8	807.8	371
3	18.2	16.3	89	146.5	0	0	0	8	2.3	8	807.7	370.2
4	18	16.2	90	146	0	0	0	8	2.2	8	807.5	369.5
5	17.8	16.2	90	145.7	0	0	0	8	2.2	8	807.3	368.9
6	17.7	16.2	91	145.8	0	0	0	8	2.2	8	807.6	368.6
7	17.8	16.3	91	146.4	14	13	13	8	2.3	8	807.8	369.1
8	18.3	16.4	89	147.2	110	79	86	8	2.3	9	808.1	370.7
9	19.1	16.5	85	148	248	143	177	8	2.5	9	808.2	373.2
10	20.1	16.5	80	148.4	394	226	247	8	2.8	8	808.3	376.2
11	21.1	16.5	76	148.2	508	271	299	8	3	8	808.5	379
12	21.9	16.4	72	147.5	585	291	339	8	3.1	8	808.1	381.1
13	22.5	16.3	69	146.7	600	284	357	8	3.3	8	807.7	382.7
14	23.1	16.2	67	146.1	556	232	362	8	3.4	8	807.3	384
15	23.4	16.1	65	145.9	491	193	338	8	3.4	8	806.8	385
16	23.5	16.2	65	146.1	393	177	276	8	3.5	8	806.3	385.5
17	23.2	16.2	67	146.5	269	132	201	8	3.5	8	805.8	384.8
18	22.5	16.2	69	146.7	144	72	118	8	3.3	8	806	382.7
19	21.6	16.3	73	147	42	22	38	8	3	8	806.2	379.9
20	20.7	16.3	77	147.3	0	0	0	8	2.8	8	806.4	377.3
21	20	16.4	80	147.5	0	0	0	8	2.6	8	807	375.5
22	19.6	16.4	83	147.8	0	0	0	8	2.5	8	807.6	374.4
23	19.3	16.4	84	148	0	0	0	8	2.3	7	808.2	373.7
24	19	16.5	86	148	0	0	0	8	2.3	7	808.1	372.9
August												
1	18.2	16.1	88	144.1	0	0	0	7	2.2	8	809.8	369.2
2	17.9	16	89	143.4	0	0	0	7	2.2	8	809.7	368.1
3	17.7	15.9	90	142.5	0	0	0	7	2.1	8	809.5	367.1
4	17.5	15.8	90	141.6	0	0	0	7	2.1	8	809.3	366.2
5	17.3	15.8	91	141.2	0	0	0	7	2.1	8	809.1	365.5
6	17.2	15.8	91	141.2	0	0	0	7	2.1	8	809.4	365
7	17.2	15.8	91	141.7	5	2	5	7	2.1	8	809.6	365.4
8	17.7	15.9	89	142.2	102	102	74	7	2.2	8	809.9	367.1
9	18.6	15.9	85	142.4	256	192	164	7	2.4	8	810.1	369.5
10	19.7	15.9	79	142.2	416	275	236	7	2.6	8	810.3	372.4
11	20.8	15.8	74	141.7	539	314	293	7	2.9	8	810.4	375.5
12	21.7	15.8	70	141.2	625	333	333	7	3	8	810	378
13	22.4	15.7	67	140.6	635	310	356	7	3.1	8	809.5	379.8
14	23	15.6	65	140	584	245	367	7	3.2	8	809	381.2
15	23.3	15.5	63	139.3	513	209	341	7	3.2	8	808.5	382.2
16	23.4	15.5	63	139	408	195	274	7	3.2	8	808	382.3
17	23	15.5	64	139.4	273	137	199	7	3.2	8	807.4	381.2
18	22.2	15.6	68	140.2	131	70	106	7	3	8	807.7	378.9
19	21.1	15.8	73	141.5	26	15	24	7	2.7	8	807.9	376
20	20	15.9	78	142.8	0	0	0	7	2.4	8	808.1	373.4
21	19.3	16	82	143.6	0	0	0	7	2.3	8	808.8	371.8
22	18.9	16.1	84	144	0	0	0	7	2.3	7	809.4	370.9
23	18.7	16.1	85	144	0	0	0	7	2.2	7	810.1	370.4
24	18.4	16.1	86	144	0	0	0	7	2.2	7	810	369.8

Kunming

HOUR	TEM	DEW	RH	X	TH	NR	DF	WD	WS	CC	AP	LW
September												
1	17	14.6	86	131	0	0	0	7	2.3	7	811.9	359.6
2	16.7	14.6	88	130.9	0	0	0	7	2.2	8	811.8	358.9
3	16.5	14.5	88	130.7	0	0	0	7	2.2	8	811.7	358.1
4	16.3	14.5	89	130.4	0	0	0	7	2.1	8	811.5	357.5
5	16.1	14.5	90	130.1	0	0	0	7	2.1	8	811.3	356.9
6	15.9	14.5	91	129.9	0	0	0	7	2.1	8	811.6	356.3
7	16	14.5	91	130	0	0	0	7	2.2	8	811.9	356.4
8	16.4	14.5	89	130.3	68	70	53	7	2.3	8	812.2	357.6
9	17.2	14.5	85	130.5	207	154	141	7	2.5	8	812.5	359.8
10	18.3	14.5	79	130.4	359	258	210	7	2.7	8	812.7	362.5
11	19.4	14.4	74	129.9	478	309	261	7	2.9	8	812.9	365.5
12	20.3	14.3	70	129.2	561	338	295	7	3	8	812.4	367.8
13	21.1	14.2	67	128.3	572	323	313	7	3.2	8	811.8	369.7
14	21.6	14.1	64	127.5	517	252	320	7	3.3	8	811.2	371.1
15	22	14	63	126.9	448	213	293	7	3.3	8	810.6	372
16	22.1	14	63	127	344	187	232	7	3.3	8	810.1	372.1
17	21.6	14.1	65	127.8	210	126	155	7	3.3	8	809.6	371.2
18	20.8	14.2	68	128.9	83	52	70	7	3	7	809.9	369.1
19	19.7	14.4	73	130	7	3	7	7	2.7	7	810.1	366.3
20	18.7	14.5	78	130.9	0	0	0	7	2.4	7	810.4	363.9
21	18	14.6	81	131.1	0	0	0	7	2.4	7	811	362.3
22	17.7	14.6	83	131	0	0	0	7	2.4	7	811.6	361.3
23	17.5	14.5	84	130.6	0	0	0	7	2.4	7	812.2	360.6
24	17.2	14.5	85	130.3	0	0	0	7	2.3	7	812.1	359.9
October												
1	14	11.8	87	109.1	0	0	0	8	2.2	7	814.2	340.3
2	13.8	11.8	88	108.8	0	0	0	8	2.1	7	814.1	339.6
3	13.6	11.8	89	108.7	0	0	0	8	2.1	7	814	339
4	13.5	11.7	89	108.6	0	0	0	8	2.1	7	813.8	338.7
5	13.3	11.7	91	108.6	0	0	0	8	2	8	813.6	338.2
6	13	11.8	92	108.8	0	0	0	8	2	8	814	337.7
7	13	11.9	92	109.5	0	0	0	7	2.1	8	814.4	338
8	13.5	12	91	110.5	51	79	38	7	2.1	8	814.8	340.1
9	14.5	12.2	86	111.3	199	224	118	7	2.5	8	815.1	342.9
10	15.9	12.2	79	111.7	360	368	170	8	2.9	8	815.3	346.5
11	17.3	12.1	73	111	475	427	208	8	3.3	8	815.6	349.8
12	18.3	11.8	68	109.4	553	461	230	8	3.5	8	814.8	351.8
13	19	11.5	64	107.2	547	416	249	8	3.6	8	814.1	352.6
14	19.6	11.1	61	105.1	473	317	258	8	3.7	8	813.3	353
15	19.9	10.9	59	103.6	396	276	230	8	3.7	8	812.9	353.3
16	20	10.8	59	103.2	286	235	174	8	3.6	7	812.4	353.2
17	19.6	10.9	60	103.8	150	143	103	8	3.5	7	812	352.1
18	18.6	11.1	64	105	34	30	30	8	3.2	7	812.4	349.7
19	17.2	11.3	70	106.4	0	0	0	8	2.8	7	812.7	346.7
20	16	11.6	76	107.8	0	0	0	8	2.5	6	813.1	344.2
21	15.2	11.7	81	108.7	0	0	0	8	2.4	6	813.5	342.7
22	14.8	11.8	83	109.1	0	0	0	8	2.3	6	814	342
23	14.5	11.8	84	109.1	0	0	0	8	2.2	6	814.5	341.5
24	14.2	11.8	86	108.9	0	0	0	8	2.2	7	814.4	340.7

Kunming

HOUR	TEM	DEW	RH	X	TH	NR	DF	WD	WS	CC	AP	LW
November												
1	10	7.5	85	81.4	0	0	0	9	2.6	5	813.8	312.9
2	9.7	7.5	87	81.4	0	0	0	9	2.5	6	813.8	312.3
3	9.5	7.5	87	81.3	0	0	0	9	2.5	6	813.6	311.6
4	9.3	7.4	88	80.9	0	0	0	9	2.4	6	813.5	310.9
5	9	7.3	90	80.4	0	0	0	9	2.4	6	813.3	309.9
6	8.5	7.3	92	80.1	0	0	0	9	2.4	6	813.7	308.6
7	8.4	7.3	93	80.4	0	0	0	9	2.4	6	814.1	308.4
8	8.9	7.5	91	81.2	32	51	26	9	2.5	7	814.5	310.5
9	10.2	7.7	85	82.2	190	316	94	9	3	7	814.7	313.9
10	12.1	7.7	76	82.7	385	553	126	8	3.5	7	815	318.5
11	13.9	7.6	67	82.1	526	634	152	8	3.9	7	815.3	322.7
12	15.3	7.2	61	80.2	632	713	156	8	4.3	7	814.4	325.1
13	16.3	6.7	55	77.4	632	661	177	9	4.6	6	813.4	325.7
14	17	6	51	74.4	532	494	207	9	4.9	6	812.5	325.5
15	17.4	5.6	49	72.1	428	410	191	9	4.8	6	812.1	325.2
16	17.5	5.3	48	71	286	308	150	9	4.7	6	811.7	324.6
17	16.9	5.4	50	71.5	123	160	80	9	4.7	6	811.3	323.2
18	15.7	5.8	54	72.9	9	6	9	9	4.1	6	811.8	320.7
19	14.1	6.2	61	75	0	0	0	9	3.6	5	812.3	317.7
20	12.6	6.6	69	77	0	0	0	9	3.1	4	812.7	315.3
21	11.6	7	74	78.6	0	0	0	9	3	5	813.1	314
22	11	7.2	78	79.6	0	0	0	9	2.9	5	813.5	313.6
23	10.7	7.3	80	80.1	0	0	0	9	2.8	5	813.9	313.4
24	10.3	7.4	82	80.4	0	0	0	9	2.7	5	813.8	312.8
December												
1	6.9	4.3	84	65	0	0	0	9	2.7	6	813	293.1
2	6.6	4.3	86	65.2	0	0	0	9	2.6	6	813	292.8
3	6.5	4.4	87	65.5	0	0	0	9	2.5	6	812.8	292.6
4	6.3	4.4	87	65.5	0	0	0	9	2.5	6	812.7	292.2
5	6	4.2	89	65	0	0	0	9	2.4	6	812.5	291.2
6	5.5	4.1	91	64.3	0	0	0	9	2.4	6	812.8	289.5
7	5.2	4	92	63.9	0	0	0	8	2.5	7	813.2	288.5
8	5.6	4.1	91	64.2	7	4	7	8	2.5	7	813.5	289.8
9	6.6	4.3	85	65.1	113	226	63	8	2.9	7	813.9	292.5
10	8.3	4.5	78	66	285	464	104	8	3.4	7	814.3	296.7
11	10.1	4.4	70	66	426	574	131	8	3.9	7	814.6	300.9
12	11.5	4.1	63	64.5	540	681	138	8	4.3	7	813.6	303.3
13	12.6	3.5	57	61.8	565	673	147	9	4.6	7	812.7	303.9
14	13.5	2.8	52	59.1	491	538	171	9	5	6	811.7	303.8
15	14	2.3	49	57.1	404	457	161	9	5	6	811.3	303.6
16	14.2	2	48	56.2	276	354	131	9	5	6	810.8	303.2
17	13.8	2.1	49	56.4	122	190	74	9	5	6	810.4	302.2
18	12.7	2.4	53	57.4	8	4	8	9	4.4	6	810.9	300.2
19	11.3	2.8	59	58.9	0	0	0	9	3.9	5	811.4	297.7
20	9.9	3.2	65	60.5	0	0	0	9	3.3	5	811.8	295.7
21	8.9	3.6	71	62.1	0	0	0	9	3.1	5	812.2	294.7
22	8.2	3.9	75	63.3	0	0	0	9	3	5	812.6	294.3
23	7.7	4.1	79	64.1	0	0	0	9	2.9	5	813	294
24	7.3	4.2	82	64.5	0	0	0	9	2.8	5	813	293.4